

The copyright of this thesis vests in the author. No quotation from it or information derived from it is to be published without full acknowledgement of the source. The thesis is to be used for private study or non-commercial research purposes only.

Published by the University of Cape Town (UCT) in terms of the non-exclusive license granted to UCT by the author.



BASE METAL HEAP AND TANK LEACHING OF A PLATREEF FLOTATION CONCENTRATE USING AMMONIACAL SOLUTIONS

**By
Caroline Muzawazi**

**Supervisor
A/Professor: Jochen Petersen**

Submitted in fulfilment of the requirements for the award of the degree of Master of Science in
Chemical Engineering

Department of Chemical Engineering, University of Cape Town

February 2013

Declaration

I know the meaning of plagiarism and I declare that the work I am submitting is my own and I duly acknowledged other people's work with an acceptable form of referencing.

.....
Caroline Muzawazi

.....
Date

Abstract

The technical feasibility of the ammonia leaching process of a Platreef flotation concentrate was investigated in different reactor settings i.e. shake flasks, columns and batch stirred tank reactors, respectively. The process investigated aims to use either a heap leaching environment or tank leaching of untreated low-grade concentrates under ambient conditions and mild temperatures. This process is proposed as an alternative primary treatment method for the recovery of base metal sulphides from a PGM containing concentrate that cannot be extracted economically by conventional milling, smelting and refining methods. Copper and nickel are recovered from chalcopyrite and pentlandite, respectively, prior to PGM recovery from the residue.

The composition of the concentrate was: 2.02% Cu, 3.17% Ni and 14.1% Fe. The major base metal sulphides were CuFeS_2 and $(\text{FeNi})_9\text{S}_8$. To optimise the leaching conditions, parameters such as buffering capacity, ammonia concentration, temperature and pulp density were studied. In the shake flasks the best conditions obtained were 4 M NH_4OH , 4 M $(\text{NH}_4)_2\text{CO}_3$ and a pH range between 9 and 10 at ambient temperature in which 84% Cu and 91% Ni were extracted in 5 days. These conditions were used as the base case in the columns and batch stirred tank reactors.

The rate of reaction increased with increase in ammonia concentration and temperature in both stirred tank reactors and columns. Ammonia concentration had the most significant effect on the total amount of Cu and Ni extracted. The reaction was found to be first order at lower ammonia concentration (i.e. < 3 M in tanks and < 4 M in columns), and zero order at higher ammonia concentration in both reactor systems. Within the range of variables studied the activation energy for Ni dissolution was 16 kJ/mol in both tanks and columns, indicating a diffusion controlled reaction. The activation energy for Cu dissolution in tank and column systems was 36 kJ/mol, indicating mixed kinetic control. The leaching kinetics were characterised by fitting to different shrinking core models (surface kinetic, diffusion layer and mixed control) and for Ni was found to be best described by diffusion control through the surface layer, whilst a mixed control model was observed to describe best the leaching kinetics of Cu dissolution. However, in both Ni and Cu dissolution all the data had high correlations for all three models. In terms of gas-liquid mass transfer k_La values were estimated to be approximately 22 times higher in the stirred tank reactors in comparison to

the columns. It appears the columns are strongly oxygen supply limited, whereas in tanks this is not the case in the range of values tested.

A potential drawback of using ammonia in a heap leach operation is that it is too volatile, causing significant loss of reagent to the atmosphere and potential environmental impact around such operations. Ammonia losses were measured during the process, by measuring the total ammonia lost from the reactor and recovered in the wash bottles in 4 days. The total ammonia lost ranged from 7 to 10% in stirred tank reactors and 6 to 16% in columns. Tank leaching proved to be a better environment as a possible alternative route for the leaching of Platreef minerals at high ammonia concentration with higher extraction rates, rapid dissolution kinetics and reduced ammonia losses.

University of Cape Town

Acknowledgements

I believe if one can see farther, it is by standing on the shoulders of academic giants. I offer my sincerest gratitude to my supervisor, A/Professor Jochen Petersen, who has supported me throughout my thesis with his patience, knowledge and insight, whilst allowing me the room to work in my own way. I attribute the level of my Masters degree to his encouragement, guidance and effort from the initial to the final level enabling me to develop an understanding in the project and to become a better Engineer. One simply could not wish for a better supervisor.

I owe my deepest gratitude to Frances Pocock (now retired), Emmanuel Ngoma, and Sue Jobson for the pleasant working environment they provide. I would also like to acknowledge James Mwase, Adri Uys and Keboihle Molatudi, CeBER and the analytical team. I am indebted to many of my colleagues who supported me in various respects during completion of the project.

Thank you Daddy for being my inspirational mentor, you are the best Dad anyone could be blessed with. Clementine Muzawazi and Joseph Sigauke, thank you for your understanding love through the duration of my studies. I offer my regards and blessings to you.

“Thank you Lord for giving me strength to plod on and for never giving up on me”

Table of Contents

Declaration.....	i
Abstract	ii
Acknowledgements	iv
Table of Contents	v
List of Figures	ix
List of Tables	xi
List of Pictures	xii
ACRONYMS.....	xiii
List of abbreviations	xiii
List of elements and compounds	xiii
List of symbols	xiv
1.0 INTRODUCTION.....	1
1.1 Background information	1
1.2 Problem statement	4
1.3 Aim	4
1.4 Research questions.....	5
1.5 Objective	5
1.6 Outline of the research	5
2.0 LITERATURE REVIEW	6
2.1 Occurrence of base metal sulphides associated with PGMs in South Africa	6
2.1.1 Platreef.....	7
2.1.2 Merensky reef	7
2.1.3 Upper Ground (UG) 2	7
2.2 Traditional method of processing PGM bearing minerals	8
2.3 Properties of chalcopyrite	9
2.4 Properties of pentlandite	9
2.5 Leaching reagents for copper and nickel sulphides	10
2.6 Common ways to extract Cu from chalcopyrite and Ni from pentlandite	10
2.7 Ammoniacal leaching process.....	11
2.7.1 Advantages of ammoniacal leaching.....	12
2.8 Applications of ammonia leaching technology	12
2.9 Types of reagents used as ammoniacal lixiviants.....	15

2.10 Feasibility studies on the ammoniacal leaching process.....	16
2.10.1 Copper dissolution studies	16
2.10.2 Nickel dissolution studies	16
2.11 Dissolution mechanism for chalcopyrite.....	17
2.12 Dissolution mechanism for pentlandite.....	19
2.13 Speciation of ammonia.....	19
2.13.1 Thermochemistry	20
2.14 Thermodynamics of ammoniacal leaching	21
2.14.1 Ratios of NH_3 and NH_4^+	23
2.15 Solubility of ammonia.....	25
2.16 Kinetics of ammoniacal leaching of copper	26
2.16.1 Effect of kinetic variables on rate of copper dissolution from chalcopyrite.....	27
2.17 Kinetics of ammoniacal leaching of nickel from metallic Ni and Ni sulphides.....	31
2.18 Limitation and challenges – passivation	31
2.18.1 Iron oxide – the result of passivation	33
2.18.2 Ammonia losses	35
2.19 Types of leaching.....	35
2.19.1 Percolation leaching	35
2.19.2 Agitation leaching	36
2.19.3 Advantages and disadvantages of leaching	38
2.20 Uses of the by-product - ammonium sulphate.....	39
3.0 EXPERIMENTAL MATERIALS AND METHODS.....	40
3.1 Introduction	40
3.2 Platreef concentrate preparation	40
3.3 Reagents	42
3.4 Equipment description	42
3.4.1 Shake flasks	42
3.4.2 Columns.....	43
3.4.3 Batch stirred tank reactor.....	45
3.5 Analytical methods	46
3.5.1 Acid digestion for solids.....	46
3.5.2 Atomic absorption spectroscopy (AAS).....	46
3.5.3 Inductive coupled plasma spectrometer (ICP).....	47

3.5.4 Ammonium analysis	47
3.5.5 Iron assay method.....	48
3.5.6 pH analysis.....	48
3.5.7 Redox potential analysis	48
3.6 Safety, health and environmental aspects of ammonia	49
3.7 Experimental procedures.....	49
3.7.1 Process variables	50
3.8 Experimental design	50
3.9 Experimental program	51
3.9.1 Investigation of ammoniacal leaching Platreef concentrates in shake flasks	51
3.9.2 Investigation of ammoniacal leaching of Platreef concentrates in columns.....	52
3.9.3 Investigation of the ammoniacal leaching process in batch stirred tank reactors..	53
3.9.4 Procedure for ammonia leaching of a Platreef concentrate in shake flasks	54
3.9.5 Procedure for ammonia leaching of a Platreef concentrate in columns	54
3.9.6 Procedure for ammonia leaching of Platreef concentrates in batch stirred tanks ...	54
3.9.7 Quantification of Ammonia Loss - Ammonia Vapour.....	55
4.0 RESULTS	56
4.1 Shake flasks.....	56
4.1.1 Trial run	56
4.1.2 Buffering effect	57
4.1.3 Ammonia concentration	59
4.1.4 Results of Fe	60
4.1.5 Redox potential vs. pH	60
4.2 Optimal conditions observed in shake flasks	61
4.3 Results of columns.....	62
4.3.1 Effect of the ratio of NH_4OH to $(\text{NH}_4)\text{CO}_3$ on the Cu and Ni extracted.....	62
4.3.2 Effect of ammonium concentration on the rate of Cu and Ni extraction	63
4.3.3 Effect of temperature on the rate of Cu and Ni extraction	64
4.4 Results of leaching in batch stirred tank reactors	65
4.4.1 Effect of pulp density	65
4.4.2 Effect of ammonia concentration	67
4.4.3 Effect of temperature.....	68
4.5 Results of the measurement of ammonia losses	69

4.5.1 Ammonia losses in batch stirred tank reactors	69
4.5.2 Ammonia losses in columns	70
5.0 DISCUSSION	73
5.1 Activation energy in batch stirred tank reactor tests	73
5.2 Activation energy in columns.....	75
5.3 Kinetic data analysis	77
5.3.1 Shrinking core model in batch stirred tank reactors.....	78
5.3.2 Shrinking core model in columns	81
5.4 Reaction order in terms of NH_3 in a batch stirred tank reactor	84
5.5 Reaction order in terms of NH_3 in a column	86
5.6 Gas-Liquid mass transfer in columns and stirred tank reactors	86
5.7 Evaporation rates of ammonia in batch stirred tank reactor system.....	89
5.8 Evaporation rates of ammonia in columns	90
6.0 CONCLUSIONS AND RECOMMENDATIONS.....	91
7.0 REFERENCES.....	94
8.0 APPENDICES.....	103

List of Figures

Figure 2.1: Quasi-equilibrium Pourbaix diagram for the Ni-NH ₃ -H ₂ O system at 25 °C.....	20
Figure 2.2: Ni(II) speciation for 0.1 M total nickel in 6 M total ammonia at 60 °C	20
Figure 2.3 (a) and (b): E _H -pH diagram for Cu-Fe-S-NH ₃ and Ni-S-NH ₃ at 25 °C.	21
Figure 2.4: E _H -pH diagram for Fe-NH ₃ -H ₂ O-CO ₃ at 25 °C	22
Figure 2.5: Percentage of NH ₄ ⁺ and NH ₃ as a function of pH.....	23
Figure 2.6: Percentage of H ₂ CO ₃ , HCO ₃ ⁻ and CO ₃ ²⁻ as a function of pH.	24
Figure 2.7: Schematic representation of ammonia oxidation leaching of chalcopyrite	32
Figure 2.8: Schematic representation of ammoniacal leaching of pentlandite.	33
Figure 2.9: Stability fields for iron oxides and jarosite (KFe ₃ (SO ₄) ₂ (OH) ₆).....	33
Figure 2.10: Types of leaching and some of the sub-types of leaching	35
Figure 2.11: Typical Heap leach operation.	36
Figure 3.1: Process flow diagram of the ammoniacal leaching process	49
Figure 4.1: Trial run graph of %Ni and %Cu extraction and pH against time	56
Figure 4.2: Graphs of Cu and Ni extraction using different buffer solutions.....	58
Figure 4.3 (a) and (b): Cu and extraction using different total ammonia concentrations	59
Figure 4.4 (a) and (b):Cu and Ni extracted at different total NH ₃ concentrations.....	63
Figure 4.5 (a) and (b): Effect of temperature on amount of Cu and Ni extracted	65
Figure 4.6 (a) and (b): % Cu and Ni extraction using different pulp densities	66
Figure 4.7 (a) and (b): Effect of NH ₃ concentration on amount of Cu and Ni extracted.....	67
Figure 4.8 (a) and (b): Cu and Ni extracted at different temperatures.....	68
Figure 4.9 (a) and (b): NH ₃ losses at different NH ₃ concentrations and temperature in tanks	70
Figure 4.10: NH ₃ losses at different ammonia concentration in columns.....	71
Figure 5.1 (a) and (b): %Cu extraction and initial rates of reaction vs. temperature in tanks.	73
Figure 5.2 (a) and (b): %Ni extraction and initial rates of reaction vs. temperature in tanks .	74
Figure 5.3: %Cu extraction and initial rates of reaction vs.temperature in columns.....	75
Figure 5.4: %Ni extraction and initial rates of reaction vs. temperature in columns	76
Figure 5.5: Graph of the surface reaction model for Cu dissolution in tank reactors.....	78
Figure 5.6: Graph of product layer diffusion model for Cu dissolution in tank reactors.....	79
Figure 5.7: Graph of mixed control model for Cu dissolution in stirred tank reactors.....	79
Figure 5.8: Graph of the surface reaction model for Ni dissolution in tank reactors.	80
Figure 5.9: Graph of product layer diffusion model for Ni dissolution in tank reactors	80
Figure 5.10: Graph of mixed control model for Ni dissolution in the tank reactors.....	81

Figure 5.11: Graph of surface reaction model for Cu dissolution in columns.	81
Figure 5.12: Graph of product layer diffusion model for Cu dissolution in columns.....	82
Figure 5.13: Graph of mixed control model for Cu dissolution in columns.	82
Figure 5.14: Graph of surface reaction model for Ni dissolution in columns.	83
Figure 5.15: Graph of product layer diffusion model a for Ni dissolution in columns.	83
Figure 5.16: Graph of mixed control model for Ni dissolution in columns.	84
Figure 5.17 a) and b): Log dX/dt vs. log $[NH_3]$ in tank reactors Cu and Ni conversion.	85
Figure 5.18 (a) and (b): Log dX/dt vs. log $[NH_3]$ in columns for Cu and Ni.	86

University of Cape Town

List of Tables

Table 2.1: Characteristics of Bushveld PGM Ore Types	6
Table 2.2: Classification of leaching reagents	10
Table 2.3: Properties of ammonia and ammonium salts	15
Table 2.4: Properties of aqueous solutions of NH_4^+ salts.....	24
Table 2.5: Solubility of ammonia in distilled water	25
Table 2.6: Solubility of oxygen in distilled water at different temperatures and salinity	29
Table 2.7: Advantages and disadvantages of different types of leaching	38
Table 3.1: Particle size analysis of the concentrate sample	41
Table 3.2: Major base metals and gangue elements of the concentrate sample	41
Table 3.3: Mineral abundances of base metal sulphides and gangue (wt. %).....	42
Table 3.4: Overall experimental plan of all experiments carried out.....	50
Table 3.5: Experimental design of shake flask experiments	52
Table 3.6: Experimental design of column experiment, pH 9 to 10	52
Table 3.7: Experimental design of experiments carried out in the batch stirred tank reactor .	53
Table 4.1: Results of redox and pH for one run conducted in shake flasks	60
Table 4.2: Table of Cu(II) to Cu(I) ratio at a pH of 9.25	61
Table 4.3: The effect of the ratio of NH_4OH to $(\text{NH}_4)_2\text{CO}_3$ concentration in columns	62
Table 4.4: Cu and Ni extraction obtained at different ammonia concentration	63
Table 4.5: Total amount of Cu and Ni extracted in 5 days	66
Table 4.6: Ammonia losses observed in the tank leaching system.....	69
Table 4.7: Ammonia losses observed in the column leaching system.....	71
Table 5.1: k and R^2 values for the slope of the regression lines in Figure 5.1 (a).	74
Table 5.2 : k and R^2 values for the slope of the regression lines in Figure 5.2 (a).	74
Table 5.3: k and R^2 values for the slope of the regression lines in Figure 5.3 (a).	76
Table 5.4: k and R^2 values for the slope of the regression lines in Figure 5.4 (a)	77
Table 5.5: Estimated $k_L a$ values in columns at different temperatures	87
Table 5.6: Estimated $k_L a$ values in tank reactors at different temperatures	87
Table 5.7: Rates of oxygen mass transfer at ambient temperature and pressure.	89
Table 5.8: Evaporation rates of ammonia in stirred tank reactor system.....	89
Table 5.9: Evaporation rates of ammonia in the column system.....	90

List of Pictures

Picture 2.1: Chalcopyrite	9
Picture 2.2: Pentlandite	9
Picture 2.3: Typical tank leaching operation.	37
Picture 2.4: Typical pressure leaching	38
Picture 3.1: Fritsch sample divider	41
Picture 3.2: Rotary micro riffler	41
Picture 3.3: Shake flask experiment	42
Picture 3.4: Columns and schematic diagram of the heap leach process	43
Picture 3.5: Support rock coated with slurry	44
Picture 3.6: Support rock coated with slurry	44
Picture 3.7: Tank leaching experiment – Applikon® reactor	45
Picture 3.8: NOVA 60 spectroquant.	47

ACRONYMS

List of abbreviations

AAS	Atomic Absorption Spectroscopy
BMS	Base Metal Sulphides
CESL	Cominco Engineering Services Limited
DRC	Democratic Republic of Congo
ICP	Inductively Coupled Plasma
NIOSH	National Institute for Occupational Safety and Health
PGE	Platinum Group Element
PGMs	Platinum group minerals
UG 2	Upper Ground 2
USA	United States of America

List of elements and compounds

CO_3^{2-}	Carbonate
CN^-	Cyanide
Co	Cobalt
Cr	Chromium
Cu	Copper
CuFeS_2	Chalcopyrite
$\text{Cu}(\text{NH}_3)_n^+$, $\text{Cu}(\text{NH}_3)_m^{2+}$	Cupra-ammine, where n ranges from 1 to 2 and m from 1 to 4
CuS	Covellite
Cu_2S	Chalcocite
Fe	Iron
$(\text{Fe},\text{Ni})_9\text{S}_8$	Pentlandite
$\text{Fe}(\text{OH})_3$	Iron hydroxide
FeS	Pyrite or Iron Sulphide
$\text{Fe}_{(1-x)}\text{S}$	Pyrrhotite
H	Hydrogen
H_2O	Water
H_2SO_4	Sulphuric acid
Mg	Magnesium

N	Nitrogen
NH ₃	Ammonia
(NH ₄) ₂ CO ₃	Ammonium carbonate
NH ₄ Cl	Ammonium chloride
NH ₄ OH	Ammonium hydroxide
NH ₂ SO ₃ ⁻	Sulphamate
(NH ₄) ₂ SO ₄	Ammonium sulphate
Ni	Nickel
Ni(NH ₃) _q ²⁺	Nickel ammine, where q ranges 1 to 6
NiSO ₄	Nickel sulphate
Ni ₂ S ₃	Nickel sulphide
OH ⁻	Hydroxide
O ₂	Oxygen
Pd	Palladium
Pt	Platinum
Rb	Rubidium
Rh	Rhodium
Ru	Ruthenium
S	Sulphur
S ₂ O ₃ ²⁻	Thiosulphate
S ₃ O ₆ ²⁻	Thionate
S ₄ O ₆ ²⁻	Polythiomate

List of symbols

A	Pre-exponential factor
C	Concentration of reactants
c*	Equilibrium concentration
c _b	Bulk concentration of oxygen in solution
E _a	Activation energy
E _H	Oxidation potential
k	Rate of reaction (min ⁻¹)
k	Partition coefficient

k_a	Solubility product
$k_L a$	Oxygen liquid mass transfer where k_L is the mass transfer coefficient and “a” is the specific gas-liquid interfacial area
k_r	Surface reaction model apparent rate constant (s^{-1})
k_m	Mixed model apparent rate constant (s^{-1})
n	Reaction order
P_g	Power input by the impeller (W)
R	Universal gas constant (8.314 J/mol/K)
r_{O_2}	Rate of oxygen supplied or consumed
T	Temperature ($^{\circ}C$ or K)
V	Volume (m^3)
V_s	Superficial gas velocity (ms^{-1})
X	Fraction of reacted particle

1.0 INTRODUCTION

1.1 Background information

Most of the world's supply of platinum and palladium and the associated base elements such as copper (Cu) and nickel (Ni) are obtained from mines within four major layered igneous intrusions. These are the Bushveld Complex in South Africa, the Stillwater Complex in the U.S.A., the Great Dyke in Zimbabwe, and the Noril'sk Complexes in Russia (Gruenewaldt et al., 1985). The South African PGM industry is dominated by three major players, namely Anglo-Platinum, Impala Platinum and Lonmin, all of which are fully vertically integrated and produce pure PGMs. After the Merensky and Upper Ground (UG) 2 reefs, the Platreef is the third most significant platinum group element (PGE) containing ore type in the Bushveld Complex. The Platreef is a 10 to 400 m thick pyroxenitic unit at the base of the Northern limb of the mafic Bushveld Complex. Merensky reef ores are the easiest to treat, followed by UG 2 and then Platreef ores with lower average PGE grades.

Traditionally, the extraction of platinum group minerals (PGMs) can be broken down into four parts namely: mining, processing, smelting and refining. The processing of Platreef ores poses a number of challenges due to the nature of the mineralogy and the subsequent smelting requirements. The mining operations on the three reefs utilise froth flotation for recovery of value minerals to concentrates. The fine grain sized Platreef ore and its PGM association primarily with bismuth and antimony affect the floatability, resulting in low efficiencies. Low-grade concentrates, associated with high pyrrhotite dilution are produced. This leads to high smelting costs, smelter integrity risks and/or large environmental impact as large quantities of iron sulphide (FeS) are converted to Fe slag and sulphur dioxide (SO₂) gas. The platinum to palladium (Pt:Pd) ratio of the Platreef ore is approximately 1:1 which is low compared to 2.33 and 1.21 for the Merensky and UG 2, respectively (Cawthorn, 1999). The lower average ratios result in high volumes of ore and high mass pulls to get relatively low-grade concentrates.

Mwase et al. (2012) established that a two-stage process, involving preliminary treatment of base metals (using acid heap bioleaching), followed by a secondary treatment of the PGMs (cyanide leaching) yielded reasonable extraction of the valuable minerals from the Platreef concentrates. Mwase et al. (2012) observed that the precious metals became more amenable

to cyanide leaching after a pre-leaching stage to remove the base metals. However, acid bioleaching in heaps would require multiple stages of caustic washing to remove residual acid which could otherwise potentially form hydrogen cyanide (which would constitute a significant health risk) in the cyanide leaching stage. Mwase et al. (2012) obtained extractions of 52% copper and 95% nickel in four weeks. In the acid heap bioleaching stage thermophilic microorganisms (operating at a temperature of 65 °C) are used to extract base metals from the concentrate material. Iron oxidising bacteria catalyse the oxidation of sulphur compounds to elemental sulphur and sulphur oxidising bacteria catalyses oxidation of the sulphur to produce sulphuric acid. This enhances the acidic environment for the process to take place and aids mineral dissolution. However, the process is sensitive to variations in temperature and air supply, and also to the presence of certain metals toxic to the microorganisms. The present project proposes an alkaline ammoniacal leach pre-treatment stage which eradicates the need for thorough caustic washing of the heaps, since the conditions remain in the alkaline region in both treatment processes and avoids the use of microorganisms.

Ammoniacal leaching is a hydrometallurgical process that allows selective extraction of base metal sulphides from an ore by forming stable metal-ammine complexes, whilst being inert to iron and acid consuming gangue. The leaching of base metals in mildly alkaline ammonia solution is a well-established technique and finds application in the Caron and Sherritt Gordon processes for the extraction of copper, nickel and cobalt in the alkaline region (pH > 9) as these form stable soluble ammine complexes. However, these processes are operated under high temperatures and pressure and/or after pre-treatment of the ore, which is energy intensive and uneconomical for low-grade ores. The process investigated here proposes to use heap leaching environments or tank leaching of untreated low-grade concentrates under ambient conditions and mild temperatures. This process is proposed as an alternative primary treatment method for the recovery of base metal sulphides from a PGM containing concentrate that cannot be economically extracted by conventional milling, smelting and refining methods. Copper and nickel are recovered from chalcopyrite and pentlandite, respectively, prior to PGM recovery from the residue.

Literature on heap leaching with ammonia is very scant, with Dutrizac (1981) being the only definite reference which has shown success with column leaching of a chalcopyrite ore for

over 3 months, but there was no explanation given why the process would not be feasible at the commercial scale. Chuanhui et al. (2000) also studied the possibility of using ammonium salts on copper sulphides in a heap leaching environment for 7 days in a column and obtained 30% copper extraction from copper oxide ore confirming that ammoniacal leaching of heaps works. Although there are anecdotal references to cases where this has been tried industrially, especially at Escondida in the 1990s, there is to the author's knowledge, no large-scale ammonia heap leach in operation at present.

Alexander Mining, a copper, gold and silver mining company has demonstrated at pilot scale a new ammonia heap leaching process AmmLeachTM for copper oxide deposits at its Leon copper project in Argentina. The process has successfully gone through the development and feasibility study stage. AmmLeachTM, a wholly owned subsidiary, has been incorporated to develop and commercialize the ammonia leaching technology. Alexander Mining has secured a patent for its ore processing method of ammoniacal leaching in the Democratic Republic of Congo (DRC) to process copper and cobalt oxides (Balashov, 2012). No technical details are available. Prior to the DRC patent, Welham et al. (2010) obtained a patent on the method of ammonia leaching of oxide and sulphide ores of copper, zinc, nickel, uranium, lead and vanadium at ambient temperatures. The invention involves curing of the ore through the application of a curing agent, which is an oxidising agent such as hypochlorite, nitrate, chlorate, perchlorate, hydrogen peroxide, calcium peroxide, ferric and cupric etc. The cured ore is then leached at atmospheric temperature and pressure with ammonium carbonate solution. In 1975, Dixon and Madigan obtained a patent for the process of ammoniacal leaching of sulphide ores or concentrates to form soluble complex amines. The process includes the step of treating the materials suspended in ammoniacal solutions of ammonium nitrate or ammonium chloride with air or oxygen at near atmospheric temperature and pressure. To the author's knowledge no studies on the ammonia heap leaching of pentlandite or other nickel sulphides have been carried out.

Although not explicitly stated in the literature, a potential drawback of using ammonia in a heap leach operation is that it is too volatile, causing significant loss of reagent to the atmosphere and potential environmental impact around such operations. Hence tank leaching might prove a better environment where vaporised ammonia could be controlled and will be investigated as a possible alternative route for the leaching of Platreef minerals.

Literature also mentions mineral passivation as a possible problem to the ammoniacal leaching system. The formation of ferric oxides can hinder the transfer of metal ions into solution and easy access of oxygen and ammonia to the surface of sulphide (Lundstron et al., 2011; Beckstead and Miller, 1977a; Stanczyk and Rampacek, 1966; Donnay et al., 1958; Forward, 1953).

1.2 Problem statement

Alternative routes for the treatment of Platreef concentrates are being sought. A two-stage process, consisting of a heap bioleach for base metal recovery (Cu and Ni), followed by cyanidation heap leaching to target the PGMs (Pt, Pd, Ru and Rb) from the Platreef concentrates has been developed. One concern around the proposed project is the switch from the acidic bioleach environment to the alkaline needed for cyanide leaching. This may require lengthy rinsing of idle heaps, or physical re-stacking with intermediate washing of the heaps after the primary treatment stage so as to remove all the protons which would react with the CN^- ion in the second stage and result in formation of hydrogen cyanide, which is a toxic gas. Ammonia leaching as an alkaline process is being proposed as a possible alternative process for base metal extraction. This will enable the two-stage processes to remain in alkaline conditions.

1.3 Aim

This project aims to apply ammonia leaching at mild temperatures and ambient pressure and without pre-treatment of the concentrates by using heap leaching principles. It is a lab scale investigation into the technical viability of the ammoniacal leaching of Platreef low-grade concentrates. Ammonia losses during the ammoniacal leaching process have been identified as a possible technical barrier; hence quantification of ammonia losses and the possibility of a tank leaching environment were investigated as an alternative route to heap leaching of the low grade concentrates. Given that the process operates in an alkali regime, proceeds rapidly even at ambient conditions, rejects Fe and uses a cheap and readily available reagent, it could be an attractive route as an alternative to acid bioleaching, especially in the context of the proposed two-stage process.

1.4 Research questions

- ❖ Is the ammonia leaching process technically feasible for the leaching of Platreef flotation concentrates as a pre-treatment method to extract base metals, copper and nickel prior to PGM recovery?
- ❖ What pH, ammonia concentration and temperature enable optimum Ni and Cu extraction?
- ❖ Are the ammonia losses experienced during the leaching process significant enough to render the process unsuitable for heap leaching?
- ❖ Is tank leaching more preferable to heap leaching using an ammoniacal lixiviant?

1.5 Objective

- ❖ To carry out a preliminary laboratory scale investigation on the feasibility of ammonia leaching of Platreef minerals in different reactor settings.
- ❖ To determine the effect of varying the temperature, ammonia concentration and pH on Cu and Ni recoveries.
- ❖ To quantify the rate of ammonia losses occurring during the leaching process.
- ❖ To compare the amount of base metal extraction using heap leaching and tank leaching environments.

1.6 Outline of the research

This thesis consists of six chapters. The first chapter is the introduction section which gives an overview of the study. The second chapter is the literature review. This section reviews the mineralogy of the Platreef ore and its associated reefs, the ammonia leaching technology for the extraction of Cu and Ni, including the chemistry and thermodynamics of the leaching of chalcopyrite and pentlandite in ammoniacal lixivants and some of the commercial applications. Chapter three describes the experimental set-up and procedures and the instrumental analysis that were used in the research. In chapter four the experimental results are presented. The results section includes the results on the technical feasibility of the ammoniacal leaching process of the Platreef flotation concentrate in the laboratory, and the effects of different parameters on the process such as temperature, pulp density, ammonia concentration, etc. Chapter five is the discussion section which includes determination of the activation energy of chalcopyrite and pentlandite, modelling of the kinetic results in terms of the shrinking core model, reaction order with respect to NH_3 and discussion of the measured evaporation rates of ammonia. Chapter six is the conclusions and recommendations section.

2.0 LITERATURE REVIEW

2.1 Occurrence of base metal sulphides associated with PGMs in South Africa

Platinum group minerals (PGMs) occur in many copper-nickel ores where base metal sulphides (BMS) pentlandite, chalcopyrite, pyrrhotite and pyrite are present, particularly for reef type ore bodies. The Bushveld Complex has an estimated area of 66 000 km² (Implats, 2012). It is a two-billion year old igneous intrusion occurring in the northern part of South Africa, unique in the range and economic significance of its contained mineral wealth. The Bushveld Complex hosts layers rich in PGMs, chromite, nickel, copper, cobalt, vanadium, iron and gold. The precious metals are recovered as the main products and the base metals as by-products of platinum mining. The Bushveld Complex consists of three PGM bearing horizons, the Platreef, Merensky and UG 2 reefs. Three main categories of mode of occurrence of PGMs were identified: PGMs associated with BMS; PGMs associated with chromite or other oxides and PGMs enclosed in silicates.

Table 2.1 presents a summary of some of the characteristics of the PGM ore types mined in the Bushveld complexes.

Table 2.1: Characteristics of Bushveld PGM Ore Types (Adapted from Newell (2008a))

Characteristic	Merensky Reef	Platreef	UG 2 Reef
Thickness (m)	0.9 – 1.2	3 – 90	0.45 – 0.65
PGM (g/t)	5 – 9	3-4	6-7
Grade: Ni	0.13	0.36	0.07
Cu	0.08	0.18	0.018
Gangue minerals	50-80% pyroxene 20-40% plagioclase 3-5% chromite 0.5-5% talc	80-90% pyroxene 10-20% plagioclase 3-5% chromite 0.5-3% talc	60-90% chromite 5-25% pyroxene 5-15% plagioclase 1-5% talc
PGM grain size	20-150 microns	40-200 microns	3-10 microns
Main PGMs	30-40% Cooperite(PtS) + Braggite (Pt, Pd)S, 3% Au/Ag 10-30% Kotuldkite (PdTe) + Michenerite (PdBiTe) 10-15% Ru phases 5-8% Sperrylite (PtAs ₂) 3-6% Isoferroplatinum (Pt ₃ Fe)	Moncheite [(Pt,Pd)(Bi,Te) ₂ -PtTe ₂] + Merenskyite [(Pd,Pt)(Bi,Te) ₂ - PdTe ₂]>>Sperrylite (PtAs ₂)>Isoferroplatinum (Pt ₃ Fe)>Braggite (Pt,Pd)S	Cooperite(PtS)>Laurite (RuS ₂) > Braggite (Pt,Pd)S> Malanite (CuPt _{1.5} Ir _{0.5} As ₄) > Isoferroplatinum (Pt ₃ Fe) > Sperrylite(PtAs ₂)

2.1.1 Platreef

Kinnaird et al. (2005) defined the Platreef as “the lithologically variable unit dominated by pyroxenite which is irregularly mineralized with PGE, Cu and Ni, between the Transvaal meta-sedimentary footwall and Archaean basement of the overlying main zone gabbro-norite”. The Platreef is a contaminated, frequently xenolith-rich unit that is geologically more complex than any of the PGE reefs, but which is also thicker and carries sufficiently consistent grade to allow large-scale open-pit mining along some areas of its strike (Kinnaird and Nex, 2003; Bye, 2001; Viljoen and Schurmann, 1998). The complex altered ores require innovative design to process them (Vermaak et al., 2007). PGM floatability of the Platreef ore is affected by PGE bismuths, tellurides and arsenides which are more abundant compared with sulphides contributing to the low PGE recoveries (Shamaila and O'Connor, 2008; Shackleton et al., 2007; Vermaak et al., 2007). The Platreef is not well-developed and the base metal sulphide and PGE mineralisations are erratic. The PGM assemblage tends to be associated with BMS along grain boundaries and enclosed in silicate (Lindsay, 1988; Kinloch, 1982).

2.1.2 Merensky reef

In the Merensky reef the major base metal sulphides are pyrrhotite, pentlandite, chalcopyrite and pyrite (Kingston and El-Dousky, 1982; Schweltnus et al., 1976; Vermaak and Hendricks, 1976). These occur interstitially between cumulus and intercumulus silicates (orthopyroxene and plagioclase respectively). The PGMs are normally found in association with the sulphides as inclusions or along sulphide/silicate grain boundaries. They also occur, to some extent, as inclusions in silicate and in close association with chromite. The dominant PGMs are cooperite and braggite with subordinate amounts of sperrylite, Pt-Pd tellurides, laurite and Pt-Fe alloy (Lindsay, 1988).

2.1.3 Upper Ground (UG) 2

The UG 2 ore is a platinum-bearing chromite-rich ore that contributes a growing proportion of PGM production from the Bushveld Igneous Complex, and contains two major gangue phases, chromite and pyroxene, which are significantly different in chemical and physical properties, posing certain problems and challenges. The PGMs and base metal sulphides occur interstitially (Lindsay, 1988) along chromite grain boundaries and locked in chromites. Penberthy et al. (2000) discovered that the PGM assemblage of the UG 2 consists mainly of

PGE-sulphides (predominantly cooperite, braggite, malanite and laurite) as well as a significant proportion of alloys and various tellurides.

2.2 Traditional method of processing PGM bearing minerals

The processing of PGMs generally comprises several steps, the major steps being comminution (crushing and grinding), concentration of ore by physical techniques such as flotation and gravity concentration, pyrometallurgical concentration, which involves smelting and converting to produce a PGM-rich Ni-Cu sulphide matte. The smelting process is based on two stages, the first stage producing a furnace matte followed by a converting stage which produces a matte for the refining stages. The first stage is concerned with gangue material removal (oxide and silicate) by using high temperatures to melt the PGM rich concentrates. Concentrates are dried in either flash/spray driers and pneumatically fed into an electric furnace. Smelting typically takes place at 1 350 °C although up to 1 600 °C for ores with higher Cr and Mg oxide content. Matte is tapped at one end of the furnace at 1 200 °C while slag is removed from the other end at 1 350 °C (Newell, 2008b). Traditional methods are energy-intensive and not economical when the ore is low-grade. Electrical energy accounts for about 40% of the direct smelting costs.

The second smelting stage is a converting process that produces a Ni-Cu matte containing all the PGMs. Nearly all the iron and most of the S (primarily FeS) are removed by oxidation and fluxes such as Si are added to form an Fe-rich slag that is skimmed off and returned to the primary furnaces. Some producers recover the entrained PGMs contained in the converter slag by milling and flotation by means of a sulphuric acid process. A Peirce-Smith converter vessel is employed, operating at 1 250 °C with oxygen injection. The off-gas is collected to produce sulphuric acid, which is used in the refining stage. One producer replaced the Peirce-Smith vessels with an Ausmelt furnace which allows continuous production. The converter matte is then sent for refining where the first stage removes the base metals (Newell, 2008b).

Base metals are a valuable by-product of PGM extraction, particularly nickel. Base metal refining begins with their removal from the converter matte, which generally employs conventional hydrometallurgy consisting of a combination of atmospheric and pressure leaching with sulphuric acid. The base metals are separated by solvent extraction and subsequently electrowon to produce cathode grade Ni and Cu, while Co is generated as a

sulphate. Some producers use the Sherritt-Gordon ammonium leach technology which produces NiSO_4 and cathode Cu as final products. Anglo America employs slow cooling over 5 days of the converter matte to promote the growth of coarse crystals of Ni_2S_3 and Cu_2S , which are parted by magnetic separation, which simplifies the base metal refining process and reduces the hold-up time of PGMs (Newell, 2008b). At Anglo and Impala Platinum (Lamya, 2007) the BMs are extracted first and then the residues are processed to recover PGMs, whilst other producers have PGM leaching before the BM refinery.

2.3 Properties of chalcopyrite



Picture 2.1: Chalcopyrite (source: Nevada-outback-gems.com/chalcopyrite (2012))

Chalcopyrite (CuFeS_2) has a molecular mass of 183.53 g/mol. It is the most abundant and main copper mineral, mined primarily for the production of copper. It has a brassy - golden yellow colour. Its density is between 4.1 and 4.3 g/cm³. Pure chalcopyrite consists of approximately 30.43% Fe, 34.63% Cu and 34.94% S by mass. It has a metallic lustre. It reacts with ammonia to precipitate red iron hydroxide and leaves a blue solution.

2.4 Properties of pentlandite



Picture 2.2: Pentlandite (source: www.galleries.com/pentlandite (2013))

Pentlandite ($\text{Fe,Ni}_9\text{S}_8$) has a molecular mass of 771.94 g/mol and is the principal ore of nickel and a minor ore of iron (usually has Ni:Fe ratio of 1:1). Pure pentlandite consists of approximately 32.56% Fe, 34.21% Ni and 33.23% S by mass. It's soluble in ammonia and gives a violet-blue colour. It has a density which ranges between 4.6 and 5.0 g/cm³. It has a brassy-bronze yellow colour. Pentlandite has a metallic lustre and is magnetic on heating.

2.5 Leaching reagents for copper and nickel sulphides

Many different solvents have been introduced and investigated over the years for copper and nickel sulphide leaching purposes. Table 2.2 outlines the classification of leaching reagents with reference to copper and nickel sulphides. Considering that an alkaline environment is being sought, ammoniacal leaching is currently the only available option.

Table 2.2: Classification of leaching reagents (Adapted from Gupta and Mukherjee (1990))

Category	Reagent	Examples
Acids and acidic salts	Concentrated Sulphuric acid	Copper sulphide concentrates, laterites, copper oxide ores, ores containing secondary copper sulphides
	Nitric acid	Sulphides of Cu, Ni and Mo, Mo scrap, uranium concentrates, zirconium oxide
	Hydrochloric acid	Illemenite, nickel matte, reduced cassiterite
	Ferric chloride/sulphate	Base metal sulphide concentrates
	Cupric chloride	Base metal sulphide concentrates
Alkalis	Ammonium hydroxide plus air	Nickel sulphide, copper sulphide, reduced laterite
Aqueous chlorine	Aqueous chlorine, hypochlorous acid	Sulphide concentrates of Cu, Ni, Zn, Pb

2.6 Common ways to extract Cu from chalcopyrite and Ni from pentlandite

There are many chalcopyrite and pentlandite hydrometallurgy methods that have been studied over the years. These include bioleaching, sulphuric acid, nitric acid, chloride and pressure leaching. Bioleaching is the extraction of a metal from sulphide ores or concentrates using microorganisms e.g. *Acidithiobacillus ferrooxidans*. The GEOCOAT™ process was developed by GeoBiotics of Lakewood Colorado for heap bioleaching of minerals. It involves the coating of concentrates onto a suitable substrate, usually barren rock, then stacking the coated material in a conventional heap fashion. Bioleaching is environmentally acceptable but the kinetics are slow and the process is sensitive to variations in temperature and air supply, and also to the presence of certain metals toxic to the micro-organisms, and the process does not recover the precious metals in the ore. Modern bioleaching technologies include the BioCop™ process, the BacTech/Mintek process and the BRISA (Dresher, 2004). Chalcopyrite and pentlandite can be dissolved in strong sulphuric acid (Prater et al., 1970), by conversion of sulphides to sulphates and copper, and nickel sulphate is subsequently leached.

Though sulphuric acid is a cheap reagent, it dissolves large amounts of iron and this is not economically viable as it increases reagent costs (Swinkels and Berezowsky, 1978). Nitric acid is a good lixiviant for the extraction of copper and nickel from chalcopyrite and pentlandite, respectively, because of its powerful oxidizing effect (Roman and Benner, 1973). This concept was modified by Kennecott Copper Corporation and is reported by Davies et al. (1978), to be competitive among the hydrometallurgical processes. The U.S. Bureau of Mines' Reno Metallurgical Centre in 1969 (Haver and Wong, 1971), and Cyprus Metallurgical Process Corporation developed the ferric chloride leaching process (Kruesi et al., 1973), which produces copper powder. The chloride based system is considered very corrosive due to the properties of ferric chloride.

The HydroCopper[®] process patented by Hyvarinen and Hamalainen (1999) was developed by Outokumpu (2005) to produce high-quality copper wire rods in a chloride environment. Outokumpu built their first plant in Erdenet, Mongolia in 2006. Chloride leaching is being developed by Intec Limited in Sydney supported by a consortium of companies (Moyes, 2002; Moyes et al., 1999). Several acid sulphate pressure leach processes were developed for chalcopyrite concentrates. These include pressure leaching at two general regimes: 150 °C (partial oxidation regime) and 220 °C (total oxidation regime). Three significant pressure oxidation leach processes are CESL process (Defreyne et al., 2004; Jones, 1973), Dynatec process (Collins and Kofluk, 1998) and the total pressure oxidation process (King et al., 1994).

2.7 Ammoniacal leaching process

Ammoniacal leaching involves selective dissolution of valuable metals of an ore, using an ammoniacal lixiviant to form stable metal-ammine complexes, $M(NH_3)_x^{2+}$ where x is a number from 1 to 6 and M is the metal (Bjerrum et al., 1841; Mellor, 1928).



The ammonia ligand consists of nitrogen (N) which has a free electron pair that associates with positive charges and displaces water molecules from the inner-sphere complex of the cation. The nitrogen atom, being the donor atom, will complex to varying degrees with a fairly large range of metals, particularly those that are divalent, e.g. Cu^{2+} and Ni^{2+} . The stabilities of these ions depend on the concentration of metal ions in solution, amount of

ammonia and the types of anions present. Only traces of ferrous compounds and very small amounts of magnesium are stable in alkali ammoniacal solutions. The ammoniacal ferrous compounds quickly oxidise, whereby ferric hydroxide is precipitated (Caron, 1950). Sheng-Li et al. (2010) obtained similar results, noting that ferric ammine is not stable as it precipitates as $\text{Fe}(\text{OH})_3$ in the presence of oxygen.

2.7.1 Advantages of ammoniacal leaching

The ammoniacal leaching process is attractive because it operates at high pH (alkaline conditions), selectively dissolving copper and nickel, whilst the major wasteful components, such as iron, calcium, acid consuming minerals and other undesirable associations, remain largely insoluble. This reduces reagent consumption and costs. There are no serious equipment corrosion problems, as ammonia is generally not an aggressive reagent. Hence, leaching can be carried out under more extreme conditions, such as relatively high reagent concentration, elevated temperatures and pressure to achieve acceptable reaction rates (Gupta and Mukherjee, 1990). Ammonia leaching is also advantageous in that ammonia and the ammonium ion constitute a pH buffer system (Meng and Han, 1996) which assists in maintaining a more stable pH range. The rate of reaction in an ammoniacal heap leaching environment was found to be comparable to that of a conventional ferric sulphate-sulphuric acid system, but without the attendant problems of carbonate gangue or iron dissolution (Dutrillac, 1981). Ammonia can easily be regenerated by evaporation because ammonia is highly volatile with a vapour pressure of 890 kPa at 20 °C (Meng and Han, 1996).

2.8 Applications of ammonia leaching technology

Ammonia leaching is a proven technology and has been used commercially for the recovery of copper and nickel from sulphides, oxides, laterites, etc., using methods that require one or more of multiple leaching stages, with the need for conventional energy-intensive physical pre-treatments such as roasting and grinding, and/or elevated temperatures and pressures. These requirements would not be cost effective for extraction of low grade ores, hence the need to explore the process on a heap at near ambient conditions. Some of the ammonia leaching applications are outlined on the next page.

1. Kennecott, Alaska and Calumet and Hecla, Michigan

The earliest commercial application of the ammonia leaching technique was reported to be in use for copper extraction in 1916. Two plants were set up separately to recover copper: one by Kennecott in Alaska in March 1916 (Duggan, 1928) and another by Calumet and Hecla Mining Company in northern Michigan U.S.A in July 1916. The Calumet and Hecla mine was temporarily closed down in 1921 to 1922, during the period of the great depression in Europe (Benedict and Kenny, 1924). Kennecott produced copper oxide from copper carbonates (malachite and azurite), chalcocite and covellite, whilst Calumet and Hecla produced copper oxides from native copper using aqueous ammonia solution. Kennecott closed its Alaska mine in 1938, whilst Calumet and Hecla closed permanently in 1968 because the ore was depleted and due to a decline in copper prices.

2. Caron process

Caron (1924) invented the process of ammonia leaching of nickel ores. It is a pressure oxidative process introduced to recover nickel and cobalt from ore by drying, grinding and calcining, reductive roasting of low grade lateritic nickel oxides at 700 °C to 750 °C, followed by oxygenated-ammonia leaching. The commercial operation of this process was applied in Nicaro (Cuba) from 1944 to 1947. Yabulu, Australia in 1974, and Punta Gorda, Cuba, in 1986, adopted the process and are still operational today, whilst another operation at Marinduque (Philippines) has since closed (Fittock, 1992; Canterford, 1975).

3. Sherritt Gordon process

Sherritt's nickel refinery at Fort Saskatchewan in Alberta, Canada was commissioned in 1954 to extract nickel, copper and cobalt from sulphide ores and flotation concentrates using autoclaves at temperatures below the boiling point (~85 °C) and high pressures presumably to contain NH₃ evaporation (~928.7 kPa gauge pressure) in the presence of oxygen. Agitation was used to dissolve the oxygen, transport the oxygen in solution and remove products from mineral surface (Forward and Mackiew, 1955). To ensure maximum extraction of metals, the ammonia content of the leach solution is maintained between 3 M and 4 M of unbound ammonia, which is the highest value compatible with efficient operation (Forward, 1953). This plant is still operational today at much higher throughputs. Other plants which operate this process include Western Mining Corporation (Australia) and Impala Platinum Limited, Springs (South Africa).

4. Arbiter process

Anaconda's Arbiter plant situated in Montana was commissioned in 1974 and shut down in 1977. On November the 24th of 1977, Cox Anaconda's spokesman announced that "the market conditions were unfavourable for the Arbiter plant to continue operating and that the company's shortage of sufficient feedstock for capacity operations were the prime reasons for the decision to close it down". The process was based on ammoniacal pressure oxidative leaching in a reaction vessel to extract copper from copper concentrate containing chalcocite, covellite, bornite, native copper and/or precipitated copper concentrate and chalcopyrite from the smelter (Kuhn et al., 1974). The Arbiter process applied intense agitation to abrade the resulting iron oxide from the surface and expose fresh surface for reaction as well as to provide good transport of oxygen. The concentrate was fed in slurry form to a specially designed ammonia leaching reactor operated at 60 °C to 90 °C. They incorporated a high speed impeller (2 500 rpm) and a gauge pressure of 710 kPa.

5. Inco of Copper Cliff, Canada

Another successful process using ammonia was adopted in the 1950s by INCO of Copper Cliff, Ontario, Canada, to extract nickel, cobalt and copper from a low grade pentlandite-pyrrhotite flotation concentrate. The process includes oxidation roasting of the sulphide concentrates, followed by quenching of the calcine under reducing conditions and finally leaching in ammonia-ammonium carbonate solution (Chase, 1980). The plant was shut down a few years later because it was uneconomical and because of the pollution problems associated with the large tonnages of SO₂.

6. Escondida process

The Escondida process is a BHP Billiton process used at the Colosso plant (Antofagasta, Chile) between 1994 and 1998. The process was conducted under controlled oxidation potential to give only partial dissolution of copper in ammonia, in which chalcocite is converted to covellite giving about 40% to 50% leaching recovery. In the partial leaching process, sulphur is not oxidised to sulphate, hence, no production of by-product ammonium sulphate. This is an advantage because it saves on ammonia reagent costs. Copper in leach residue is recovered by flotation followed by smelting (Duyvesteyn and Sabacky, 1993), whereas the dissolved copper from the resulting leach liquor is recovered by solvent extraction and electrowinning.

7. AmmLeach process

The AmmLeach process is a recent technology that involves heap leaching of copper oxides. According to the patent by Welham et al. (2010), after appropriate size reduction, the ore is transported to the heap on a conveyor belt. Whilst on the belt the ore is sprayed with a solution containing 4 M NH_3 and 0.36 M sodium hypochlorite with the aim of infiltrating ~80% of the particle pore volume with the solution. The purpose of the hypochlorite is to oxidise the sulphide minerals if present (curing). The ore is constructed into a heap and the heap is left to rest for ~13 days to allow the curing solution to work. This makes the ore more amenable to ammonia leaching. Once the heap has rested, the heap is irrigated sequentially with recirculated ammonia solutions of ammonium chloride or nitrate, the raffinate and finally water. The process has been successful on pilot scale and Alexander Mining plc. intends to commercialise it.

2.9 Types of reagents used as ammoniacal lixiviants

Ammoniacal lixiviants are solutions of ammonia and an ammonium salt used to leach metals such Cu and Ni. The ammonium salt acts as a buffer. There are three types of ammonium salts commonly used for ammonia leaching, which are ammonium carbonate, chloride and sulphate. These reagents and their properties are outlined in Table 2.3.

Table 2.3: Properties of ammonia and ammonium salts

Reagents	Properties
Ammonia NH_3	Ammonia is a colourless, flammable gas with a penetrating and pungent odour. It has a molar mass of 17, a boiling point of -33.40°C , melting point of -77.70°C and specific gravity of 0.77. NH_3 is soluble in water, alcohol, etc. It is a good solvent for organic molecules (Myers, 2007).
Ammonium Carbonate $(\text{NH}_4)_2\text{CO}_3$	It is a white powder at room temperature, but chemical treatment can result in its breakdown, releasing NH_3 and CO_2 . It has a molar mass of 96.09 g/mol, a density of 1.50 g/cm^3 and a melting point of 58°C (Haynes et al., 2010).
Ammonium Sulphate $(\text{NH}_4)_2\text{SO}_4$	It has a molar mass of 132.14 g/mol. It has a density of 1.77 g/cm^3 at 20°C . The melting point is between 235 and 280°C . It's soluble in water. Its solution is acidic; pH of 0.1 M solution is 5.5 (Haynes et al., 2010).
Ammonium Chloride NH_4Cl	It has a molar mass of 53.49 g/mol. It's highly soluble in water. Solutions are mildly acidic. It reacts with a strong base to release ammonia gas. It has a specific gravity of 1.53 (Bothara, 2008; Wiberg and Holleman, 2001).

2.10 Feasibility studies on the ammoniacal leaching process

2.10.1 Copper dissolution studies

Several researchers have investigated the ammoniacal leaching process of copper dissolution, under different experimental conditions. Yamasaki (1920) investigated the rate of dissolution of metallic copper using ammonium hydroxide solutions, and his results show dissolution of copper. Lu and Graydon (1955), Halpern (1953) and Lane and McDonald (1946) also noted that copper dissolution of metallic copper occurred in ammoniacal solutions. Stanczyk and Rampacek (1966) studied the dissolution behaviour of different copper sulphides in ammoniacal medium. They established that chalcocite, covellite and bornite readily dissolved at lower temperatures in comparison to chalcopyrite and attributed the formation of hematite in chalcopyrite leaching. Habashi (1963) studied the dissolution of metallic copper in aqueous solutions of ammonia. His results showed that a corrosion process occurred in which the anodic reaction is the reduction reaction of oxygen and the cathodic reaction is the oxidation of copper. Nicol (1975) investigated the electrochemical dissolution of metallic copper and nickel and copper-nickel alloys in ammonium carbonate solutions. He found that the rate of copper and nickel oxidation was controlled by diffusion of oxygen to the surface. Dutrizac (1981) demonstrated the general feasibility of percolation leaching of chalcopyrite using an oxygenated ammoniacal medium. The process has been proved to work, though passivation of chalcopyrite was shown to be a limitation. Bell et al. (1995) also investigated the ammonia leaching process in in-situ leaching, and found significant copper recoveries (~94%) from chalcopyrite concentrates using pressure and temperature as high as 6 900 kPa and 100 °C, respectively, to mimic deep underground conditions. The high temperatures and pressures that were considered in this study are unlikely to be feasible in a real world process.

2.10.2 Nickel dissolution studies

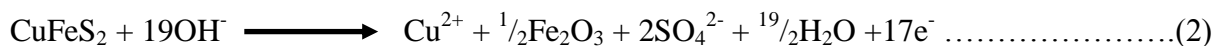
Caron (1924) received a U.S. patent after inventing the process of pre-roasting of sulphide ores and recovering nickel and cobalt (and copper if present) directly from the oxide ore produced, using ammoniacal solutions of ammonium carbonate. This process is still operational and known as the Caron process. The oxidising-ammonia leaching process for nickel sulphide concentrate pioneered by Forward (1953) has been used by Sherritt Gordon mines at Fort Saskatchewan (Canada) and by Impala Platinum Ltd. in Springs (South Africa). The nickel sulphide solution (after copper removal) is leached under high pressure of approximately 928 kPa and temperature of 85 °C in autoclaves at a relatively low speed of 150 rpm with oxygenated ammoniacal solutions of ammonium sulphate. The process allows

nickel recoveries greater than 80%. The ammonia pressure leaching of metallic nickel powders with oxygen was studied by Morioka and Shimakage (1971). It was found that the dissolution of nickel powder in ammonia solution was electrochemical in nature. The diffusion of oxygen through each solution to the nickel surface was the rate determining step. Another study on the high pressure leaching of nickel metallic powder in ammonium carbonate was carried out by Mizoguchi et al. (1978). A similar leaching behaviour was observed. The dissolution of nickel powder was described in terms of a shrinking core model with a first order reaction at the solid/liquid interface. The initial rate of dissolution was a function of the oxygen concentration, mass transfer coefficient, and particle density and radius. Bhuntunkomol et al. (1980) studied the leaching behaviour of metallic nickel in oxygenated ammonia solutions using a rotating disc. Their experimental results show that the dissolution of nickel increased with time at a fixed rate. These authors found the activation energy (E_a) as 9.6 kJ/mol using temperatures between 35 °C and 65 °C which is indicative of mass transfer control. Senaputra et al. (2008) carried out a preliminary thermodynamic and kinetic study to compare the leaching behavior of Ni, NiO, NiS and Ni₃S₂ in the form of rotating discs in oxygenated ammoniacal solutions. The authors observed the effect of different anions in the presence of Cu(II) as an oxidant. The presence of Cu(II) thiosulfate accelerated the extraction of Ni from NiO and NiS₂ due to Cu(II) redox mediation and involvement of thiosulphate ions in the solution, but the presence of thiosulphate hindered the extraction of Ni from NiS and Ni₃S₂. The authors suggest that it could have resulted from passivation by NiS₂.

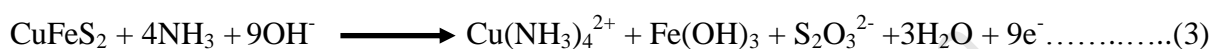
2.11 Dissolution mechanism for chalcopyrite

The leaching reaction involves an electrochemical mechanism. Chalcopyrite dissolves in oxygenated ammoniacal solution and the ammonia acts as a complexing agent and stabilises the cupric ion in the basic media as cupra-ammine complexes. Warren (1979) and Dutrizac (1981) observed that, elemental sulphur exists as a transient species, but reasons are unknown for its presence. The stable sulphur species under oxidation leaching is the sulphate anion although the reaction proceeds through the thiosulphate ($S_2O_3^{2-}$) intermediate (Forward, 1953), thionate ($S_3O_6^{2-}$), polythiomate ($S_4O_6^{2-}$) and sulphamate ($NH_2SO_3^-$). Iron is superficially dissolved or hardly dissolved by the formation of ferrous ammonium complex which quickly precipitates as hydrated ferric hydroxides in the presence of oxygen. The formation of hematite is critical and appears to influence the reaction kinetics, (Kuhn et al., 1974; Evans et al., 1964). The overall leaching reaction for chalcopyrite can be written as two

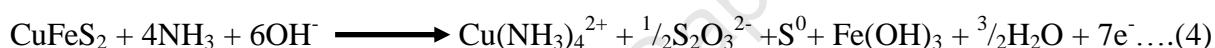
half reactions and these involve both charge transfer and chemical interaction contributions to the reactions. At the anodic site, the metal gives off electrons resulting in dissolution and formation of metal ammine complexes. The anodic reactions for the dissolution of chalcopyrite can be explained according to one model, this anodic half-cell reaction suggested by Beckstead and Miller (1977a) is:



whereas another model proposed by Warren and Wadsworth (1984) indicates the reaction as:



Neither of these two reactions account for the formation of both thiosulphate and elemental sulphur. Thus, a third model has been proposed by Reilly and Scott (1977) as:



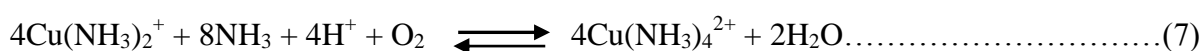
Despite the differences proposed in the anodic step, the investigators agree on the cathodic step, which is the reduction of oxygen on the mineral surface shown in equation 5. At the cathodic site, oxidants take electrons from the metal and the metal is consequently oxidised.



Beckstead and Miller (1977a) state that the cupric ion is considered to catalyse the oxygen discharge reaction and hence has the second cathodic equation as:



In 2003, Ghosh et al. found that the catalytic action of Cu(II) was attributed to the redox couple Cu(I)/Cu(II), where $\text{Cu}(\text{NH}_3)_4^{2+}$ is the oxidant and is reduced to $\text{Cu}(\text{NH}_3)_2^+$ which is subsequently oxidised by dissolved oxygen. According to Nelen and Sobol (1959) the equilibrium reaction proceeds as follows:



Cu(II) together with oxygen during ammonia leaching had a synergistic effect on the dissolution rate (Ghosh et al., 2003). To maintain maximum activity of $\text{Cu}(\text{NH}_3)_4^{2+}$, the pH must be maintained between 9 and 11. The overall reaction obtained by Beckstead and Miller (1977a) is given as:



2.12 Dissolution mechanism for pentlandite

There is no equation for ammoniacal leaching of pentlandite proposed in the literature. A general equation of nickel sulphides dissolution by Forward (1953) has been modified to give a possible pentlandite reaction pathway.



This suggests that pentlandite is leached with aqueous ammonia in the presence of oxygen, and nickel is released in the +2 state and is stabilised in the solution by formation of nickel-ammine complexes. The iron content is oxidised to form ferric oxide, whilst the sulphide component is oxidised to soluble species, predominantly sulphate.

2.13 Speciation of ammonia

Electrochemical reactions occurring in ammoniacal solutions are subject to constraints related to the speciation of ammonia. Ammonia assumes three different forms which are: free ammonia (unionised aqueous NH_3), ammonium ions (ionised NH_4^+) and metal ammines ($\text{M}(\text{NH}_3)_n^{2+}$) (Osseo-Asare et al., 1983). The stepwise formation for ammonia metal complexes was extensively investigated by Bjerrum et al. (1841). There are several speciation forms of nickel-ammines and cupra-ammines, which are stable over a wide pH range which include $\text{Cu}(\text{NH}_3)_n^+$, $\text{Cu}(\text{NH}_3)_m^{2+}$, $\text{Ni}(\text{NH}_3)_q^{2+}$, with $n = 2$ and 3 , m ranging from 1 to 4 and q ranging from 1 to 6 . The most stable species between pH 9 and 10 are $\text{Ni}(\text{NH}_3)_6^{2+}$, $\text{Cu}(\text{NH}_3)_2^+$, and $\text{Cu}(\text{NH}_3)_4^{2+}$. Although the square pyramidal $\text{Cu}(\text{NH}_3)_5^{2+}$ is known to exist at room temperature, it seems likely that the complex with four ammonia ligands, $\text{Cu}(\text{NH}_3)_4^{2+}$, is the predominant species in concentrated solutions and/or at elevated temperatures.

2.13.1 Thermochemistry

Asselin (2011) studied the stability of Fe-Ni-Co alloy systems through the use of speciation and Pourbaix diagrams. This was done at 25 °C using a total ammonia concentration of 6 M. Asselin (2011) observed that increasing the temperature reduced the stability fields of the amines. Stability regions of the amines play a central role in the selective leaching and separation of Ni and Co from sulphide and laterites. When temperature is increased from ambient to 60 °C, there is a more limited range of pH where the metallic ions are fully complexed. Ni(II) hexammine species are considerably more stable at 60 °C, pH 9 and represent over 80% of the total dissolved Ni in 6 M total ammonia and 0.1 M total nickel.

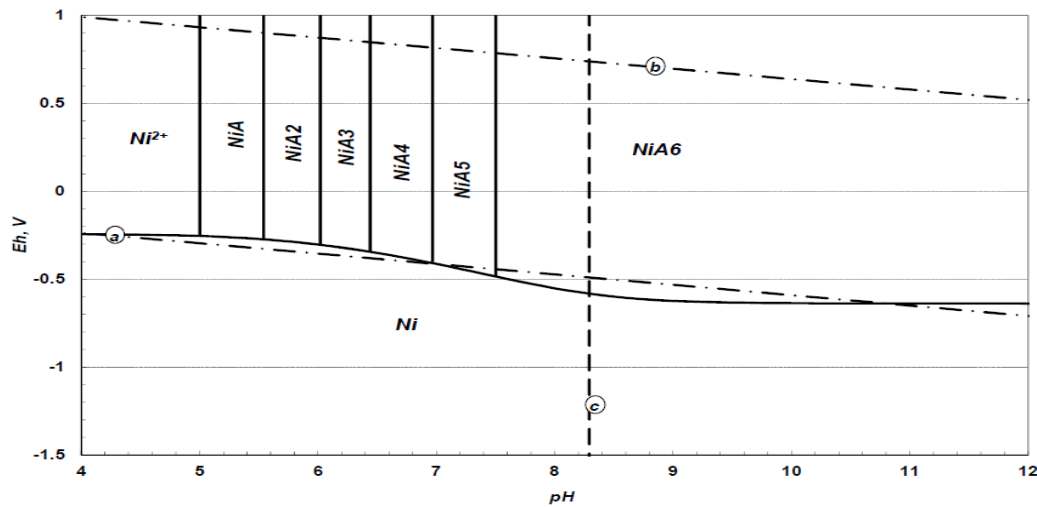


Figure 2.1: Quasi-equilibrium Pourbaix diagram for the Ni-NH₃-H₂O system at 25 °C (ambient). [Ni] = 0.1 and [NH₃]_T = 6 M. Lines a, b and c represent, respectively, the hydrogen evolution line, the oxygen reduction line and the ammonia buffer point. “NiA_n” represents the amino-nickel (II) species where “n” is the number of ammonia ligands in the complex. (Source: Asselin (2011))

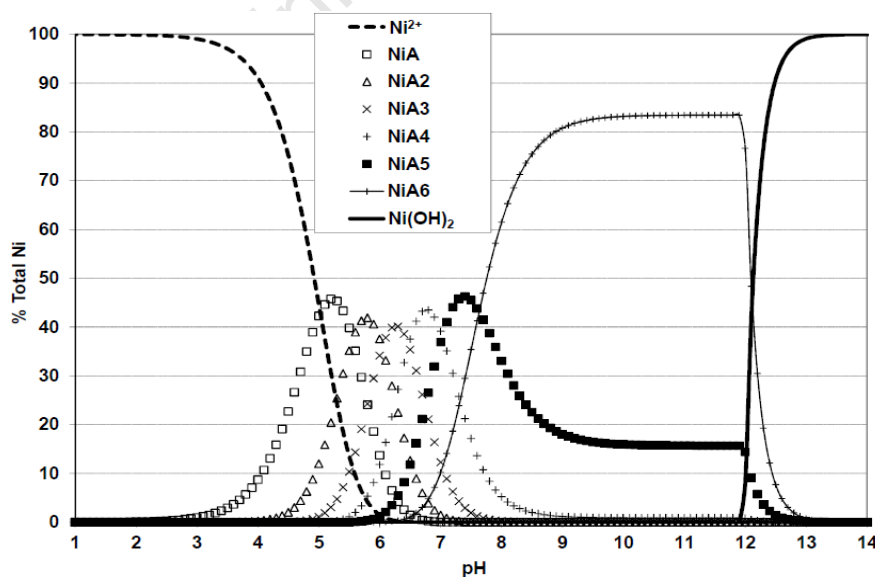


Figure 2.2: Ni(II) speciation for 0.1 M total nickel in 6 M total ammonia at 60 °C (Source: Asselin (2011))

2.14 Thermodynamics of ammoniacal leaching

The stability or instability of sulphide minerals in contact with aqueous solutions of selected composition can be summarized by means of E_H – pH diagrams. Figure 2.3 (a) defines the regions of pH and potential in which $\text{Cu}(\text{NH}_3)_4^{2+}$ and Figure 2.3 (b) $\text{Ni}(\text{NH}_3)_6^{2+}$ are stable.

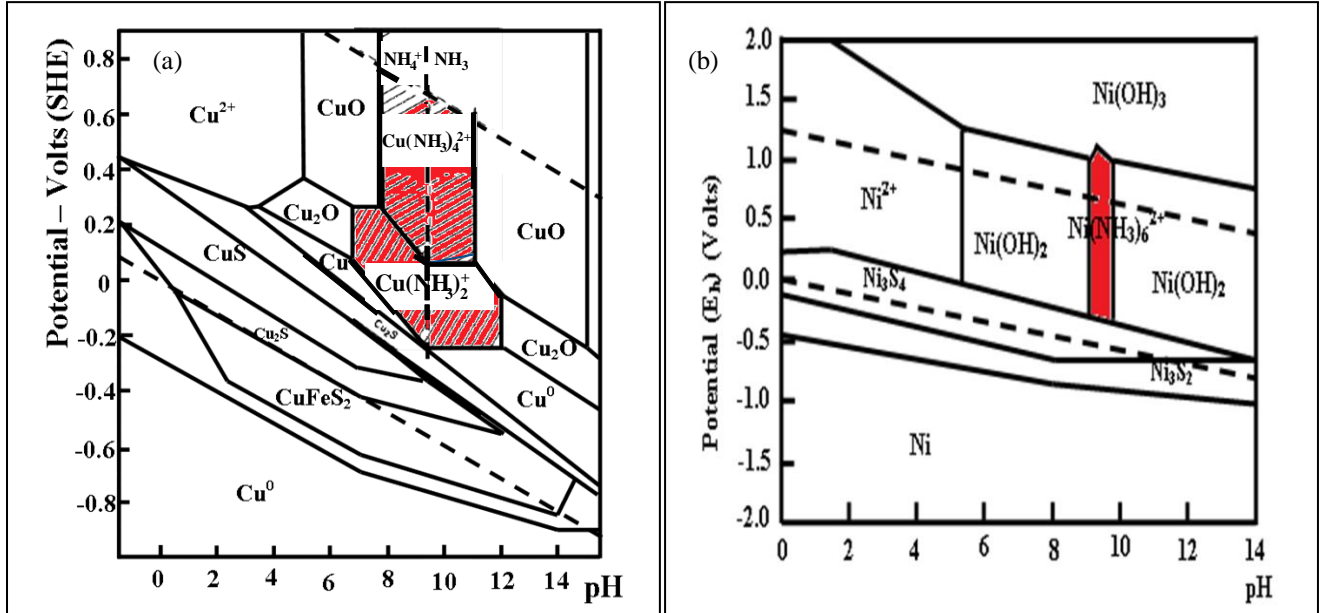


Figure 2.3 (a) and (b): E_H -pH diagram for Cu-Fe-S- NH_3 at 25 °C and 1M activity (Adapted from Peters (1976)) and E_H -pH for Ni-S- NH_3 at 25 °C at 1M activity (Adapted from Dreisinger (2000)) respectively.

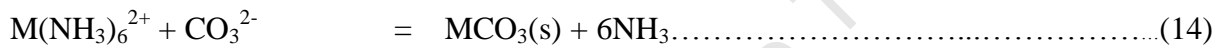
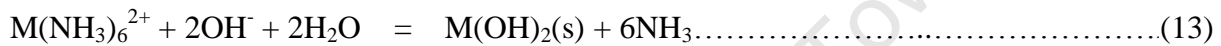
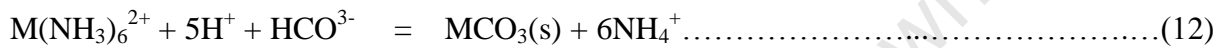
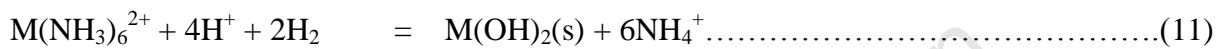
The leaching operation should be carried out under those experimental conditions which ensure maximum stability of cupra-ammine and nickel-ammine as predicted in the E_H -pH diagram. Figure 2.3 (a) shows that at pH 9, the dominant soluble copper-bearing species are $\text{Cu}(\text{NH}_3)_4^{2+}$, an oxidant, and $\text{Cu}(\text{NH}_3)_2^+$, a reductant. The ratio of these two species is dependent on the oxidation potential of the system. Meng and Han (1996) report the relationship between the potential and this ratio as:

$$E_H = 0.074 - 0.1182 \log[\text{NH}_3] + 0.0591 \log \frac{[\text{Cu}(\text{NH}_3)_4^{2+}]}{[\text{Cu}(\text{NH}_3)_2^+]} \dots\dots\dots (10)$$

where E_H is the oxidation potential.

The vertical dashed line in Figure 2.3 (a) represents the equilibrium between NH_3 and NH_4^+ . Caron (1950) and Peters (1976) reported an E_H -pH diagram for the copper-ammonia-water system which shows that $\text{Cu}(\text{NH}_3)_4^{2+}$ is stable between pH 8 and 11, and both authors used 1M activity.

Bhuntunkomol et al. (1980) reported an E_H -pH diagram for nickel-ammonia-water system with the $Ni(NH_3)_6^{2+}$ stable at a pH between 8.5 and 10.5, at 25 °C and at 1 M activity. In contrast to this, Dreisinger (2000) reports a region of stable $Ni(NH_3)_6^{2+}$ at 25 °C and 1 M activity as between pH 9 and 10 (Figure 2.3 (b)). The main thermodynamic effect of ammonia during leaching is to prevent formation of oxides and hydroxides, as these slow down the reaction between sulphide minerals and the aqueous solutions and defeat the purpose of leaching. If the pH decreases even slightly from the metal ammine stability zone, precipitation occurs and salts of metal hydroxides and carbonates form. These metal ammines can be precipitated as follows depending on the leach conditions (Osseo-Asare et al., 1983):



Equations 11 and 12 describe the metal ammine/metal hydroxide or carbonate relative stability in comparatively low pH solutions ($[NH_3] \ll [NH_4^+]$). Equations 13 and 14, on the other hand, describe the high pH ($[NH_3] \gg [NH_4^+]$) metal ammine stability limit.

In the pH range 9.2 to 9.7, as the oxidation potential is raised, the transformation of the metallic phase Fe to the oxides proceeds via aqueous ferrous ammine intermediates with low Fe concentration ($1.0 \times 10^{-4} \text{ kmolm}^{-3}$). It is the fact that Fe^{2+} forms only weak ammine complexes that permit Ni and Cu to be extracted selectively.

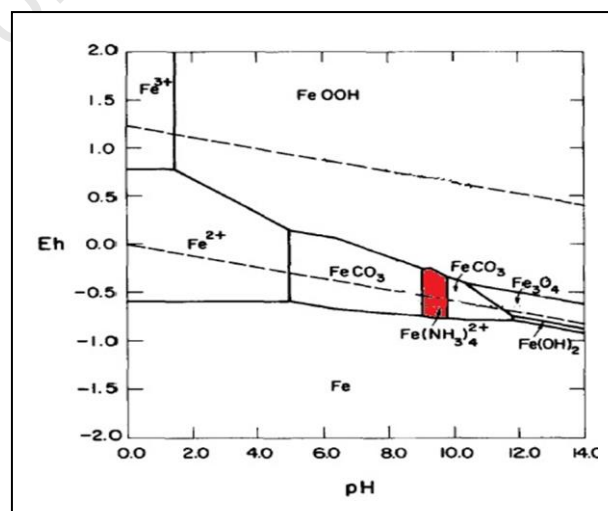


Figure 2.4: E_H – pH diagram for $Fe-NH_3-H_2O-CO_3$ at 25 °C and $[Fe] = 1.0 \times 10^{-4} \text{ kmolm}^{-3}$ (Adapted from Osseo-Asare et al. (1983))

Ferrous amines are thermodynamically stable under reducing conditions within a constrained stability window as illustrated in Figure 2.4. Iron, which is initially dissolved as a ferrous ammine complex, is quickly oxidized to the ferric state and precipitates as ferric hydroxide, eventually leaving the process in the leach residues (Das and Anand, 1995; Jandova and Pedlick, 1994). Thus, under oxidising conditions that keep nickel and copper amines in solution, iron exists as oxides.

2.14.1 Ratios of NH_3 and NH_4^+

The combination of NH_3 and NH_4^+ salts is a powerful lixiviant and the ratio of $\text{NH}_3/\text{NH}_4^+$ is significant to attain higher metal extraction rates (Tozowa et al., 1976). Addition of an ammonium salt strengthens the buffering capacity as it adds extra ammonium ions and minimises the formation of the hydroxide. According to Le Chatelier's principle, this promotes the backward reaction. The solution will therefore contain lots of unreacted ammonia for copper and nickel complexation and enough hydroxide ions to make the solution alkaline (equation 15).

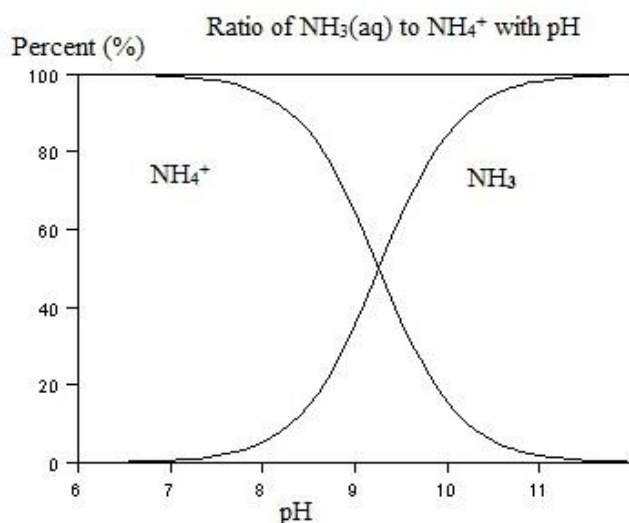


Figure 2.5: Percentage of NH_4^+ and NH_3 as a function of pH.

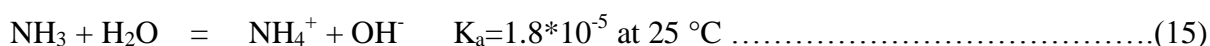


Figure 2.5 shows the ratios of the NH_4^+ ion and NH_3 , depending on the pH of the solution. The ratio will change by a factor of 10 with every unit change in pH. To obtain meaningful metal extractions, both NH_3 and NH_4^+ must be present, and such a condition minimises the tendency for the dissolved metal to precipitate out of the solution. The best leaching results are obtained when there is an equal molar proportion of NH_3 and NH_4^+ and the pH is in the

9.23 range (equilibrium conditions). NH_3 is predominant at pH above 9.23. Thus, the more alkaline the region is, the more free NH_3 molecules will be available to form metal ammines. NH_4^+ is predominant at pH below 9.23, which explains why precipitation of some metals occurs at lower pH values due to the lacking availability of NH_3 to form the soluble complexes.

Any salt containing acidic or basic ions will have pH-dependent solubilities. The ratios of the carbonates with pH are shown in Figure 2.6. In the alkaline region the HCO_3^- and CO_3^{2-} are dominant. The pK_a for this system is 10.3 at 25 °C. This improves the buffering capacity of the system.

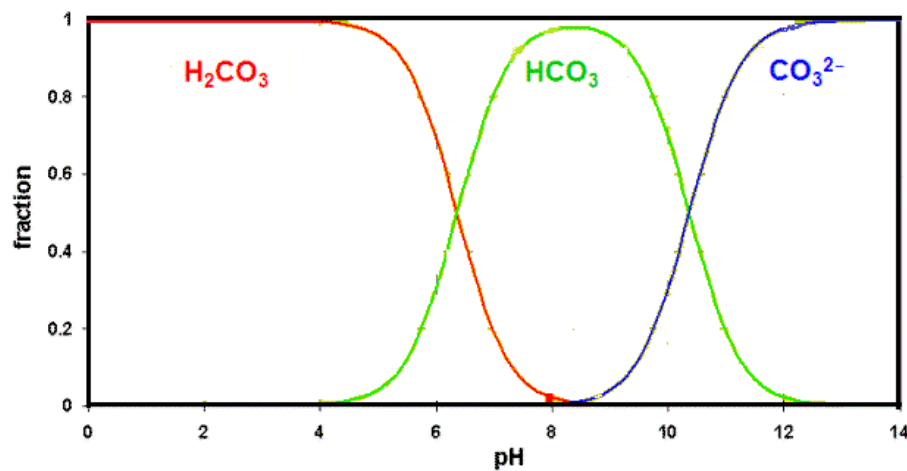


Figure 2.6: Percentage of H_2CO_3 , HCO_3^- and CO_3^{2-} as a function of pH.

Effect of the Anion

NH_4^+ salts have different buffering capacity depending on the anion present, which affects the system pH as outlined in Table 2.4

Table 2.4: Properties of aqueous solutions of NH_4^+ salts (Adapted from Kotz and Treichel (2003))

NH_4^+ salt	Acid	K_a	Base	K_b	pH of the solution
NH_4OH	NH_4^+	5.6×10^{-10}	NH_3	1.8×10^{-5}	$K_b > K_a$ basic
$(\text{NH}_4)_2\text{CO}_3$	NH_4^+	5.6×10^{-10}	CO_3^{2-}	2.1×10^{-4}	$K_b > K_a$ basic
$(\text{NH}_4)_2\text{SO}_4$	NH_4^+	5.6×10^{-10}	SO_4^{2-}	8.3×10^{-13}	$K_a > K_b$ slightly acidic
NH_4Cl	NH_4^+	5.6×10^{-10}	Cl^-	Very small	$K_a > K_b$ slightly acidic

Anions that are conjugate bases of strong acids such as Cl^- ions ($\text{pK}_a = 2.86$) and SO_4^{2-} ions ($\text{pK}_a = 1.92$) are such weak bases that they have no effect on solution pH. Hence, NH_4Cl and $(\text{NH}_4)_2\text{SO}_4$'s pH will be influenced by the NH_4^+ ion ($\text{pK}_a = 9.24$). The pK_a of CO_3^{2-} is 10.33 and is larger than the pK_a of the NH_4^+ ion, hence the solution will be basic and the $(\text{NH}_4)_2\text{CO}_3$ will be a favourable buffer in the alkaline region.

2.15 Solubility of ammonia

Solubility of ammonia with temperature

The solubility of ammonia in water decreases with increase in temperature and the dissolved or suspended materials. Solubility values at moderate temperatures are shown in Table 2.5.

Table 2.5: Solubility of ammonia in distilled water (adapted from (Jones, 1973; Windholz et al., 1976))

Temperature	Solubility in water at 101 kPa	Solubility in water at 101 kPa
0°C	895 g/l	52.6 M
20°C	529 g/l	31.1 M
40°C	316 g/l	18.6 M
60°C	168 g/l	9.9 M

Henry's law constant (K_H) for ammonia at 25 °C

The solubility of a gas in a liquid is directly proportional to the gas pressure. As the gas pressure increases, so does its solubility. This explains why ammonia leaching has been applied at high pressure, e.g. in the Sherritt-Gordon process. Henry's law describes the equilibrium distribution of volatile species between liquid and gaseous phase as:

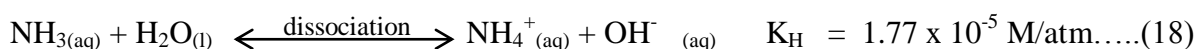
$$c_g = K_H P_g \dots\dots\dots (16)$$

where c_g is the gas solubility (M), P_g is the partial pressure of the gaseous solute (atm) and K_H is Henry's law constant (M/atm), a constant characteristic of the solute and the solvent. Henry's law describes only the equilibrium between two phases as:



*values of K_H were adapted from Robinson and Stokes (1970) and Stumm and Morgan (1996) at 25 °C

However, within the aqueous phase, partitioning of the aqueous form of a substance may occur and is accounted for using an additional equilibrium expression, such as:



This equation implies that a larger quantity of the NH_3 may actually exist within the aqueous phase at equilibrium than would be predicted by Henry's law. This can be especially significant if a dissociated species participates in an additional reaction, such as an acid-base reaction that would consume OH^- ions, and this reaction is pH-dependent (Smith and Harvey, 2007). The solubility of NH_3 gas (M) is smaller in the salt solution than in the dilute aqueous medium. Henry's law helps to predict the amount of each gas that will go into solution.

2.16 Kinetics of ammoniacal leaching of copper

Most studies have been conducted on the kinetics of leaching copper from copper sulphides and metallic copper using ammonia and oxygen (e.g. Forward, 1953; Stanczyk et al., 1966; Beckstead and Miller, 1977a; Bell et al., 1995; Rao, 2000). Yamasaki (1920) investigated the rate of dissolution of metallic copper in ammonium hydroxide by rotating copper species at constant volume and a steady current of air supply. His findings indicated that there was electrolytic dissolution of copper, and the reaction product cuprammonium compound acted as a catalyst by promoting the rate of reaction, i.e. the reaction was autocatalytic. Lu and Graydon (1955) also observed autocatalysis under air-saturated conditions. Contradictory to these findings, Halpern (1953) and Lane and McDonald (1946) found no evidence of autocatalysis, using oxygen-saturated conditions. This could have resulted due to the fact that the mechanism of the dissolution is different for the two sets of experimental conditions. When autocatalysis was observed, air was used in the reaction, but when pure oxygen was used in the system, there was no evidence of autocatalysis. Lane and McDonald (1946) investigated the reaction kinetics between metallic copper and ammonium hydroxide. They found the overall order of reaction to be zero order, but first order with respect to ammonium hydroxide concentration when using oxygenated ammonium hydroxide. Halpern (1953) investigated the kinetics of this reaction under conditions where:

- a) the chemical process itself was rate controlling,
- b) no insoluble products formed, and
- c) transport of oxygen to the copper surface was sufficiently fast that it did not influence the rate.

His findings indicate that copper readily reacts with ammonia in the presence of oxygen. Beckstead and Miller (1977b) studied the reaction kinetics of the oxidation leaching of chalcopyrite so as to determine the important chemical factors which govern the kinetic response of the system. The author found the dissolution rate in the chemically controlled

region to be limited by an electrochemical reaction at the chalcopyrite surface. Reilly and Scott (1977) studied the kinetics of chalcopyrite leaching in thoroughly aerated ammoniacal solutions. These authors found an electrochemical surface reaction model, in which the cathode reduction of oxygen on the solid surface is rate determining, satisfactorily predicts experimental behaviour in the range of experimental data. The electrochemical nature of the chemically controlled reaction has also been confirmed by Warren and Wadsworth (1978).

2.16.1 Effect of kinetic variables on rate of copper dissolution from chalcopyrite

- 1. Temperature** – As the temperature increases the rate of a reaction increases. However, high temperatures ($> 50\text{ }^{\circ}\text{C}$ - Caron (1950)) increase ammonia evaporation and promote hydrolysis. Higher temperatures also require higher ammonia and water partial pressures to maintain adequate partial pressure of oxygen. Beckstead and Miller (1977a), using a temperature range of $60\text{ }^{\circ}\text{C}$ to $105\text{ }^{\circ}\text{C}$, found that the rate of chalcopyrite dissolution in ammonia increased with increase in temperature and obtained an activation energy (E_a) of 42 kJ/mol . The author suggested that this value supported the contention that the electrochemical reaction was limited by a surface reaction mechanism. Bell et al. (1995) also found the rate to be temperature dependent, using temperatures of $20\text{ }^{\circ}\text{C}$ to $100\text{ }^{\circ}\text{C}$. The authors obtained E_a values of 31.4 kJ/mol and 37.7 kJ/mol , and suggest a surface reaction rate control. Dutrizac (1981) found the rate to increase only slightly with temperature, with an increase of 28% when temperatures were elevated from $25\text{ }^{\circ}\text{C}$ to $65\text{ }^{\circ}\text{C}$. He suggests that the very slight temperature dependence indicates that the percolation leaching reaction is likely to be under mixed control, with both the surface chemical reaction rate and the rate of oxygen transport playing significant roles. However, the author suggests that in well-aerated ammoniacal media, the chalcopyrite leaching rate increases rapidly with increasing temperature. Generally, the activation energies determined varied between 30 and 45 kJ/mol for chalcopyrite dissolution in ammoniacal solutions. The differences could have resulted from the different experimental conditions. Beckstead and Miller (1977a) used a reactor with agitation for increased mass transfer, whilst Bell et al. (1995) used a high-pressure autoclave with ideal conditions.
- 2. Ammonia concentration** – The determination of the effect of ammonia concentration is very complicated in that the ammonia reacts in four ways. Some of the ammonia is neutralised to ammonium, some is converted to sulphamate, some forms metal

ammines and some remains as unbound ammonia. Increased unbound ammonia increases the maximum extraction of the metals by a higher degree of complexation of the metal ions (Forward and Mackiew, 1955). Stanczyk and Rampacek (1966) reported that the rate of reaction increased with an increase in ammonia concentration. Reilly and Scott (1977) gave confirmatory results and noted that the leaching rate increased with increasing oxygenated ammonia concentrations using ammonia concentrations of 2.5 to 7.0 mol/L. Warren and Wadsworth (1978) reported a first order NH_3 dependence, stating that an increase in ammonia concentration increased the rate of oxidation. Dutrizac (1981) observed that the rate increased as the square root of the total ammonium concentration (0.1 to 2.0 M) but was insensitive to the ratio of NH_4OH to $(\text{NH}_4)_2\text{CO}_3$ and to a solution pH above 9.5. Beckstead and Miller, (1977a) gave somewhat contradictory information suggesting that the rate was almost independent (slightly dependent) of the ammonium hydroxide concentration using a range from 0.79 M to 4.48 M.

3. **Oxygen pressure** – Oxygen not only is an oxidising agent but also assists the ammonia complexing agent to stabilise the dissolved copper and nickel. Bjerrum et al. (1841) and Halpern (1953) observed that no copper dissolution occurred in the absence of oxygen. Bell et al. (1995) used hydrogen peroxide as an oxidant so as to provide sufficient oxidant to drive the leaching reaction. This, however, had both oxidising and reducing effects on the process. Forward (1953) showed that increased oxygen pressure accelerates the leaching action during the initial stages but has less effect as the reaction proceeds. The author also observed that variation in oxygen pressure has no effect on the ultimate extraction of nickel or copper. Beckstead and Miller (1977a) showed that below an oxygen pressure of approximately 1.25 atm, an empirical reaction order of one-half was determined with respect to oxygen pressure. Above oxygen pressures of 1.25 atm, the rate of reaction was relatively insensitive to oxygen pressure. These results were explained by an adsorption process which resulted in surface saturation with oxygen at higher pressures. Dutrizac (1981) and Chen (2009) observed that the amount of oxygen in the leaching medium is of minor importance and the significant parameter is the transport of oxygen gas into the column and subsequent dissolution into the leaching medium at the surface of the ore particle. Other dissolved substances will affect the ability of oxygen to dissolve in water at the same temperature and pressure, because there is less “room” for the

oxygen in the water. The solubility of oxygen decreases with increase in temperature up to 100 °C and increases again at higher temperature (Tromans, 1998). Oxygen solubility decreases as salinity increases. Table 2.6 illustrates the solubility of oxygen in distilled water and it will be a lot lower in solutions of higher ionic strength, such as ammonia.

Table 2.6: Solubility of oxygen in distilled water at 101.1 KPa, different temperatures and salinity (Weiss, 1970)

	Salinity (% w/w)					
	0%	1%	2%	3%	3.5%	4%
Temp °C	Solubility of oxygen in distilled water (mL/L)					
0	10.218	9.543	8.913	8.325	8.045	7.775
10	7.891	7.406	6.950	6.522	6.319	6.121
20	6.352	5.987	5.644	5.320	5.166	5.015
25	6.018	5.401	5.154	4.812	4.719	4.605
30	5.276	4.994	4.727	4.474	4.353	4.235
40	4.486	4.262	4.050	3.848	3.750	3.656
50	3.932	3.722	3.522	3.333	3.243	3.155
60	3.451	3.276	3.110	2.952	2.876	2.803

These oxygen solubility values were obtained by Weiss (1970) using the following equation:

$$\ln C^* = -177.7888 + 255.5907 \left(\frac{100}{T} \right) + 146.4813 \ln \left(\frac{T}{100} \right) - 22.2040 \left(\frac{T}{100} \right) + S \left[-0.037362 + 0.016504 \left(\frac{T}{100} \right) - 0.0020564 \left(\frac{T}{100} \right)^2 \right] \dots\dots\dots (19)$$

Where C^* is the solubility (mL/L), T is absolute temperature and S is the salinity in parts per billion.

- 4. Cupric additions** – Due to the low solubility of oxygen in aqueous solutions, an oxidant may be added, such as cupric ions. Beckstead and Miller (1977a) observed that in the presence of cupric and absence of oxygen, no reaction occurred. The authors also observed that initial cupric additions significantly increased the rate of the reaction, using a range of cupric from 0 to 30 g/l. In the absence of initial cupric addition to the system, the author obtained sigmoidal reaction curves. The sigmoidal curves showed that initially the rate was slow, and after build-up of some Cu^{2+} , the reaction rate increased significantly due to the catalytic effect of cupric ammine. According to the authors, the cupric catalyses the oxygen discharge reaction (equation

- 6). After addition of initial cupric, the initial reaction rate increased significantly, explaining the catalytic effect of the cupric concentration. The reaction rate curves became less sigmoidal in shape after cupric addition. According to Yamasaki (1920) and Tozowa et al. (1976), $\text{Cu}(\text{NH}_3)_4^{2+}$ acts as an oxidant and enhances the rate of reaction by acting as a redox mediator. Ghosh et al. (2003) used Cu(II) as an oxidation catalyst attributed by the redox couple Cu(II)/Cu(I), where cupric ammine $\text{Cu}(\text{NH}_3)_4^{2+}$ oxidises sphalerite and the reduced state cuprous ammine $\text{Cu}(\text{NH}_3)_2^+$ is subsequently re-oxidized by oxygen (equation 7). The addition of an oxidant is necessary in order to enhance the sulphide dissolution Park et al. (2007).
5. **pH** – The rate of reaction is slow at pH values less than 7, which is attributed to the low free NH_3 concentration for the reaction. At pH values between 7 and 10, the reaction rate increases as the free NH_3 concentration increases. However, when the pH is above 10, the rate is independent of pH, as the unbound ammonia concentration is high. In 1920, Yamasaki found that sodium hydroxide in small quantities increased the reaction rate, and in large quantities decreased the rate. The process pH, if low or too high, may result in formation of hydroxides and oxides. The optimal pH is 9.23, where NH_3 (un-ionised ammonia) and NH_4^+ (ionised ammonia) are in equal amounts in the ammoniacal solution, as illustrated in Figure 2.5. The solubility of ammonia in water decreases with increasing pH. Hence an optimum pH that allows appreciable solubility of NH_3 is required. Beckstead and Miller (1977a) found that the reaction rate showed a half-order dependence on initial hydroxyl ion concentration.
6. **Stirring speed** – Halpern (1953) found that in low oxygen pressure regions, the rate of leaching increased markedly with stirring speed, a characteristic of diffusion- or transport-controlled reactions, whereas at higher oxygen pressures no dependence on the rate of stirring velocity was evident. Beckstead and Miller (1977a) used a hydraulically driven reactor that enabled them to use stirring speeds up to 6 000 rpm during the ammonia-oxidation leaching of chalcopyrite. The authors observed that the stirring speed significantly influenced the rate of reaction below 3 000 rpm. The rate of reaction became insensitive to stirring speed above 3 000 rpm, and the author explained that the reaction rate depends on the surface deposit effects and/or electrochemical site activation and not mass transfer control at the higher stirring rates.

2.17 Kinetics of ammoniacal leaching of nickel from metallic Ni and Ni sulphides

The dissolution kinetics of nickel sulphides are not as well researched as those of copper, especially dissolution of pentlandite. Morioka and Shimakage (1971) found the E_a for the dissolution of metallic nickel powder in oxygenated ammonia solution to be 8 kJ/mol. Mizoguchi et al. (1978) described the dissolution of nickel powder in terms of a shrinking core model with a first order reaction at the solid/liquid interface. The initial rate of dissolution was a function of the oxygen concentration, mass transfer coefficient, particle density and radius. The author found the E_a as 6.28 kJ/mol at temperatures between 30 °C and 110 °C. Bhuntunkomol et al. (1980), using temperatures between 35 °C and 65 °C, found the E_a as 9.6 kJ/mol, which is indicative of mass transfer control. In the Caron process, nickel sulphides are first roasted at high temperatures (~750 °C) and converted to nickel oxides. The nickel oxide formed is leached with oxygenated ammonia solution at temperatures > 150 °C (Canterford, 1975; Caron, 1950). Park et al. (2007) investigated the oxidative ammonia/ammonium sulphate leaching of an artificial Cu-Ni-Co-Fe matte in an autoclave. They obtained optimum recoveries at 200 °C, 4 M total ammonia and an oxygen pressure of 1 460 kPa. At high concentrations of oxygen and pH of 6 to 8, the formation of NiO is shown on an E_H -pH diagram by Meng and Han (1996). The oxide remains as a stable phase at this pH range and the rate is very slow. Ammonia is added to complex the nickel, avoid hydrolysis of nickel ions at high pH and to raise the solution pH. At high pH values, however, nickel ammine is the most stable species, and any NiO formed initially is soon dissolved so that the rate is relatively higher. The Caron process used 7% (3.8 M) ammonia concentration and 5.1 to 7% (2.3 M to 3.2 M) carbon dioxide to leach nickel ores and silicates of nickel.

2.18 Limitation and challenges – passivation

The formation of ferric oxides can hinder the transfer of metal ions into solution (Lundstron et al., 2011) and easy access of oxygen and ammonia to the surface of sulphide particles. As a result, the dissolution process slows down considerably during the latter stage of leaching. The morphology of the hematite deposit alters the surface reaction kinetics. Beckstead and Miller (1977b) explained passivation of chalcopyrite based on the electrochemical model (Figure 2.7). They suggest that surface deposits control the reaction kinetics by hindering the transfer to and from the chalcopyrite. Donnay et al. (1958) and Stanczyk and Rampacek (1966) found similar results.

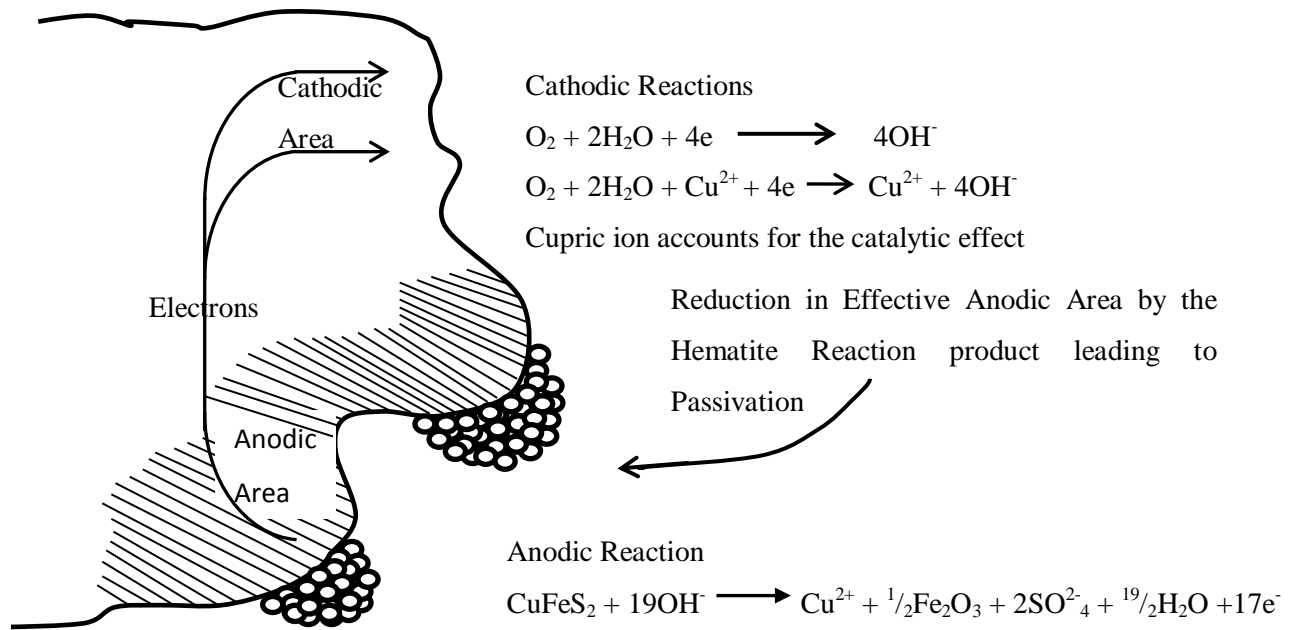


Figure 2.7: Schematic representation of the electrochemical reaction taking place during ammonia oxidation leaching of chalcopyrite. (Adapted from Beckstead and Miller (1977a))

Beckstead and Miller (1977b) observed that iron is oxidised to ferric and precipitated as iron oxide. Nucleation and growth of the hematite phase on the surface of copper-iron sulphides, particularly chalcopyrite, appears to account for a significant reduction in the rate of reaction and in many instances seems to passivate the surface. For the ammoniacal leaching experiments done by Dutrizac (1981), 3 to 10% of the total copper was leached during the 3 month tests; and similar to Beckstead and Miller (1977b): he observed that the ferric oxide product inhibited the reaction under percolation conditions. In 1979, Warren found that passivation by iron oxide occurred at 1V in reactions where oxygen was used as the oxidising agent in alkaline solutions. Bell et al. (1995) used mannitol and dextrose as iron sequestering agents, but despite reducing the ferric oxide reaction product layer (build-up), these organic compounds were also reductive in nature and decreased the rate of copper extraction.

Forward (1953) illustrated the passivation of pentlandite as shown in Figure 2.8. At any given time during the progress of the leach, the leaching pentlandite particle consists of a sulphide core surrounded by an iron oxide envelope through which the nickel and sulphur ions diffuse outward to react with oxygen at the liquid-solid interface while the oxygen diffuses inward, possibly by a mechanism associated with vacancies in the oxide lattice.

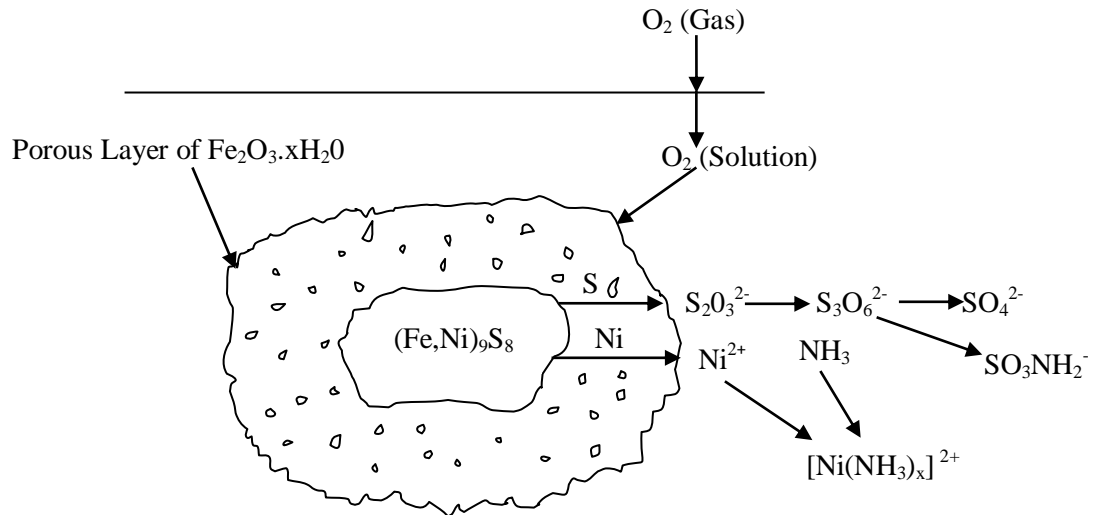


Figure 2.8: Schematic representation of ammoniacal leaching of pentlandite (Adapted from Forward (1953)).

2.18.1 Iron oxide – the result of passivation

The iron in chalcopyrite and pentlandite is oxidised in the presence of air only once it is solubilised. Initial dissolution of iron enables solubilisation of Ni and Cu components of an ore before its subsequent rejection as a hydroxide. The mineral dissolution is driven by the oxidation of sulphur. Iron is easily oxidised in alkaline conditions from Fe(II) to Fe(III). With increasing pH iron forms various iron oxide or hydroxide compounds. Ferric oxides and hydroxides can be in the form of $\text{Fe}(\text{OH})_3$ (iron hydroxide), FeOOH (goethite), or Fe_2O_3 (hematite). Iron can also form jarosite ($\text{KFe}_3(\text{SO}_4)_2(\text{OH})_6$) at low pH values. A stability diagram for the iron oxides is illustrated in Figure 2.9 wherein jarosite is stable in the region of low pH (< 3) (Babcan, 1971).

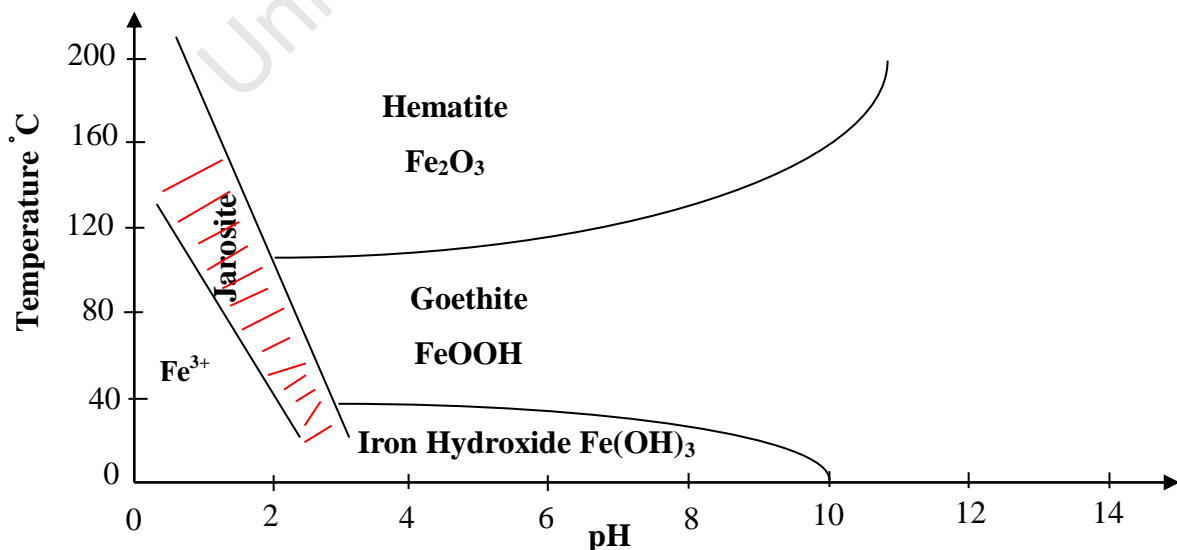
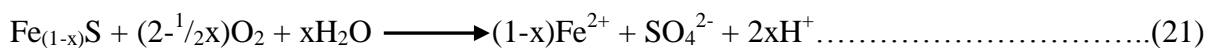
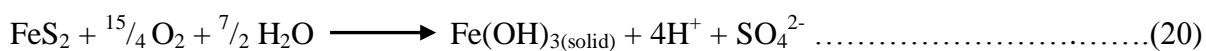


Figure 2.9 also shows that high temperatures favour the formation of hematite at the expense of goethite and that higher pH values favour the stability of goethite with respect to hematite. Jarosite and goethite coexist in nature, suggesting that the rate of transformation from jarosite to goethite at near neutral pH is fairly slow. In 1983, Dutrizac (1983) observed that extensive percolation of fresh water will convert jarosite to goethite, particularly in storage ponds in regions of high rainfall. In 1986, Chen and Cabri (1986) observed that despite the clearly defined stability regions of jarosite, goethite and hematite as derived from experiments, in nature jarosite is commonly associated with goethite, goethite with hematite, and all three can occur together. Although Figure 2.9 shows the regions of stability of the various species, kinetic effects often determine the initial products. $\text{Fe}(\text{OH})_3$ is the most difficult to filter compared to jarosite and goethite phases. $\text{Fe}(\text{OH})_3$ and FeOOH are amorphous solids whilst Fe_2O_3 and jarosite are crystalline solids. The iron oxide reaction product may inhibit the reaction. Hematite (Fe_2O_3) and goethite (FeOOH) are more stable than $\text{Fe}(\text{OH})_3$. Raising the pH of acidic Fe(III) solutions results in the precipitation of goethite.

Pyrite and pyrrhotite

Pyrite and pyrrhotite are almost inert in ammoniacal solutions. Pyrite does not react measurably with ammonia under the conditions normally used in leaching: it remains unaltered in the leach residue or else is oxidised to produce an iron oxide. Guilinger (1987) in their kinetic study of pyrite oxidation found that addition of an ammonia leachant resulted ultimately in ceasing of the pyrite reaction. X-ray diffractometry studies by Rao et al. (1993) showed that in the temperature range between 115 °C to 135 °C and pH of 10 the pyrite grain present in the concentrates did not react in the ammonia medium and remained practically inert. Peters (1976) also reports that during ammonia leaching processes, pyrite, and to a lesser extent pyrrhotite, are incompletely reacted and appear in leach residues. The author suggests that this could be as a result of a protective coating of iron oxide formed around the pyrite and pyrrhotite, which slows down their decomposition. The equations (20) and (21) shown below, illustrate the general oxidation reactions of pyrite and pyrrhotite, which result in acid production and hence a decrease in pH values.



2.18.2 Ammonia losses

Another limitation observed was ammonia losses due to evaporation. Dutrizac (1981) found losses of 5% to 20% when he investigated the ammoniacal percolation of chalcopyrite in a column. Ammonia losses appear to be the most significant technical barrier to commercial adoption of the process. The solubility of NH_3 in water will increase with decreasing pH and is reduced at higher pH. Ammonium carbonate is a volatile substance. It exists as a solid, but chemical treatment can result in its breakdown, releasing ammonia and carbon dioxide, both gases under normal conditions. Thus, the volatility of a substance is the relative ease with which it can be vaporised. In heap leaching it might be difficult to see how the need for good gas circulation for oxygen transport is compatible with the requirement to minimise ammonia evaporation, but in tank leaching, closed vessels can be operated under pressure to keep the NH_3 in the solution (used with pure oxygen) or at atmospheric pressure and the ammonia gas scrubbed off and recycled.

2.19 Types of leaching

Leaching refers to the process of extraction of metals from ores by employing suitable solvents. The leaching of metals such as copper and nickel has been extensively studied by several researchers such as Gupta (2003), Bartlett (1998) and Gupta and Mukherjee (1990). There are two possible types of leaching that can be employed on low-grade ores i.e. percolation and agitation leaching shown in Figure 2.10.

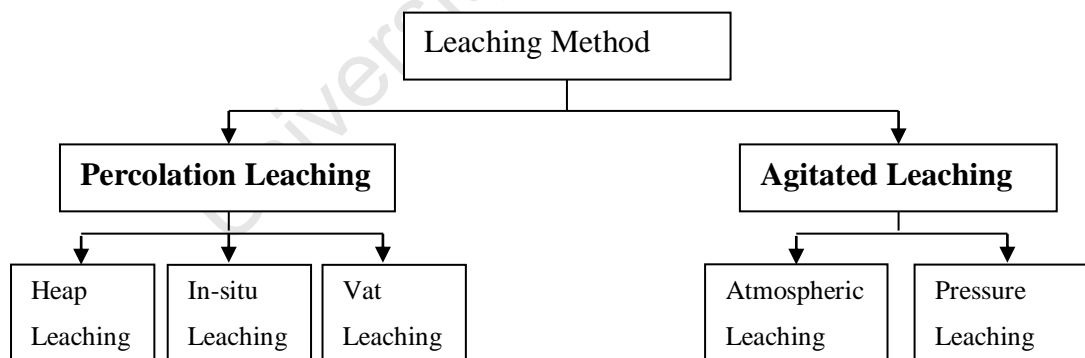


Figure 2.10: Types of leaching and some of the sub-types of leaching

2.19.1 Percolation leaching

Percolation leaching involves selective dissolution of metals by lixiviants sprinkled on the surface of a mass or pile of material stacked into a suitable heap or waste dump. The lixiviant percolates by gravity through the ore mass or agglomerated material and leaches out the valuable metals. The pregnant solution exits at the bottom of the heap into a collection

reservoir and given further treatment to recover dissolved metals. After metal recovery, the solution, possibly re-oxidised or re-acidified, is pumped to the top of the ore mass to repeat the cycle. The technique may be acid-based or alkaline-based percolation. Percolation leaching is a very slow process and may take several months to extract 50% of the target mineral but because of its low processing costs, it is an attractive process for leaching low grade ores.

In heap leaching (Figure 2.11), the heap of crushed ore or agglomerated material is placed on an impermeable plastic and/or clay-lined leach pad and leaches out the valuable metals.

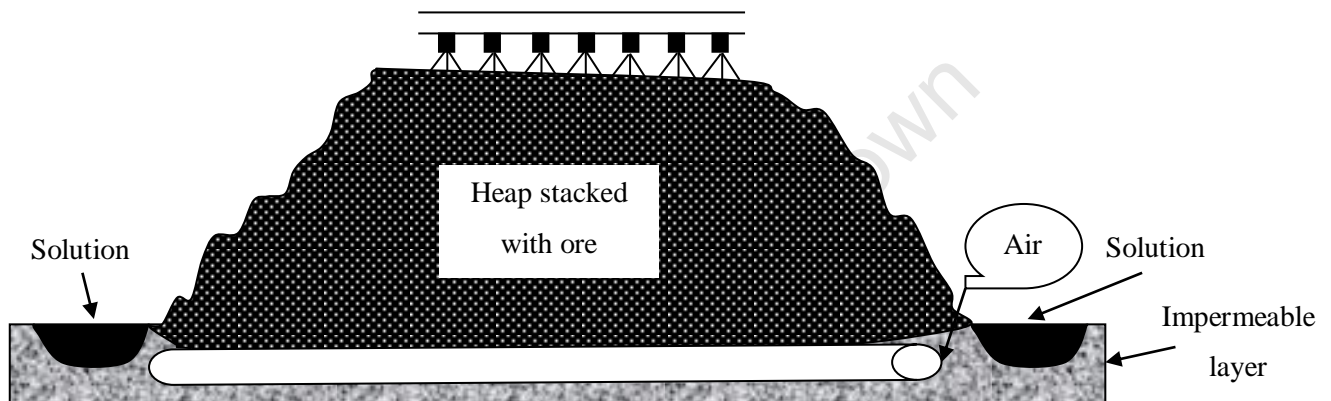


Figure 2.11: Typical Heap leach operation (Adapted from Nicol (2008)).

In in-situ leaching, the valuable metals are recovered through boreholes drilled into an ore deposit. In vat leaching, the solids are loaded into the vat (a large scale basin), and, once full, the vat is flooded with a leaching solution and left to react for a period of time. The solution is then drained and is either recycled back into the vat or is pumped to the next step of the recovery process (Bartlett, 1998; Gupta and Mukherjee, 1990).

2.19.2 Agitation leaching

Agitation leaching is a hydrometallurgical method of extracting valuable material by dissolving soluble minerals from a solid ore or concentrate within specially designed vessels. The material is ground sufficiently fine and mixed with extraction lixiviant or water to form a slurry or pulp, which can flow under gravity or when pumped. Leaching reagents (aqueous solution which acts as a solvent) are added to the tanks to achieve the leaching reaction. The duration of the leaching operation can range from less than an hour to 5 days, and several tanks are usually arranged in a cascade. In continuous systems the slurry will then either

overflow from one tank to the next, or be pumped to the next tank. Ultimately the pregnant solution is separated from the slurry using some liquid/solid separation process, and the solution passes to the next phase of recovery. Tanks are equipped with agitators (to keep the solids in suspension and effect the solid to liquid gas contact, (Altman et al., 2002)), baffles (assist with agitation by increasing the efficiency of agitation and preventing centrifuging of slurries in circular tanks; baffles avoid vortex formation) and gas introduction equipment designed to maintain the solids in suspension in the slurry, and achieve leaching. In the case of sulphide leaching, aeration is needed and is accomplished by blowing air or pure oxygen under the stirrer. Picture 2.3 illustrates a typical tank leach operation.

Agitation has a pronounced effect on leaching rates due to the heterogeneous character of the reactions which involve dissolving oxygen at the gas-liquid interface, transporting the oxygen through the solution from the liquid-solid interface. These three are increased by increased agitation. When the equilibrium between the metal on the ore surface and the metal contained by the solution is approached, the solubilisation of the metal in the ore is slowed, and the extraction is considered to be completed. Once the process is considered to be at equilibrium, the ore is separated from the extraction fluid using sedimentation, thickening or clarification. The extraction process may be continued in a separate extraction vat with clean extraction solution to enhance extraction. An agitation vat coupled with a solid-liquid separation vessel (sedimentation or clarification) is considered to be a single stage.



Picture 2.3: Typical tank leaching operation (Source: wiki.biomine.skelleftea.se (2008)).

Another branch of agitation leaching is pressure leaching (illustrated in Picture 2.4) in which milled high-grade ore or concentrate is contacted with lixiviant in high-pressure and high-temperature reactors (autoclaves). Pressure leaching is applied when the rate of oxidation or dissolution of a mineral is too slow at temperatures below 90 °C to make recovery economically viable. In the context of ammonia leaching pressure autoclaves also help control the evaporation of ammonia, even if operated at temperatures below 100 °C.



Picture 2.4: Typical pressure leaching (Adapted from Porter (2000))

2.19.3 Advantages and disadvantages of leaching

The advantages and disadvantages of agitation leaching and percolation leaching were adapted from literature (Bartlett, 1998; Gupta and Mukherjee, 1990; Gupta, 2003) and summarised in Table 2.7.

Table 2.7: Advantages and disadvantages of different types of leaching

Types	Advantages	Disadvantages
Percolation Leaching	<ul style="list-style-type: none">• Low capital and operating costs.• Operates on a large scale.• Simple atmospheric leach process.• Less risky form of technology.	<ul style="list-style-type: none">• Low and slow recoveries.• Certain ores are not amenable to percolation leaching: those that contain high amounts of clay (tend to clog) and carbonates (in a sulphuric acid leach these consume acid and form gypsum).• Heap leaching requires the availability of land.• Groundwater contamination may result.• Complex technology relative to chemical and physical features.
Agitation Leaching	<ul style="list-style-type: none">• Rapid dissolution kinetics.• High recoveries.• Allows for good process control and mass and oxygen transfer.	<ul style="list-style-type: none">• High capital and operating cost in pressure leaching.• Complex technology with high maintenance costs.• Generally non-selective leaching.• Limited volume limits maximum residence time or throughput rates.

2.20 Uses of the by-product - ammonium sulphate

Ammonia leaching of sulphide concentrates produces large quantities of ammonium sulphate as a by-product which may present disposal problems. However, ammonium sulphate can be recycled for different applications. Although ammonium sulphate is a marketable product, it is difficult to produce at sufficiently high purity in a mineral type process, requiring extensive purification (energy-intensive) and crystallisation. Some of the applications of ammonium sulphate include that it can be used as a soil fertiliser, as the sulphur reduces the soil pH and promotes protein synthesis whilst nitrogen promotes plant growth (Gowariker et al., 2009). Ammonium sulphate is not used as a sole nitrogen source because it is toxic to some crops. Ammonium sulphate may also be used as an agricultural spray adjuvant for water soluble insecticides, herbicides and fungicides, e.g. glyphosate and glufosinate herbicides (Penner et al., 2005). It may also be used in the preparation of other ammonium salts. In biochemistry ammonium sulphate precipitation is a common method of purifying proteins by precipitation and as an ingredient for many vaccines disease control (Zapp, 2009). Ammonium sulphate is also used as a food additive and may also be used as a flame retardant as it lowers the combustion temperature of a material (Ash and Ash, 2004).

3.0 EXPERIMENTAL MATERIALS AND METHODS

3.1 Introduction

A two-stage leaching process, which involves acid bioleaching of a Platreef ore to extract base metals, followed by cyanide leaching to recover precious metals from the residue has been established by Mwase et al. (2012) and is still under development. The precious metals in the Platreef ore have been observed to be more amenable to cyanide leaching after a pre-leaching stage to remove the base metals. However, moving from an acidic heap bioleaching environment to the alkaline cyanide leaching environment would require multiple washing stages of the ore so as to remove all the acid and avoid formation of toxic hydrogen cyanide, a volatile gas that rapidly evaporates at atmospheric pressure. To eliminate the multiple leaching stages, the technical feasibility of the alkaline ammoniacal leaching of the Platreef low-grade concentrate was investigated as an alternative route for base metal recovery, either in heaps or in tanks. Ammonia losses have been observed to be a possible technical barrier and quantification of the losses was carried out so as to establish the technical and environmental effects that could arise. The effect of total ammonia concentration, temperature, and pH on nickel and copper recovery were investigated as these parameters were considered to influence the process.

The ammoniacal leaching process involved subsequent phases of shake flasks, batch stirred tank reactors and column tests. The shake flask tests were conducted to test the initial parameters and establish ball-park kinetics, i.e. pH, ammonia concentration, etc. in dilute solutions. The batch stirred tank reactor leach tests were to test the ammoniacal leaching process at higher slurry concentrations at those conditions established as optimal in the shake flasks. Likewise, the columns serve to test the heap leaching properties of the material. The columns used provided more accurate extraction and ammonia consumption data under trickle bed (percolation) conditions, which would be relevant to heap leaching, whilst the stirred tank reactors provided the tank leaching environment with increased mass transfer.

3.2 Platreef concentrate preparation

The material used during the ammoniacal leaching study was a Platreef flotation concentrate supplied by Lonmin plc. A 200 kg sample of concentrate was obtained and thoroughly mixed to obtain a homogenous sample and split down to 4 kg samples using a 2-way riffle splitter

followed by a 10-way rotary splitter. To obtain the required amount of sample for leaching experiments, size analysis and base metal solid assays, the concentrate was further split using a Fritsch rotary 10-way sample divider (picture 3.1) and/or an 8-way rotary micro riffler (picture 3.2) to ensure homogeneity.



Picture 3.1: Fritsch sample divider



Picture 3.2: Rotary micro riffler

The concentrate was sized using wet screening showing the size distribution in Table 3.1.

Table 3.1: Particle size analysis of the concentrate sample

Screen Sizes (μm)	% Passing
75	97%
45	97%
38	83%

The low-grade concentrate derived from the platinum ore (PGMs) consists of the following base metal grade assay shown in Table 3.2.

Table 3.2: Major base metals and gangue elements of the concentrate sample

Mg	Al	Si	Ca	Ti	V	Cr	Mn	Fe	Co	Ni	Cu	Zn	Pb
%	%	%	%	%	%	%	%	%	%	%	%	%	%
10.0	1.79	16.2	3.56	0.067	<0.05	0.14	0.14	14.1	0.099	3.17	2.02	0.064	<0.05

Ni and Cu are the base metals of interest and their compositions are 3.17% Ni in pentlandite and 2.02% Cu in chalcopyrite, respectively. Co is present in small amounts, i.e. 0.099%, and though it can be leached in oxygenated ammonia solutions, it was not the major focus of this study. A mineralogical analysis was carried out by ALS laboratory Group using an automated

mineral liberation analyser (MLA) designed to determine the mineral speciation of the minerals. The MLA gave the mineral abundance of BMS as shown in Table 3.3.

Table 3.3: Mineral abundances of base metal sulphides and gangue (wt. %)

Mineral	Wt. % abundance
PGMs	0.06%
Chalcopyrite	4.93%
Pentlandite	7.70%
Pyrrhotite	5.27%
Pyrite	1.98%
Silicates	43.89%
Pyroxene	22.62%
Others	13.55%

3.3 Reagents

The reagents used in the investigation of the ammoniacal leaching process were ammonia solution (25% uniVAR grade), ammonium sulphate and ammonium chloride, which were supplied by Merck, and ammonium carbonate, which was supplied by Sigma Aldrich®. The leaching solution was prepared by dissolving known volumes and masses of ammonium hydroxide and ammonium carbonate, chloride or sulphate in distilled water respectively. Compressed air was used to supply the oxygen required to facilitate the ammoniacal leaching reaction.

3.4 Equipment description

3.4.1 Shake flasks

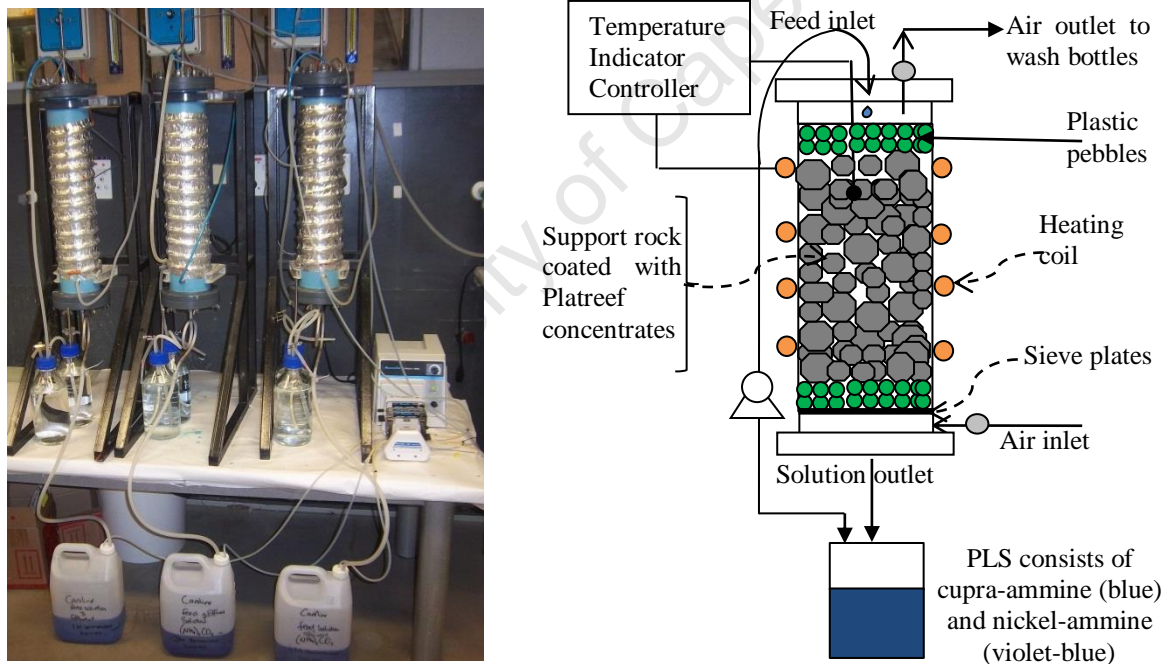
Shake flask tests were performed first, to obtain an initial indication of the feasibility of the ammoniacal leaching process on the Platreef concentrates. This enabled benchmarking of recoveries and investigation of key parameters using the set-up in picture 3.3.



Picture 3.3: Shake flask experiment - Erlenmeyer flasks on a shaking platform in a fume-hood.

3.4.2 Columns

The columns used were 0.5 m in height and 0.09 m in diameter. They consisted of a thermocouple, heating mantle, a feed pipe, solution outlet, gas inlet and outlet pipe. The thermocouple was used to monitor the temperature in the column and was placed in the ore bed. The columns consisted of an air inlet point near the bottom of the column, where compressed air was sparged into the column. Excess air from the column was released through the gas outlet pipe to wash bottles in which the ammonia was scrubbed out. A peristaltic pump was used to generate a cycle flow of solution calibrated to a feed flow-rate of 1 L/d (5 L/m²/h, a typical value for operating heaps). The slow feed rate ensured a small quantity of feed solution was sent to the column to allow clear absorption to the coated material. The lixiviant percolated through the column by the action of gravity. The pregnant leach solution (PLS) was collected at the bottom of the column in a reservoir and recycled as feed for three days. After three days the PLS was removed and fresh feed solution was placed into the container. The experiments were not done in duplicates due to time constraints.



Picture 3.4: Heap leaching experiments in columns and schematic diagram of the heap leach process

GEOCOAT preparation of concentrates

The GEOCOATTM concept developed by GeoBiotics of Lakewood Colorado (Johansson et al., 1999) was used to prepare the Platreef concentrates. Support rock was screened using + 1 mm and - 25 mm sieves. Slurry was made by mixing the Platreef concentrates with distilled

water in the ratio of solids to liquids of 5:3. The slurry, a thick sludge, was used for coating dry unreactive support rock in a bucket and tumbled to form an even coating using a mass ratio of concentrate to support rock of 1:9. The weight ratio of concentrates to support rock was found to depend strongly on the type of concentrate used, and it is usually in the range 1:5 to 1:10 (Harvey et al., 2002). The hydrophobic nature of the concentrate assists in the formation of the coating and no binding agents are required (Harvey et al., 2002).



Picture 3.5: Uncoated support rock



Picture 3.6: Support rock coated with slurry

The GEOCOAT heap process prevents the compaction of fines and ensures uniform distribution of air and solution to all parts of the heap. This aims to utilise the advantage of heap leaching (low capital and operating costs) while avoiding its drawbacks (long leach times, mineral occlusion) (Petersen and Dixon, 2002).

Packing of the column (Picture 3.4)

Each column was loaded with a 5 cm layer of plastic pebbles to cover the bottom surface of the column to allow for air distribution. Each column was packed to $\frac{2}{3}$ of its height with support rock coated with slurry. After packing with coated material the top layer was covered with a 5cm layer of plastic pebbles to enhance the distribution of the feed solution.

Pump calibration procedure

Distilled water of density 1 g/mL was used to calibrate the pump. A small beaker was filled with distilled water. One end of a tube (the size to be used in the feed) was placed into the beaker and the other end placed in an empty measuring cylinder via a peristaltic pump. The water was pumped from the beaker into the measuring cylinder for 5 min. Each time the pump speed was adjusted, until a pump speed that enabled the final volumetric reading in the

cylinder to be 3.5 mL in 5 min was obtained. This set the pump to feed the columns at a rate of 1 L/d.

Sampling procedure

After recycling the feed and effluent every 3 days, the solution was removed and a sample was taken. Before sampling, the volume of the effluent was measured. Fresh solution was placed into the reservoir. During the experiments, pH and redox were measured using a pH and redox meter, respectively. The samples were filtered and Cu, Ni and Fe extracted were analysed using AAS and ICP analysis.

Recovery of concentrate material

At the end of the column experiments the concentrate was recovered by releasing the contents of the column into a 20 L bucket. The plastic pebbles were washed off any concentrate in the bucket and collected. The slurry was washed off the support rock by placing it onto a 5.6 mm sieve and pouring water to remove slurry into the 20 L bucket. Some filter paper was weighed and used to filter contents of the bucket using a pressure filter press. The filter cake was dried in an oven, weighed and sampled.

3.4.3 Batch stirred tank reactor

A 2 L Applikon[®] reactor, consisting of a lipseal stirrer with a three bladed mixing impeller, aeration pipe, sample pipe, liquid addition pipe, baffles and a jacket was used for tank leaching. The experiments were done in duplicates using 2 Applikon[®] reactors.



Picture 3.7: Tank leaching experiment – Applikon[®] reactor under batch mode

The reactor had a glass jacket that enabled even temperature distribution throughout the reactor through a natural water convection mechanism. Compressed air was sparged into the

reactor to meet the oxygen requirements. Air leaving the reactor was passed through a reflux condenser to reduce evaporation losses of leach solution during leaching. The air leaving the reactor was scrubbed off ammonia gas by passing through two wash bottles, connected in series. A careful mass balance on N_2 gases in the tank and wash bottles showed good closure with no significant portions of NH_3 in the off-gas. Mass balances around the system showed the desired emission levels of less than 25 ppm of ammonia were released to the atmosphere. Sampling was done through a sample pipe dipped close to the bottom using a syringe connected to a tube. Make-up solution was added via the liquid addition pipe.

3.5 Analytical methods

The measurement of metal composition of each leaching solution was made by AAS and ICP analysis. Iron was monitored on a daily basis using a UV Spectrophotometer to ensure no significant dissolution occurred. Ammonia was analysed using the NOVA 60 Spectroquant photometer. pH and redox potential were measured using a pH and redox meter, respectively.

3.5.1 Acid digestion for solids

Unleached samples and leached residues were acid digested before AAS or ICP analysis to convert the solids into liquid form for AAS. Acid digestion was done using 3 acids: 6 mL of HCl, 4 mL of HF and 2 mL of HNO_3 . These 3 acids were added into Easy-prep vessels together with 0.2 g of solid sample. The vessels were placed into a MarcsXpress (CEM) microwave and ramped to a temperature of 210 °C. The ramp time was 30 min at a pressure of 800 psi. The ramp is automatically broken into 2 parts - the last 30 °C are done in 10 min. The power application starts low and increases to 1 600W as temperature increases. After the digestion a holding time of 15 min allows the pressure and power to drop whilst the liquid cools down. This enables the volatile elements to be retained and no solution is lost.

3.5.2 Atomic absorption spectroscopy (AAS)

AAS is a spectro-analytical procedure for the qualitative and quantitative determination of chemical elements employing the absorption of optical radiation (light) by free atoms in the gaseous state. This technique was used for determining the concentration of a particular element in a sample. The electrons of the atoms in the atomizer can be promoted to higher orbitals for a short period of time only absorbing defined energy (wavelength) quantities. Each wavelength corresponds to only one element. Solids were acid digested before analysis.

3.5.3 Inductive coupled plasma spectrometer (ICP)

In ICP analysis, the sample was heated to a high temperature in an inductively coupled argon stream which ionised the elements. The ionised elements emitted a characteristic wavelength of light, the intensity of which is proportional to the amount of the element in the sample. The ICP measures the light spectra emitted by elements in solution. Solids were put through an acid digestion cycle so that the metals were in solution before ICP analysis. The ICP has a measuring detection limit of 1 ppb to 10 ppb.

3.5.4 Ammonium analysis

The ammonia analysis was performed using a spectroquant NOVA 60 photometer (picture 3.8) with ammonium test kits obtained from Merck. The analysis is based on the fact that ammonium nitrogen ($\text{NH}_4\text{-N}$) occurs partly in the form of ammonium ions and partly as ammonia. A pH-dependent equilibrium exists between the two forms. In strongly alkaline solution ammonium nitrogen is present almost entirely as ammonia, which reacts with hypochlorite ions present in the reagents of the kit to form monochloramine. This in turn reacts with a substituted phenol to form a blue indophenol derivative that is determined photometrically. Analysis of the ammonium ion is done immediately after sampling. The sample must first be filtered to remove turbid material. The samples are diluted with distilled water as desired. The pH of the sample must be within the range of 4 to 13. If the pH is not within this range the sample pH is adjusted with either sulphuric acid or sodium hydroxide. 5 mL of reagent $\text{NH}_4\text{-1}$, 0.10 mL of the sample and 1 level micro-spoon of reagent $\text{NH}_4\text{-2}$ are added into a test tube and the mixture is vigorously shaken until the $\text{NH}_4\text{-2}$ reagent has completely dissolved. The mixture is left to stand for 15 min (reaction time), then analysed using the NOVA 60 spectroquant at a wavelength of 690 nm.

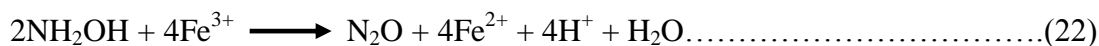


Picture 3.8: NOVA 60 spectroquant – photometer used for ammonia analysis.

3.5.5 Iron assay method

The iron assay procedure is based on two facts:

- ✓ The formation of orange red complexes when Fe^{2+} is mixed with 1-10 phenanthroline. Three molecules of 1-10 phenanthroline chelates with one Fe^{2+} ion.
- ✓ The reduction of Fe^{3+} by hydroxylamine according to the stoichiometry shown below:



By first reducing all the Fe^{3+} present in a sample, total iron can be determined by use of the 1-10 phenanthroline complexing agent. A blank solution comprising of 2 mL acetate buffer, 2 mL 1-10 phenanthroline solution and 1 mL of milliQ water is prepared. The spectrophotometer is set to a wavelength of 510 nm and zero calibrated. A standard curve is prepared by diluting a standard ferrous iron stock to 10, 20, 30, 40, and 50 mg/L. To quantify the total dissolved iron, acetate buffer and indicator solutions are added into a test tube (as described previously) together with 1 mL of the sample. A small spatula of hydroxylamine (approximately 0.5 to 1.5g) is added and the mixture is shaken for 2 minutes. The mixture is allowed to stand for 5 minutes. The total iron concentrations were determined using a Unicam, Helios, α .v4.04 UV Spectrophotometer.

3.5.6 pH analysis

pH was measured using a Metrohm, 713 pH meter. The pH meter used consisted of a measuring probe connected to an electronic meter that measured and displayed the pH reading. The pH meter was calibrated before each measurement to ensure precision, so as to increase the reproducibility of the potential of the glass electrode. Two standard buffer solutions were used for calibration, pH 7 which was essentially a “zero point” and pH 9 as it was close to the point of interest, i.e. samples were basic. The electrodes when not in use were stored in a bridge electrolyte 3 M KCl, to avoid membrane dehydration and the consequent loss of functionality of the electrode.

3.5.7 Redox potential analysis

The redox potential was measured using a Metrohm, 827 redox meter with a platinum ring electrode and 3 M KCl AgCl electrolyte. The redox meter was calibrated before each measurement to ensure precision and increase the reproducibility of the potential of the glass electrode by placing it into a standard solution with a redox potential of 468 mV. The reading obtained was used to calculate the accuracy of the probe. The procedure was repeated to confirm calibration.

3.6 Safety, health and environmental aspects of ammonia

Some of the properties of ammonia are listed in section 2.9. At room temperature, ammonia is a gas. Flammability hazard rating is 1 (slight fire hazard) and auto-ignition temperature is 651 °C. It is extinguished by water spray or fog (AB ACHEMA, 2006). Ammonia must **always** be handled with caution and pre-cautions stated on the MSDS (Appendix B) must be followed. At high concentrations, ammonia is hazardous. Exposure to ammonia can occur through inhalation, skin contact, eyes and ingestion. Ammonia gas is severely irritating to the eyes and to the moist skin and mucus membranes of humans. Liquid ammonia causes severe eye damage that may lead to blindness and can cause freezing and third-degree burns of the skin. Ammonia has no cumulative effects on the environment as it does not last long in the environment, i.e. it has only a few days atmospheric lifetime. Because of the short lifetime of ammonia it is considered to be biodegradable as it is converted to N₂ gas (which is a less harmful component of air), through nitrification and denitrification. Because of its high alkalinity and solubility in water, ammonia can alter the pH balances of surface water, soil and plants. Should they be exposure to high concentrations for any length of time, these changes in pH could be detrimental to both flora and fauna. Disposals must be done in an environmentally safe manner, such as in large amounts of water.

3.7 Experimental procedures

The general ammoniacal leaching process is outlined in Figure 3.1. The concentrates were leached with a buffered ammoniacal lixiviant in different reactor systems. There was constant monitoring of the pH using the pH meter, redox potential using the redox meter and Fe extracted using the UV Helios Spectrophotometer at a wavelength of 510nm. Each sample obtained was filtered and sent for AAS and ICP analysis.

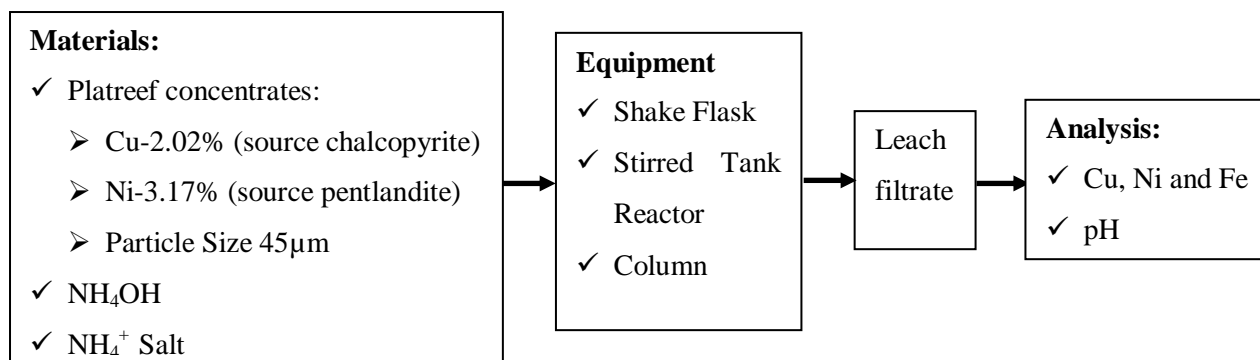


Figure 3.1: Process flow diagram of the ammoniacal leaching process

3.7.1 Process variables

- a) Reagent concentration – The total ammonium concentration was investigated using equimolar concentrations of ammonium hydroxide and ammonium salt e.g. 0.5 M NH_4OH and 0.5 M $(\text{NH}_4)_2\text{CO}_3$.
- b) Reagent pH – This varied according to the lixiviant, but was in all cases in the alkaline region, based on experiments conducted and literature. When the pH dropped out of the required region, a few mL of buffered ammoniacal lixiviant was added to return it to the required range of between 9 and 10.
- c) Buffering effect - Solutions were buffered to obtain and maintain the required pH using various combinations of ammonium hydroxide and ammonium salt. The ammonium salts investigated in the ammoniacal leaching process were ammonium sulphate, ammonium carbonate and ammonium chloride.
- d) Temperature - Room temperature is economically preferred, given the tonnage and grade of the material to be treated. Other temperatures investigated were 30 °C, 40 °C, 50 °C and 60 °C.

3.8 Experimental design

To investigate the ammoniacal leaching process feasibility of the Platreef concentrates, several parameters were explored initially in shake flasks. The ball park kinetics established in shake flasks were used in columns and batch stirred tank reactors. When one parameter was investigated all other parameters were kept constant.

Table 3.4: Overall experimental plan of all experiments carried out

Reactor	✓ Investigated Parameters			
	pH	Ammonia concentration	Temperature	Pulp density
		(M)	(°C) \pm 0.1°C	% w/v
Shake Flasks	✓	✓		
Columns		✓	✓	
Stirred tank reactors		✓	✓	✓

3.9 Experimental program

The experiments were carried out in three phases, as follows:

- ❖ Investigation of the technical feasibility of the ammoniacal leaching process of Platreef concentrates in:
 - ✓ Shake flasks
 - ✓ Columns and
 - ✓ Batch stirred tank reactors.

3.9.1 Investigation of the feasibility of the ammoniacal leaching process of a Platreef flotation concentrate in shake flasks

During this phase, the following experiments were conducted:

- a) A series of experiments were conducted to establish if the leaching process was technically viable for the present type of concentrate. Initially no extraction occurred, until it was observed that the pH played an important role in ensuring the reaction occurred.
- b) Investigation of the optimal pH range.
- c) Understanding the buffering effect of different ammoniacal salts so as to choose the better buffer.
- d) An investigation of the effect of total ammonia concentration on the extraction of base metals.

Experimental design 1 in shake flasks

Table 3.5: Experimental design of shake flask experiments, pulp density – 1% w/v at ambient temperature

Shake Flask Experiment	pH range	Ammonia Concentration
1	6 to 10*	5 M NH_4OH , 5 M $(\text{NH}_4)_2\text{CO}_3$
2	9 to 10	5 M NH_4OH, 5 M $(\text{NH}_4)_2\text{CO}_3^*$
3	9 to 10	5 M NH_4OH, 5 M $(\text{NH}_4)_2\text{SO}_4^*$
4	9 to 10	5 M NH_4OH, 5 M NH_4Cl^*
5	9 to 10	0.5 M NH_4OH, 0.5 M $(\text{NH}_4)_2\text{CO}_3^*$
6	9 to 10	1 M NH_4OH, 1 M $(\text{NH}_4)_2\text{CO}_3^*$
7	9 to 10	2 M NH_4OH, 2 M $(\text{NH}_4)_2\text{CO}_3^*$
8	9 to 10	3 M NH_4OH, 3 M $(\text{NH}_4)_2\text{CO}_3^*$
9	9 to 10	4 M NH_4OH, 4 M $(\text{NH}_4)_2\text{CO}_3^*$
10	9 to 10	5 M NH_4OH, 5 M $(\text{NH}_4)_2\text{CO}_3^*$

* The bold are the parameters under investigation in the matrix

3.9.2 Investigation of the ammoniacal leaching of a Platreef concentrate in columns

During this phase, the following experiments were conducted:

- Effect of total ammonia concentration on the amount of copper and nickel extraction.
- Effect of temperature on the rate of ammoniacal leaching of copper and nickel.

Experimental design 2 in columns

Table 3.6: Experimental design of column experiment, pH 9 to 10

Column Experiment	Investigated Parameters	
	Ammonia Concentration	Temperature ($^{\circ}\text{C}$) $\pm 1^{\circ}\text{C}$
1 (Base Case)	4 M NH_4OH, 4 M $(\text{NH}_4)_2\text{CO}_3^*$	Ambient
2	4 M NH_4OH, 2 M $(\text{NH}_4)_2\text{CO}_3^*$	Ambient
3	4 M NH_4OH, 2 M $(\text{NH}_4)_2\text{CO}_3^*$	Ambient
4	2 M NH_4OH, 1 M $(\text{NH}_4)_2\text{CO}_3^*$	Ambient
5	1 M NH_4OH, 0.5 M $(\text{NH}_4)_2\text{CO}_3^*$	Ambient
6	0.5 M NH_4OH, 0.25 M $(\text{NH}_4)_2\text{CO}_3^*$	Ambient
7	0.5 M NH_4OH , 0.25 M $(\text{NH}_4)_2\text{CO}_3$	40 $^{\circ}\text{C}^*$
8	2 M NH_4OH , 1 M $(\text{NH}_4)_2\text{CO}_3$	40 $^{\circ}\text{C}^*$

* The bold are the parameters under investigation in the matrix

3.9.3 Investigation of the ammoniacal leaching of a Platreef concentrate in batch stirred tank reactors.

During this phase, the following experiments were conducted:

- Effect of pulp density on the amount Cu and Ni extracted.
- Effect of ammonia concentration and calculation of initial rate of extraction at different ammonia concentration.
- Effect of temperature and calculation of the activation energy.

Experimental design 3 on batch stirred tank reactors

Table 3.7: Experimental design of experiments carried out in the batch stirred tank reactor, pH 9 to 10

Stirred tank experiment	Investigated parameters at constant impeller speed 500 rpm		
	Total Ammonia Concentration	Temperature $\pm 0.1^\circ\text{C}$	Pulp Density
1	4 M NH_4OH , 4 M $(\text{NH}_4)_2\text{CO}_3$	50 $^\circ\text{C}$	1% w/v*
2	4 M NH_4OH , 4 M $(\text{NH}_4)_2\text{CO}_3$	50 $^\circ\text{C}$	2% w/v*
3	4 M NH_4OH , 4 M $(\text{NH}_4)_2\text{CO}_3$	50 $^\circ\text{C}$	5% w/v*
4	4 M NH_4OH , 4 M $(\text{NH}_4)_2\text{CO}_3$	50 $^\circ\text{C}$	10% w/v*
5	4 M NH_4OH , 4 M $(\text{NH}_4)_2\text{CO}_3$	50 $^\circ\text{C}$	20% w/v*
6	0.5 M NH_4OH, 0.5 M $(\text{NH}_4)_2\text{CO}_3$*	50 $^\circ\text{C}$	2% w/v
7	1 M NH_4OH, 1 M $(\text{NH}_4)_2\text{CO}_3$*	50 $^\circ\text{C}$	2% w/v
8	2 M NH_4OH, 2 M $(\text{NH}_4)_2\text{CO}_3$*	50 $^\circ\text{C}$	2% w/v
9	4 M NH_4OH, 4 M $(\text{NH}_4)_2\text{CO}_3$*	50 $^\circ\text{C}$	2% w/v
10	4 M NH_4OH , 4 M $(\text{NH}_4)_2\text{CO}_3$	Ambient temp*	2% w/v
11	4 M NH_4OH , 4 M $(\text{NH}_4)_2\text{CO}_3$	30 $^\circ\text{C}$*	2% w/v
12	4 M NH_4OH , 4 M $(\text{NH}_4)_2\text{CO}_3$	40 $^\circ\text{C}$*	2% w/v
13	4 M NH_4OH , 4 M $(\text{NH}_4)_2\text{CO}_3$	50 $^\circ\text{C}$*	2% w/v
14	4 M NH_4OH , 4 M $(\text{NH}_4)_2\text{CO}_3$	60 $^\circ\text{C}$*	2% w/v

* The bold are the parameters under investigation in the matrix

3.9.4 Procedure for ammonia leaching of a Platreef concentrate in shake flasks

To investigate the feasibility of the ammoniacal leaching of Platreef concentrates, each Erlenmeyer flask was loaded with 1 g of the concentrates (1% w/v pulp density) and 100 mL of buffered ammoniacal lixiviant. The mixture was agitated by placing it on a shaking platform. Air was supplied through passive aeration as the flasks shook. All experiments were carried out in a fume hood under ambient conditions. The molarity of the lixiviant was changed depending on the experiment. The shake flasks were placed such that a series of them were under one condition. Two flasks were removed as daily samples and were assumed to represent progress in all the remaining flasks. These were vacuum filtered using 0.45 µm membrane filter papers. The filtrate's pH and redox potential were measured using a pH and redox meter respectively and Fe, Cu and Ni recoveries were analysed using AAS and ICP analysis.

3.9.5 Procedure for ammonia leaching of a Platreef concentrate in columns (heap leaching)

Column leaching experiments were investigated to demonstrate the heap leaching behaviour of the Platreef concentrates using the GEOCOATTM method, mild temperature and atmospheric pressure. The column was packed as outlined in section 3.4.2, using the coated support rock. The column was fed from the top via a peristaltic pump calibrated to a flow-rate of 1 L/d. The lixiviant percolated through the column by the action of gravity. The pregnant leach solution (PLS) was collected at the bottom of the column into a reservoir and recycled as feed for three days. Dutrizac (1981) observed that recycling gave favourable extractions, due to the cupric ammine catalytic effect. The PLS was analysed for copper and nickel using AAS and ICP analysis, and ammonia concentration was measured using a NOVA 60 spectroquant photometer (section 3.5). Additionally, pH and redox potential were monitored. At the end of the experiments the concentrate was washed off the support rocks and recovered via pressure filtration for further analysis and possible additional test work.

3.9.6 Procedure for ammonia leaching of a Platreef flotation concentrate in batch stirred tanks (tank leaching)

Tank leaching experiments were carried out in 2 L Applikon[®] reactors as shown in Picture 3.7 to investigate higher pulp densities and the effect of changing the parameters that were established in shake flasks. 1 L ammoniacal solution of desired concentration was placed

into the reactor together with the required pulp density. Mixing and gas dispersion of the slurry in the reactor was achieved through agitation, using a three blade turbine impeller connected to a controlled stirrer motor rotating at 500 rpm. The reactor was operated in batch mode for the duration of 5 days. Samples were taken on a daily basis or during required time intervals. Ammonia lost and taken out during sampling was replaced with fresh buffered ammoniacal lixiviant of the same molarity to maintain the volume constant and the pH within the required range. The reactor was connected to a constant temperature water bath that circulated heated water through the reactor jacket to keep the system at the desired temperature. The temperature in the water bath was monitored using a thermometer to ensure that the displayed temperature was correct. Compressed air was continuously supplied to the reactor at a flow-rate of 120 cm³/min. pH and redox potential were constantly monitored using the pH and redox meter, respectively. Fe concentrations were analysed using a UV spectrophotometer. At the end of the leaching process, the leached concentrate was filtered and washed with distilled water. Leach residues were dried and either re-leached to obtain maximum recovery or analysed using AAS via acid digestion, whilst the filtrate was analysed for Cu, Ni and Fe recoveries using AAS and ICP analysis.

3.9.7 Quantification of Ammonia Loss - Ammonia Vapour

Experiments were set up as described above, and the effect of different ammonia concentrations and temperatures on the rate of ammonia loss was monitored. The gas stream, consisting of ammonia, air and water vapour, exits the top of the stirred tank reactor or column and flows into an ammonia scrubber unit. The ammonia scrubber unit utilised two scrubbing stages, the first and second stages used distilled water in ordinary wash bottles. Mass balances around the system showed that the scrubber unit reduced the ammonia concentration in the off-gas to less than 25 ppm prior to venting to the atmosphere. Quantification of ammonia losses was done by analysing the initial ammonia concentration and the final concentration in the reactor or column's reservoir. These were balanced by analysing the ammonia dissolved in the wash bottles and that which had reacted with the base metals. The analysis of ammonia was done using a NOVA 60 spectroquant photometer (section 3.5).

4.0 RESULTS

Prior to tank and column leaching experiments, the representative concentrate samples were subjected to a series of shake flask leaching experiments to assess the leaching behaviour of samples over short time intervals. This enabled studying the leaching behaviour of the concentrate samples at different time periods and ammonia concentrations. Results are presented sequentially from shake flasks to columns followed by stirred tank results.

4.1 Shake flasks

4.1.1 Trial run

Figure 4.1 illustrates a trial run conducted in order to understand the ammoniacal leaching process on a shaking platform. The data shown is for an experiment carried out with 1% w/v solids, 5 M NH_4OH and 5 M $(\text{NH}_4)_2\text{CO}_3$ at ambient temperature. Ni extraction increased to 71% after 2 ½ days and gradually fell to 59% by day 4. It was observed that on day 4 there was a pH drop that occurred, from a pH of 9.40 to a pH of 8.94, and this could have resulted in the formation of $\text{Ni}(\text{OH})_2$ precipitates. Cu extraction continuously increased throughout the run. However, the rate of extraction reduced slightly as the pH dropped on day 4. The leach residues from the 4th day were re-leached with fresh solution at a pH of 9.41 to observe the pH effect. The Ni extraction increased from 59% to 91% in two days. This is likely due to an increase in pH, since a fresh solution was used. Cu extraction increased from 71% obtained on day 4 to 84% after being leached in fresh solution.

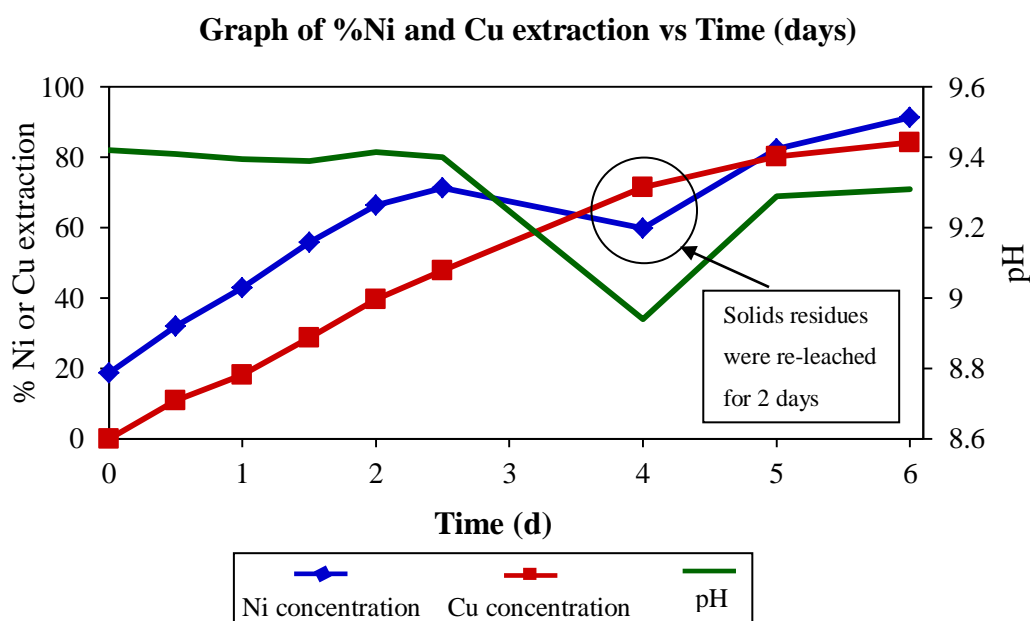


Figure 4.1: Trial run graph of %Ni and %Cu extraction against time and pH vs. time, 5 M NH_4OH and 5 M $(\text{NH}_4)_2\text{CO}_3$ ammoniacal lixiviant, ambient temperature, 1% w/v pulp density

The pH of the ammoniacal solution was found to be of great importance during the ammoniacal leaching process with regards to the OH^- ion required for the dissolution reaction and the production of free ammonia needed for the leaching reaction and prevention of metal precipitation. The shake flasks established the best pH range as between 9 and 10 through which maximum extraction of Ni and Cu may be obtained and precipitation of these metals reduced. $\text{Ni}(\text{NH}_3)_6^{2+}$ and $\text{Cu}(\text{NH}_3)_4^{2+}$ and $\text{Cu}(\text{NH}_3)_2^+$ are the most stable ammonia Ni and Cu complexes within the pH region of 9 to 10, which is outlined in section 2.14 by the E_{H} -pH diagram. Ammonia loss could have also contributed to the pH drop, as these were open flasks placed on a shaking platform. If a pH drop was noted after sampling and pH measurements, buffered ammoniacal solution was added to the system in all further experiments.

In order to study the effects of other parameters, the optimum pH obtained was maintained in all other experiments. The right buffering capacity was required in order to maintain the pH in the required range obtained as between 9 and 10.

4.1.2 Buffering effect

$(\text{NH}_4)_2\text{CO}_3$, NH_4Cl and $(\text{NH}_4)_2\text{SO}_4$ are the ammonium salts that were investigated in order to find a suitable buffer salt for the lixiviant. The most favourable salt obtained was $(\text{NH}_4)_2\text{CO}_3$. The buffer solution was obtained by dissolving known quantities of ammonium hydroxide (5M) and one of the ammonium salts (5M). The experiment was carried out at room temperature and using 1% w/v pulp density. Adding an ammonium salt to the system (shown in equation 15) adds lots of extra ammonium ions and minimises the formation of the hydroxide. According to Le Chatelier's principle, this promotes the backward reaction. The solution will therefore contain lots of unreacted ammonia for copper and nickel complexation and enough hydroxide ions to make the solution alkaline.

Figure 4.2 illustrates 3 graphs: graph (a) shows results of using ammonium sulphate buffer salt, graph (b) results of using ammonium chloride as a buffer salt and graph (c) results of using ammonium carbonate as the buffer salt. Graph (c) shows results of ammonium carbonate as a buffer with better copper and nickel recoveries in comparison to graph (b) for the ammonium chloride buffer and graph (a) for the ammonium sulphate buffer. For %Cu and %Ni extraction, graph (c) reached 77% and 90% respectively, graph (b) had 12% and 12% respectively and graph (a), had 12% and 6% after 6 days of leaching, respectively. The

pH stability for the $(\text{NH}_4)_2\text{CO}_3$ is better than for NH_4Cl and $(\text{NH}_4)_2\text{SO}_4$. Graph (c) indicates a pH range between 9 and 10, whilst the pH for graph (a) and (b), rapidly declined from pH 10 to as low as pH 5.

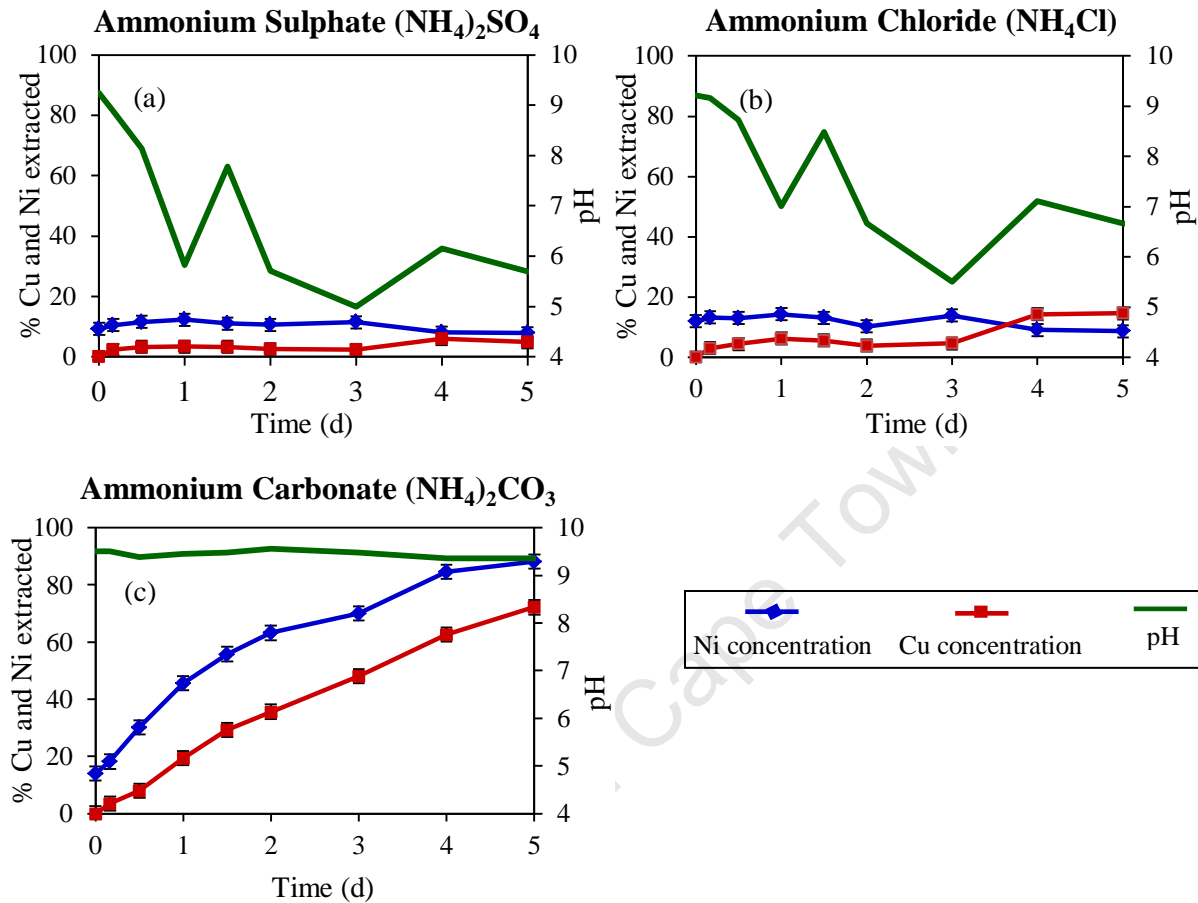


Figure 4.2: Graphs of Cu and Ni extraction using different buffer solutions. Graph (a) 5 M NH_4OH and 5 M $(\text{NH}_4)_2\text{SO}_4$, Graph (b) 5 M NH_4OH and 5 M NH_4Cl and Graph (c) 5 M NH_4OH and 5 M $(\text{NH}_4)_2\text{CO}_3$ ammoniacal lixiviant. All experiments at ambient temperature (25 °C) and pressure and used 1% w/v pulp density.

Ammonium carbonate has a higher pK_a than the other two salts. The high pK_a value of the CO_3^{2-} ($\text{pK}_a = 10.3$), together with the pK_a of ammonia ($\text{pK}_a = 9.23$) give $(\text{NH}_4)_2\text{CO}_3$ a rather broad buffering range in the more alkaline pH range, unlike NH_4Cl and $(\text{NH}_4)_2\text{SO}_4$. Anion Cl^- has a $\text{pK}_a = 2.86$ and is a conjugate base for a strong acid, and is thus a weak base. Hence, it has no effect on pH as well as the SO_4^{2-} with a $\text{pK}_a = 1.92$. This is why NH_4Cl and $(\text{NH}_4)_2\text{SO}_4$ have lower buffering capacities. A high pK_a results in less ammonia losses (Kotz and Treichel, 2003). Hence, it was concluded that the ammonium carbonate salt was a better buffer and in all experiments that followed ammonium carbonate was used.

4.1.3 Ammonia concentration

To study the effect of the total ammonia concentration on the rate of leaching solutions, equimolar amounts of ammonium carbonate and ammonium hydroxide were used. The optimum ammoniacal solution obtained was 4 M NH_4OH and 4M $(\text{NH}_4)_2\text{CO}_3$ using different equimolar ammonia concentrations ranging from 0.5 M to 5 M of the NH_4OH and $(\text{NH}_4)_2\text{CO}_3$ each in the investigation, with 1% w/v solids at ambient temperature. The optimal concentration obtained copper recoveries of 73% and nickel recoveries of 93% within 4 days as shown in Figure 4.3 (a) and (b). The analytical error for each triplicate analysis was $\pm 3\%$.

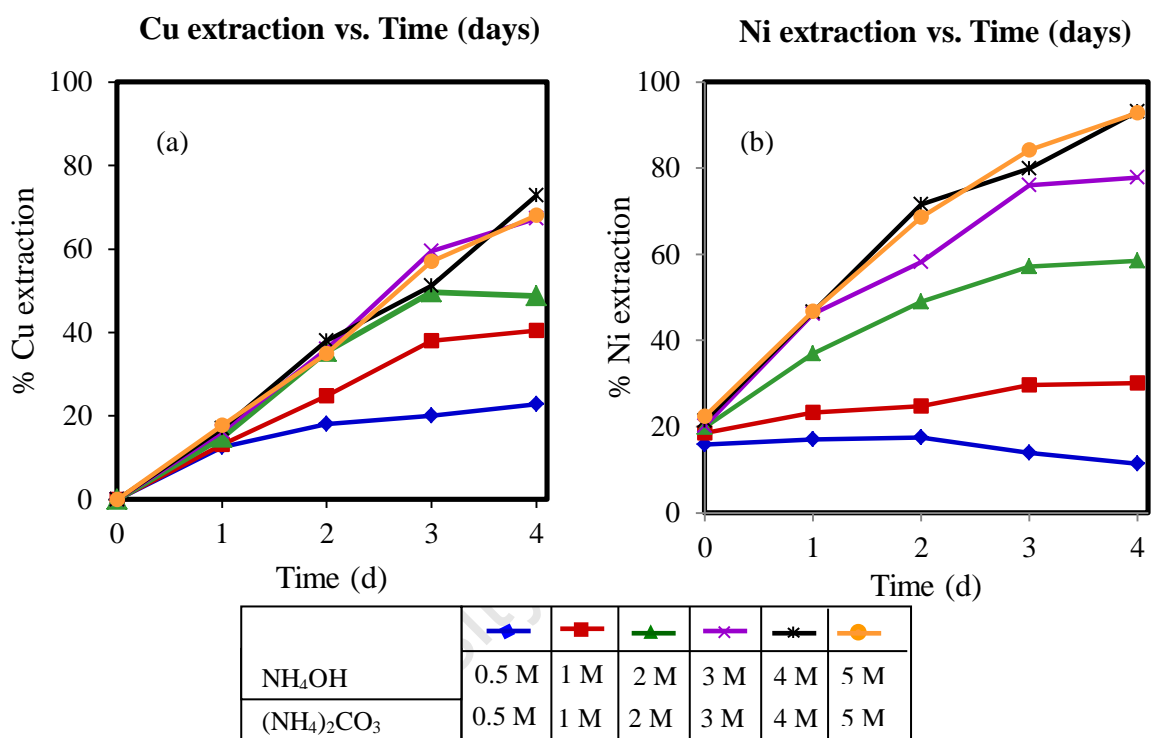


Figure 4.3: Graph (a) of Cu extraction using different total ammonia concentrations, ambient temperature and pressure and 1% w/v pulp density. Graph (b) of Ni extraction using different total ammonia concentrations, ambient temperature and pressure and 1% w/v pulp density.

Generally, it was observed that as the concentration of the ammoniacal lixiviant increased, the extraction of Cu and Ni and the pH stability increased. The pH values of all the flasks except those with a molarity of 1 M remained within the required range of 9 to 10. The pH of the flasks with 1 M molarity dropped below 9 on day 3 to a pH of 8.89. 5 mL of buffered solution of the same strength was added to increase the pH to 9.03. The Cu dissolution rate observed in 1 M, 2 M, 3M, 4 M and 5 M could have resulted from a drop in pH with time as these were open shake flasks and ammonia was lost.

4.1.4 Results of Fe

Fe was monitored on a daily basis using a UV Spectrophotometer at a wavelength of 510 nm and the results compared with those obtained using AAS analysis. These gave Fe concentrations approximately 2 mg/L to 10 mg/L, thus indicating that iron is superficially dissolved or hardly dissolved. In the presence of air, oxidising conditions exist, hence any iron dissolved is immediately oxidised to the ferric form, which subsequently precipitates as iron hydroxide or oxide and this could have been the reason for low Fe. As discussed in section 2.1.7, it is of added advantage that iron does not dissolve in ammoniacal solutions.

4.1.5 Redox potential vs. pH

The general trend was that, as the experiment proceeded, the pH decreased slightly, whilst the redox potential increased. The redox potential for all experiments carried out in the shake flasks had a range from 0 mV to 90 mV. Table 4.1 gives typical results obtained for one run carried out in the shake flasks. Other runs had similar redox-pH changes.

Table 4.1: Results of redox and pH for one run conducted in shake flasks at 4M ammonia concentration, 1% w/v

Time (d)	0	0.5	1	1.5	2	2.5	4	6.5	8.5
pH	9.50	9.41	9.40	9.39	9.42	9.40	9.16	9.29	9.20
Redox potential (V)	0.000	0.047	0.058	0.063	0.047	0.0555	0.084	0.087	0.070

Typically, alkaline redox potentials are low. According to the Nernst equation (equation 10 – repeated for clarity), the redox is a result of the ratio of the concentration of $\text{Cu}(\text{NH}_3)_2^+$ and $\text{Cu}(\text{NH}_3)_4^{2+}$ (Meng and Han, 1996).

$$E_H = 0.074 - 0.1182 \log[\text{NH}_3] + 0.0591 \log \frac{[\text{Cu}(\text{NH}_3)_4^{2+}]}{[\text{Cu}(\text{NH}_3)_2^+]} \dots\dots\dots (10)$$

where E_H is the oxidation potential:

The pH of the system was maintained in the range of 9 to 10 and in this region $\text{Cu}(\text{NH}_3)_4^{2+}$ acts as an oxidant such that the ratio of $\text{Cu}(\text{NH}_3)_4^{2+} / \text{Cu}(\text{NH}_3)_2^+$ is positive as the Cu(II) ions are the predominant form. With known ammonia concentration and E_H , the Cu(II)/Cu(I) ratio can be estimated as illustrated in Table 4.2. The redox potentials were measured using a combined Pt and Ag/AgCl reference electrode (Metrohm). The measured redox potentials were converted to E_H versus the standard hydrogen electrode (SHE) by the correction factor

of the Ag/AgCl reference electrode (adding 208 mV for 3 M KCl junction electrolyte (Altmaier et al., 2010). Free NH_3 is calculated using the solubility constant and pH of the system. For example, given a certain E_H at a pH of 9.25, the NH_3 to NH_4^+ ratio is 1:1 and the ratio of Cu(II) to Cu(I) may be determined using equation 10 as illustrated in Table 4.2.

Table 4.2: Table of Cu(II) to Cu(I) ratio at a pH of 9.25 and k_s of NH_3 of 1.8×10^{-5}

Redox (V)		0	0.03	0.06	0.09
E_H (V)		0.208	0.238	0.268	0.298
Cu(II):Cu(I) ratios					
NH_3	NH_4^+	ratio	ratio	ratio	ratio
0.5	0.5	46:1	149:1	479:1	1542:1
1	1	185:1	596:1	1917:1	6169:1
2	2	740:1	2382:1	7667:1	24674:1
3	3	1666:1	5360:1	17251:1	55517:1
4	4	2961:1	9530:1	30668:1	98697:1
5	5	4627:1	14890:1	47919:1	154215:1

As the concentration of free ammonia increases the $\text{Cu}(\text{NH}_3)_4^{2+}$ increases, hence increasing the oxidising potential of the Cu(II) ions in the reaction. This could be the reason why the rate of reaction is higher at higher ammonia concentration and also more Cu and Ni is extracted due to autocatalysis. An increase in the value of E_H is indicative of an increase in the ratio of Cu(II) to Cu(I) at the same free ammonia concentration.

4.2 Optimal conditions observed in shake flasks

The ammoniacal leaching process is sensitive to pH changes. The best pH range established in the shake flasks was between 9 and 10 with minimal precipitation, as copper and nickel ammine complexes are more stable. The best buffer salt that maintained the pH within the required region and enabled better Cu and Ni extraction was $(\text{NH}_4)_2\text{CO}_3$. The best ammoniacal lixiviant concentration which gave the best Cu and Ni extraction of 73% and 93% respectively was a solution of 4M NH_4OH and 4M $(\text{NH}_4)_2\text{CO}_3$. These conditions were implemented in columns and tanks as the base case to enable better exploration of the ammoniacal leaching process. Initial tests in the shake flask showed that hardly any Fe, Mg, Al or Ca was dissolved in the leaching tests and in subsequent experiments these elements were not analysed.

4.3 Results of columns

A comparison between the base case ammoniacal lixiviant and that with half the ammonium carbonate was studied in order to investigate the effect of the $(\text{NH}_4)_2\text{CO}_3$ on the Cu and Ni extraction in columns. An investigation of different ammonia concentrations was also done using the columns. 1 L of ammoniacal lixiviant was recycled through the system every 3 days before a fresh solution was placed, maintaining a flow-rate of 1 L/d. The effect of temperature was observed at two different temperatures, i.e. ambient temperature (25 °C) and 40 °C due to time constraints.

4.3.1 Effect of the ratio of NH_4OH to $(\text{NH}_4)_2\text{CO}_3$ on the Cu and Ni extracted

Initially experiments were carried out for 42 days, in two columns using different ratios of $\text{NH}_4\text{OH}:(\text{NH}_4)_2\text{CO}_3$ i.e. 4 M NH_4OH :4 M $(\text{NH}_4)_2\text{CO}_3$ (base case) and 4 M NH_4OH :2 M $(\text{NH}_4)_2\text{CO}_3$. This gives a ratio of ammoniacal lixiviant of 1:1 and 2:1, respectively. Table 4.3 outlines the total %Cu and %Ni extraction. These experiments were carried out at ambient temperature and pressure with air flow-rate at 80 mL/min. The column experiments were run over a long period and due to time constraints experiments were not done in duplicate. This might compromise the replicability of the experiments, however, the results obtained were sufficient in showing that the process is technically feasible (research objective). Samples were sent in duplicates with an experimental error of $\pm 3\%$.

Table 4.3: The effect of the ratio of NH_4OH to $(\text{NH}_4)_2\text{CO}_3$ concentration in columns in 42 days

Column	Ratio	NH_4OH	$(\text{NH}_4)_2\text{CO}_3$	Cu	Ni
A	1:1	4 M	4 M	87%	69%
B	2:1	4 M	2 M	90%	64%

It was observed that the %Ni extraction using the 1:1 and 2:1 ammoniacal lixiviant was comparable with 69% and 64% Ni extraction, respectively. The %Cu extracted was slightly higher in the 2:1 ratio at 90%, but with only a 3% extraction difference with the 1:1 ratio. The results obtained were comparable with slightly higher Cu extracted in the 2:1 and in order to reduce costs of the reagents the ratio of 2:1 was used in all other column experiments in the study as ammonium carbonate is more expensive than ammonium hydroxide.

4.3.2 Effect of ammonium concentration on the rate of Cu and Ni extraction

The effect of ammonium concentration was investigated further in column leach tests at ambient temperature and pressure and using an air flow-rate of 80 mL/min. The extractions of Cu and Ni in columns A and B are shown in Table 4.3 and for columns C, D and E are shown in Table 4.4. Samples were sent in duplicates with an Error of $\pm 3\%$.

Table 4.4: %Cu and %Ni extraction obtained at different ammonia concentration in 42 days

Column	NH ₄ OH	(NH ₄) ₂ CO ₃	Cu	Ni
C	2 M	1 M	81%	18%
D	1 M	0.5 M	42%	14%
E	0.5 M	0.25 M	24%	4%

The %Cu and Ni extraction over a 42 day period are illustrated in Figure 4.4 (a) and (b). The amount of base metals extracted from the concentrates increased at a more or less constant rate and did not show any sign of slowing in the course of the experiment. Higher %Cu and %Ni extraction was obtained in columns with concentrates being leached with more concentrated ammoniacal lixiviant. This was in agreement with observations made in shake flasks. However, the amount of Ni leached in the columns was less than the copper extracted, which is the opposite of what was observed in the shake flasks. Given the linear rate of extraction the process is likely to be reagent limited relative to shake flask experiments.

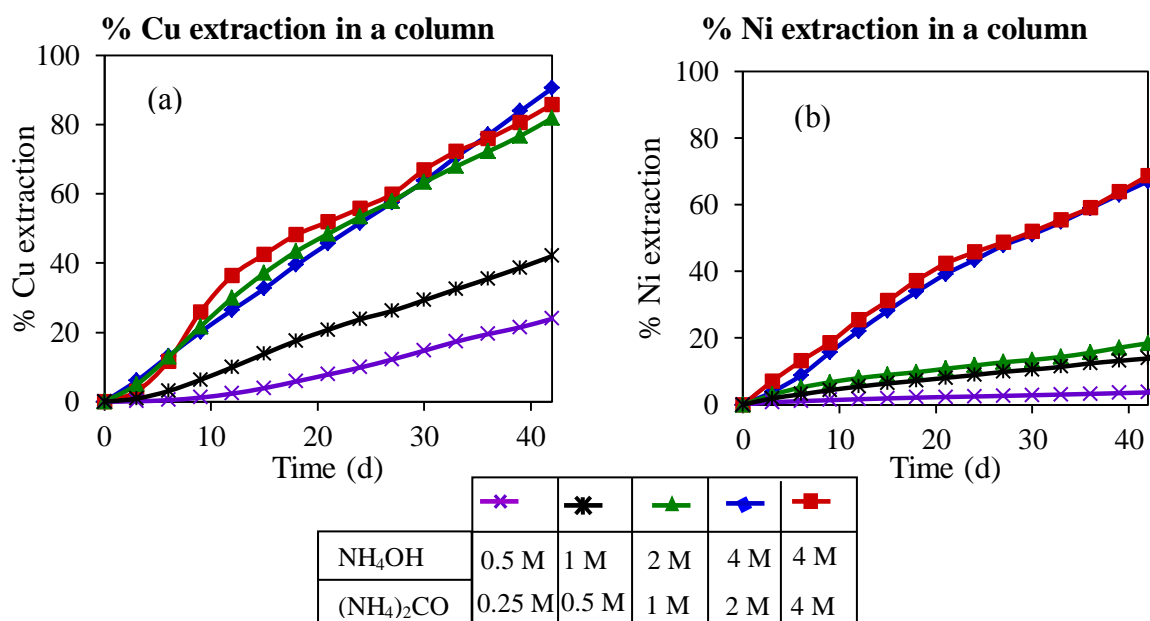


Figure 4.4 (a) and (b): %Cu and %Ni extracted respectively at different total ammonia concentrations, at ambient temperature and pressure, 80 mL/min of air.

Dutrizac (1981) obtained 3 to 10 % Cu recoveries from a high grade chalcopyrite ore with 4.78% Cu in 3 months using a total ammonium concentration of 2 M NH_3 and ore P_{95} of 0.297 mm. Dutrizac (1981) suggests that this could have been as a result of Fe_2O_3 build-up which inhibited the reaction. In the experiments under study the concentrates had a P_{97} of 0.45 μm size and were coated onto coarse support rock and leached. It is postulated that ferric oxide did not inhibit the reaction as the particle size used was small. Chuanhui et al. (2000) obtained 30% Cu recovery in 1 week with P_{80} of 1.7 mm and all passing 2 mm.

4.3.3 Effect of temperature on the rate of Cu and Ni extraction

The effect of temperature on Cu and Ni extraction in the columns is presented in Figure 4.5 (a) and (b) respectively. The experiments were carried out at 40 °C and compared with those carried out at ambient temperature. A higher temperature tends to increase the amount of Cu and Ni extracted within the same period. As illustrated in Figure 4.4 (a) and (b), at 1 M ammonia concentration, Cu extracted increased from 24 to 60%, whilst at 4 M, Cu increased from 81 to 100% when temperature was increased from ambient to 40 °C in 42 days. Ni extraction increased from 4 to 9% using 1 M ammonia concentration and 20 to 50% for 4 M ammonia concentration when temperature was increased from ambient to 40 °C in 42 days. The curves are all linear, including the 4 M NH_3 Cu curve which goes up to 100% in a linear manner. Linear leach profiles normally relate to reagent limited leaching. Bell et al. (1995) found temperature dependence of the leaching rate in a high-pressure autoclave at 6 900 kPa pressure and temperature range of 20 to 100 °C demonstrating in-situ leaching, whilst Dutrizac (1981) obtained a 28% Cu extraction increase after increasing the temperature from 25 °C to 65 °C. Dutrizac (1981) noted that at higher temperatures, the results became less reproducible. Chuanhui et al. (2000) during their one week column run also observed an increase in Cu extraction after increasing the temperature from 25 °C to 41 °C. The analysis of activation energy is presented in section 5.2.

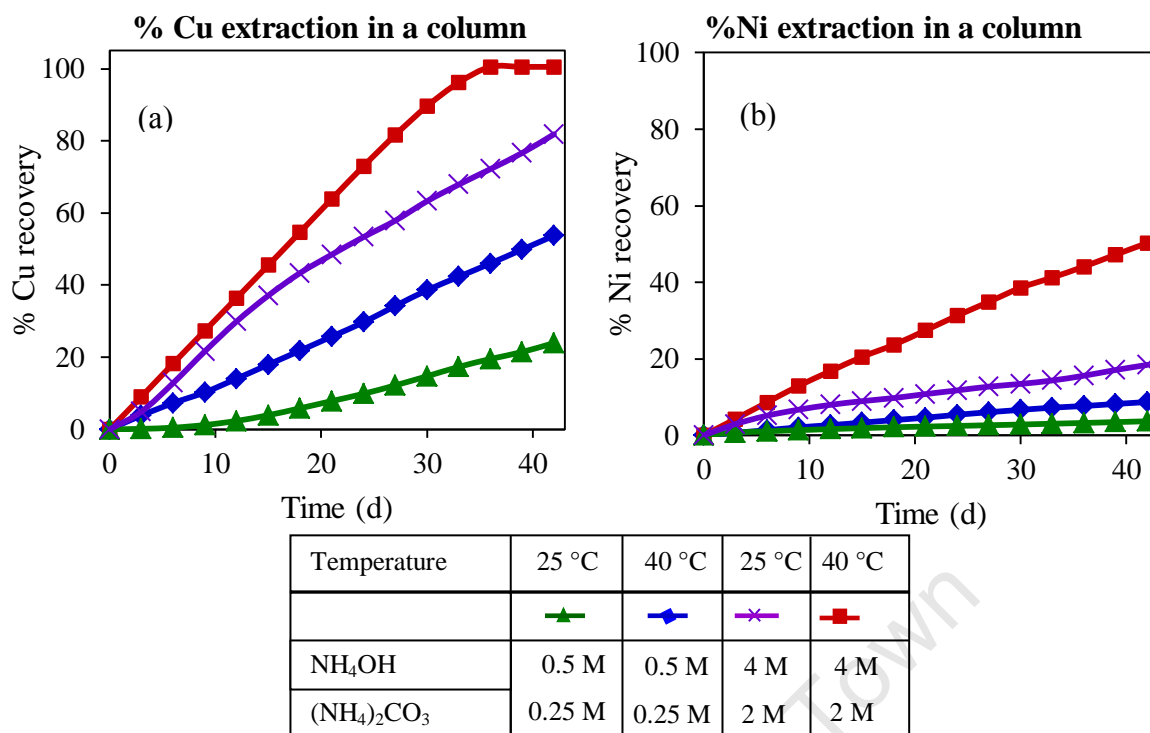


Figure 4.5 (a) and (b): Effect of temperature on amount of Cu and Ni extracted using 1M and 4M total NH_3 concentrations at ambient temperature and pressure, 80 mL/min of air.

4.4 Results of leaching in batch stirred tank reactors

4.4.1 Effect of pulp density

The batch leach tests enabled higher slurry concentrations to be investigated and a more controlled ammonia environment. Figure 4.6 (a) and (b) illustrate the effect of pulp density using 4 M NH_4OH and 4 M $(\text{NH}_4)_2\text{CO}_3$ at 50°C, 500 rpm and air flow-rate of 120 cm³/min. The curves start at approximately 20%, showing a significant amount of Ni is in soluble form, which could be an oxidized form of Ni. This case is not the same for Cu, as Cu is gradually extracted from 0. Two Applikon[®] reactors were used in all experiments to observe any analytical error (shown by the error bars). Generally, good extractions were obtained at the optimal conditions (section 4.2) despite the fact that different pulp densities were used. 100% Cu extraction was observed for 2% and 5% w/v pulp densities and 100% Ni extraction was observed for the 5% w/v pulp density. The extraction of Cu and Ni over the first day marginally increases as pulp density increases from 1 to 5% but then declines when moving from 5 to 20% pulp density. The increase observed from 1 to 5% could have resulted from an increase in $\text{Cu}(\text{NH}_3)_4^{2+}$ which acts as a redox mediator and hence autocatalysis by the $\text{Cu}(\text{NH}_3)_4^{2+}$ improves the amount of Cu and Ni extracted.

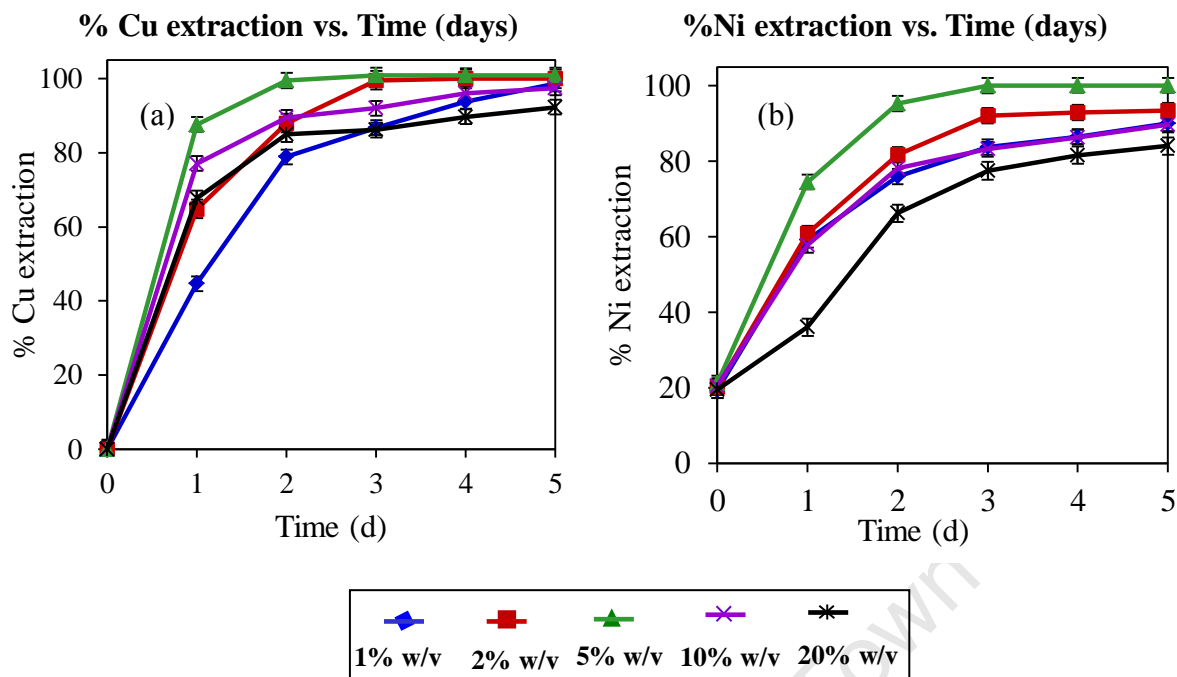


Figure 4.6 (a) and (b): % Cu and Ni extraction using different pulp densities, 4 M NH_4OH , 4M $(\text{NH}_4)_2\text{CO}_3$, pH 9.35, 500 rpm, 50 °C and 120 cm^3/min air flow-rate. 2 Applikon[®] reactors were used to reduce analytical error.

Despite the slight decrease in % extraction of base metals when pulp density was increased from 5 to 20%, Table 4.5 shows that the total amount of Cu and Ni extracted went up in a linear manner. This shows that the effect of the pulp density is largely negligible over 5 days.

Table 4.5: Total amount of Cu and Ni extracted in 5 days

Pulp Density	Cu		Ni	
	% Cu extraction	Cu released	% Ni extraction	Ni released
1%	99	199 mg/L	90	285 mg/L
2%	100	404 mg/L	93	592 mg/L
5%	100	1019 mg/L	100	1587 mg/L
10%	98	1970 mg/L	90	2843 mg/L
20%	92	3727 mg/L	84	5327 mg/L

*The Cu concentration is the total amount of Cu and Ni extracted in 5 days including the initial extraction of approximately 20%

However, before the reaction reaches completion, for example after day 1, they are kinetic effects as a result of the different solid to liquid ratio shown by the different slopes in Figure 4.6. To ensure that the reaction was not limited by mass transfer at the gas-liquid interface, the reaction was studied at dilute solid phase concentration (2% w/v) in the subsequent experiments.

4.4.2 Effect of ammonia concentration

In Figure 4.7 (a) and (b) the amount of Cu and Ni extracted at different ammonia concentration but with all other conditions kept constant is shown. The effect of ammonia concentration was studied using different ammonia concentrations at 50°C, 500 rpm impeller speed, air flow-rate of 120 cm³/min and 2% w/v pulp density. The results show that there is an increase in the initial rate of leaching as the ammonia concentration increased, showing a significant effect on the leaching of Cu and Ni. Studies by Forward (1953) have shown that an increase in free (unbound) ammonia increases the rate of leaching and maximum extraction of Cu and Ni metals. This is in agreement with Stanczyk and Rampacek (1966), Reilly and Scott (1977) and Dutrizac (1981). At 0.5 M NH₄OH and 0.5 M (NH₄)₂CO₃, after an initial increase, the extraction of both Cu and Ni remained low and unchanged over the following days. After day 1, the extraction rate of Cu and Ni declines for the highest ammonia concentration but not as rapid as the other concentrations. After 3 days, near complete extraction of Cu and Ni is observed when 4 M NH₄OH and 4 M (NH₄)₂CO₃ is used and the % extraction does not increase any further after 3 days, whilst at 2 M NH₄OH and 2 M (NH₄)₂CO₃ and 1 M NH₄OH and 1 M (NH₄)₂CO₃ the amount of Ni extracted has a linear profile.

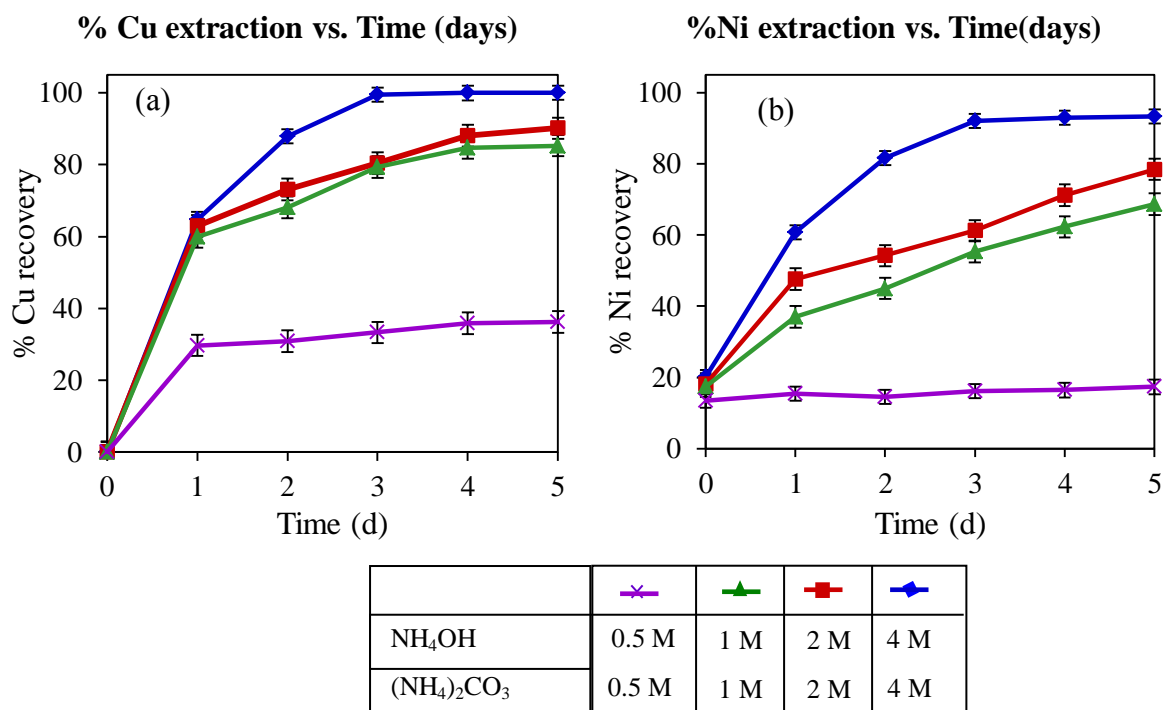


Figure 4.7 (a) and (b): Effect of ammonia concentration on amount of Cu and Ni extracted, 2% w/v, pH 9.35, 500 rpm, 50 °C and 120 cm³/min air flow-rate. 2 Applikon® reactors were used in each experiment to reduce analytical error.

4.4.3 Effect of temperature

The effect of temperature on the rate of Cu and Ni extraction is shown in Figure 4.8 (a) and (b). The effect of temperature was determined using 4M ammonium hydroxide and 4M ammonium carbonate, 500 rpm impeller speed, air flow-rate of 120 cm³/min and 2% w/v pulp density. The amount of initial copper and nickel extracted seemed to be depended on the concentration of ammonia with little variation with temperature. However, the results suggest that an increase in temperature increases the overall rate at which Cu and Ni are extracted from chalcopyrite and pentlandite concentrates, respectively, which is in agreement with Beckstead and Miller (1977a), Bell et al. (1995) and Dutrizac (1981). It must be noted that there was a considerable reduction in the volume of the solution due to evaporation as the temperature increased. 15 mL of buffered ammoniacal lixiviant of the same molarity was added to the reactor to replace 10 mL of sample taken and 5 mL of that evaporated and thus maintain more or less constant volume and pH. This could, however, have resulted in a slight increase in the overall molarity.

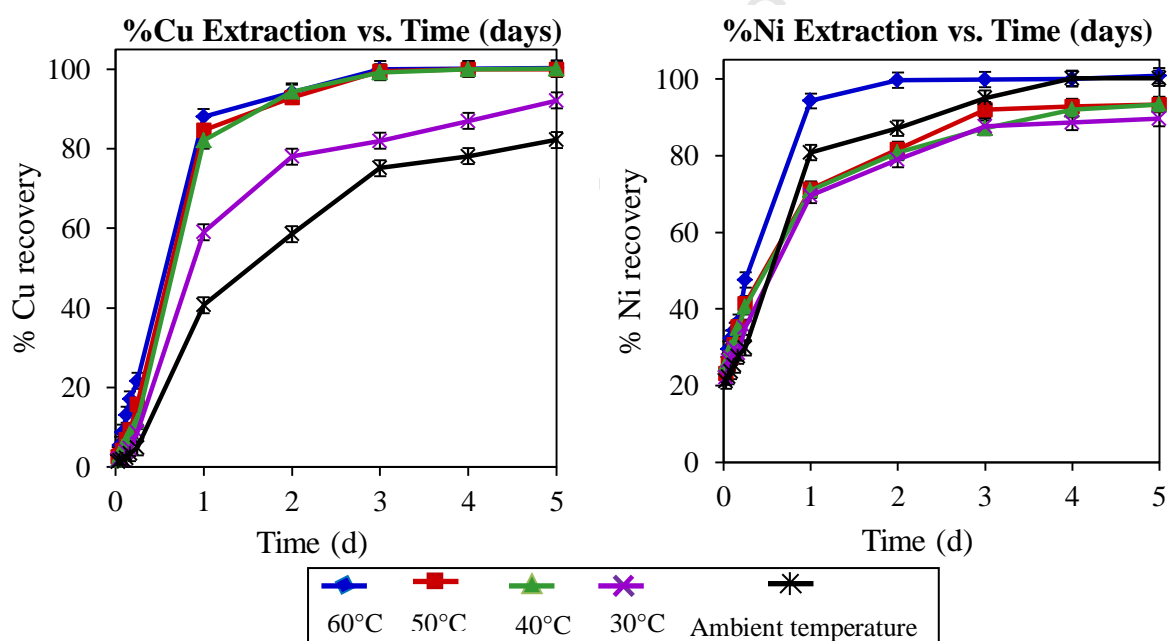


Figure 4.8 (a) and (b): Cu and Ni extracted at different temperatures using 2% w/v, 4 M NH₄OH, 2M (NH₄)₂CO₃, pH 9.35, 500 rpm and 120 cm³/min air rate. 2 Applikon® reactors were used in each experiment to reduce analytical error.

The Ni curves (Figure 4.8 (b)) start at approximately 20%; showing a significant amount of Ni is soluble, possibly in an oxidized form. This case is not the same for Cu, as Cu is gradually extracted from 0.

4.5 Results of the measurement of ammonia losses

Ammonia losses were observed to increase as temperature and ammonia concentration increased. In both the stirred tank reactor and the column, almost all the ammonia was scrubbed off in the first wash bottle, with residual ammonia being washed in the second bottle. A careful mass balance of NH_3 in the tank and wash bottles showed good closure. To quantify the ammonia losses, the equation used was:

$$(\text{NH}_3)_{\text{total}} = (\text{NH}_3 + \text{NH}_4^+ + \text{Cu}(\text{NH}_3)_n^{2+} + \text{Ni}(\text{NH}_3)_n^{2+})_{\text{reactor}} + (\text{NH}_3 + \text{NH}_4^+)_{\text{wash bottles}} + \text{other losses beyond wash bottles and bound to other species not desired} \dots\dots\dots(23)$$

This provided an estimated value of the ammonia being lost. It was observed that the ammonia losses were greatest when the experiment started, but reduced as the days progressed.

4.5.1 Ammonia losses in batch stirred tank reactors

Table 4.6 shows the ammonia lost in the first and second wash bottles and the total ammonia lost from the reactor and recovered in the wash bottles in 4 days. From this table it is observed that more ammonia is lost in the first wash bottle with residual ammonia being scrubbed off in the second wash bottle.

Table 4.6: Ammonia losses observed in wash bottles 1 and 2 in the tank leaching system (*WB is wash bottle)

NH_4OH (M)	$(\text{NH}_4)_2\text{CO}_3$ (M)	Temp	WB 1(M)	%WB 1	WB2 (M)	%lost in WB 2	Total lost in WB (M)	Total % lost in WB
4	4	50 °C	1.341	11.18%	0.044	0.37%	1.385	11.54%
2	2	50 °C	0.508	8.47%	0.034	0.56%	0.541	9.03%
0.5	0.5	50 °C	0.065	4.33%	0.042	2.8%	0.107	7.13%
4	4	40 °C	1.24	10.33%	0.021	0.18%	1.261	10.51%
4	4	ambient	1.05	8.28%	0.011	0.07%	1.061	8.35%

Figure 4.9 (a) shows the total ammonia accumulation with time in the two wash bottles lost from the stirred tank reactor with time at different ammonia concentrations. These results show a more or less linear increase in ammonia lost with time. At lower concentrations, less ammonia is lost. For example, at the same temperature of 50 °C, 0.107 M of NH_3 was lost when 0.5 M NH_4OH and 0.5 M $(\text{NH}_4)_2\text{CO}_3$ was used, compared to 1.39 M ammonia lost

when 4 M NH_4OH and 4 M $(\text{NH}_4)_2\text{CO}_3$ was used. The solubility of NH_3 gas (M) is smaller in the concentrated solution than in the dilute aqueous medium, hence, increase in ammonia concentration results in an increase in ammonia loss. Figure 4.9 (b) shows the total ammonia scrubbed off in the wash bottles with time and how it is affected by temperature. An increase in temperature also resulted in a higher loss in ammonia. For example, looking at 4 M NH_4OH and 4 M $(\text{NH}_4)_2\text{CO}_3$ at different temperatures, more ammonia was lost at 50 °C (1.385 M) in comparison to ammonia lost at 40 °C (1.261 M) and the least lost at ambient temperature (1.061 M). Although somewhat higher evaporation is observed at higher temperatures, this effect is not dramatic and not consistent. Evaporation rates are discussed in section 5.6.

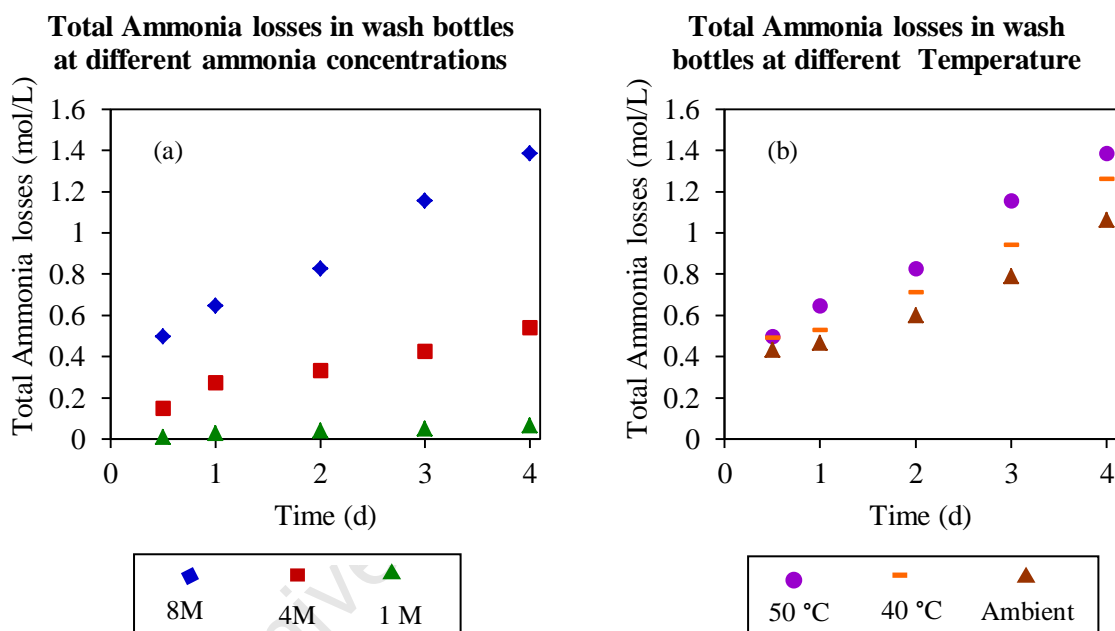


Figure 4.9 (a): % Ammonia losses at different ammonia concentrations and (b) Ammonia losses at different temperature 2% w/v, 4 M NH_4OH , 4M $(\text{NH}_4)_2\text{CO}_3$, pH 9.35, 500 rpm and 120 cm^3/min air rate

A significant increase in ammonia lost with ammonia concentration at the same temperature (Figure 4.9 (a)) was observed in comparison to an increase in temperature at the same ammonia concentration (Figure 4.9 (b)).

4.5.2 Ammonia losses in columns

Table 4.7 shows the ammonia lost in the first and second wash bottles and the total ammonia lost from the reactor and recovered in the wash bottles. Fresh feed of 1 L was replaced for leaching in columns every 3 days. Ammonia losses were measured in 3 days for each

ammoniacal solution before fresh feed solution was replaced and fresh distilled water replaced in the wash bottles. Table 4.7 shows that more ammonia was lost in the first wash bottle with residual ammonia being scrubbed off in the second wash bottle. However, unlike in the tanks where the ammonia lost in the wash bottle 2 was negligible, reasonable amounts were scrubbed off in the column's second wash bottle.

Table 4.7: Ammonia losses observed in wash bottles 1 and 2 in the column leaching system (WB is wash bottle)

NH ₄ OH (M)	(NH ₄) ₂ CO ₃ (M)	Temp	WB 1(M)	% WB 1	WB2 (M)	%lost in WB 2	Total lost in WB (M)	Total % lost in WB
4	4	ambient	1.14	9.46%	0.54	4.53%	1.68	13.99%
4	2	ambient	0.73	9.13%	0.32	4.01%	1.05	13.14%
2	1	ambient	0.37	9.35%	0.10	2.50%	0.47	11.85%
1	0.5	ambient	0.13	6.60%	0.02	0.75%	0.15	7.35%
0.5	0.25	ambient	0.05	5.05%	0.01	1.00%	0.06	6.05%
2	1	40 °C	0.46	11.5%	0.15	3.75%	0.61	15.25%
0.5	0.25	40 °C	0.08	8.00%	0.02	2.00%	0.10	10.00%

Figure 4.10 shows the total ammonia accumulation with time in the two wash bottles lost from the column with time at different ammonia concentration. These results show an increase in ammonia lost with time. More ammonia is lost in the more concentrated reactions. Evaporation rates are calculated in section 5.

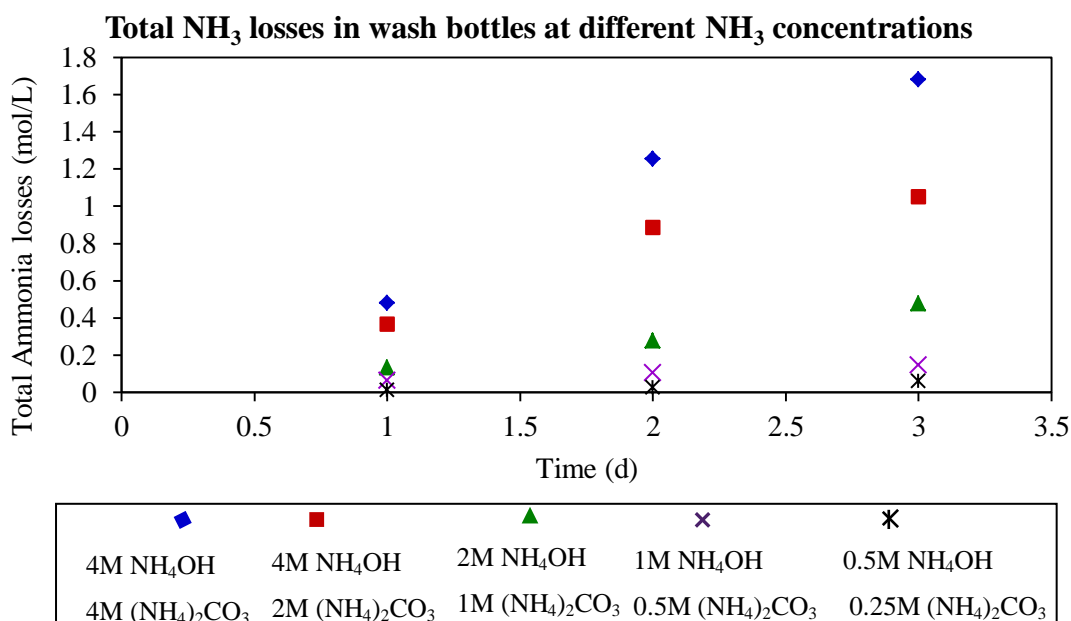


Figure 4.10: % Ammonia losses at different ammonia concentrations, at ambient temperature and pressure, pH 9.35, 500 rpm and 80 mL/min air flow-rate

Only two temperatures were used to study the effect of temperature. An increase in temperature resulted in a higher loss in ammonia. For example, in Table 4.7 it can be observed that for 2 M NH_4OH and 1 M $(\text{NH}_4)_2\text{CO}_3$, the ammonia lost increased from 0.47 M to 0.61 M when the temperature was increased from ambient to 40 °C, with a 5% difference in ammonia lost.

University of Cape Town

5.0 DISCUSSION

5.1 Activation energy in batch stirred tank reactor tests

Figure 4.8 (a) and (b) show a fairly linear profile from the first few minutes of the reaction up to day 1. The gradient of these curves is a reflection of the initial rates of reaction. When temperature was varied, samples were taken in 5 min intervals for the first 20 min, then every 40 min for 2 h and then on an hourly basis for another 2 h as illustrated in Figure 5.1 (a) and 5.2 (a). Arrhenius plots of the temperature dependence data are shown in Figure 5.1 (b) and 5.2 (b). These show the initial rate in units of min^{-1} against the inverse of absolute temperature (K^{-1}) for Cu and Ni in 4 h. This was done because a certain amount of Ni extraction was very instantaneous, such that after 40 min approximately 25% of the Ni was leached into the solution whilst Cu gradually increased initially from 0 to obtain a fairly linear regression passing through the origin. To quantify the activation energy, initial rate constants were calculated by determining the initial slope from a linear regression over the first 5 data points for Cu and Ni, respectively. The Arrhenius equation used for regression analysis is:

$$\log k = \frac{E_a}{2.303 RT} + \log A \dots \dots \dots (24)$$

k = initial leach rate (min^{-1}), A = pre-exponential factor, E_a = activation energy (J), R = universal gas constant (8.314 J/mol/K), T = absolute temperature (K).

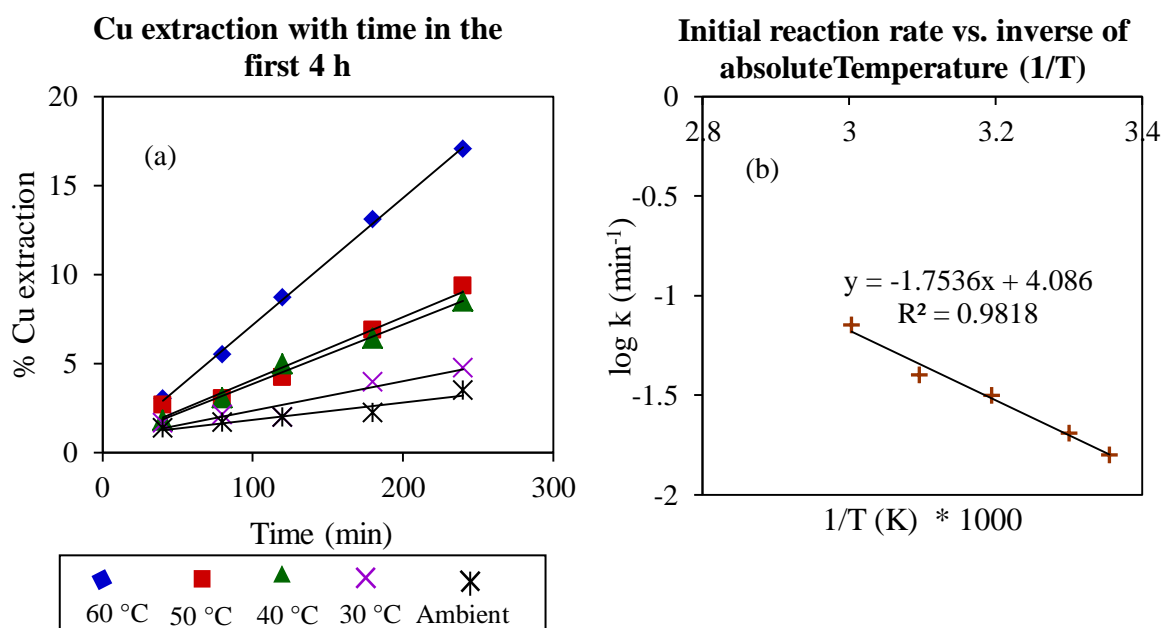


Figure 5.1: Graph (a) is a plot of the %Cu extra extraction in the first 4 hours at different temperatures and Graph (b) is the plot of the initial rates of reaction against the inverse of the absolute temperature.

Table 5.1: k and R² values for the slope of the regression lines in Figure 5.1 (a).

Temperature (°C)	Reaction rate k	R ²
60	0.0713	0.999
50	0.0398	0.978
40	0.0316	0.992
30	0.0204	0.991
25	0.0158	0.945

Table 5.1 and 5.2 are the k and R² values obtained for the slope of the regression lines in Figure 5.1 (a) and 5.2 (a), respectively. The slopes are fairly linear with high correlation values. The rate of reaction increases as the temperature increases.

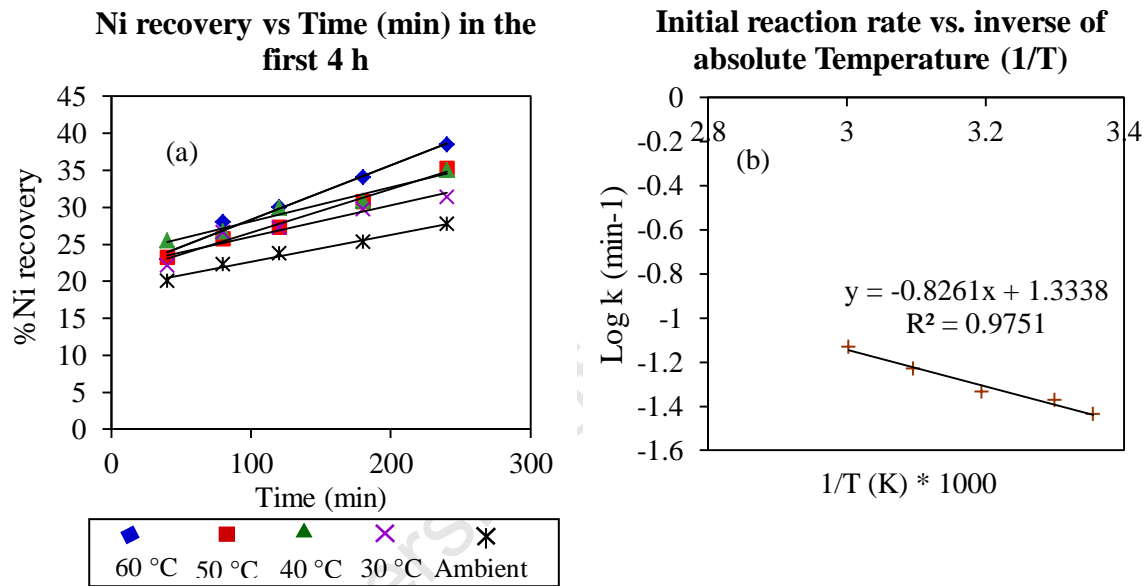


Figure 5.2: Graph (a) is a plot of the %Ni extraction within the first 4 hours at different temperatures and Graph (b) is the plot of the initial rates of reaction against the inverse of the absolute temperature

Table 5.2 : k and R² values for the slope of the regression lines in Figure 5.2 (a).

Temperature (°C)	Reaction rate k	R ²
60	0.0620	0.957
50	0.0588	0.990
40	0.0464	0.965
30	0.0385	0.945
25	0.0323	0.994

Within the range of variables studied an E_a of 33.6 kJ/mol was obtained for Cu extraction and 15.8 kJ/mol for Ni extraction was obtained. Most of the Cu extracted was from chalcopyrite and most of the Ni from pentlandite. This indicates a mixed control reaction with respect to copper and a transport controlled reaction with respect to nickel. Beckstead and Miller

(1977a) obtained an E_a of 42 kJ/mol, and they suggest that the reaction was limited by a surface reaction rate mechanism.

5.2 Activation energy in columns

The effect of temperature in columns was tested only at ambient temperature (25 °C) and at 40 °C due to time constraints. Temperature was varied for columns operated with 1 M and 4 M total ammonia concentration. Arrhenius plots of the temperature dependence data are shown in Figure 5.3 (b) and 5.4 (b). These show the initial rate in units of min^{-1} against the inverse of absolute temperature (K^{-1}) for Cu and Ni in 15 days. To quantify the activation energy, initial rate constants were calculated by determining the initial slope from a linear regression over the first 5 data points for Cu and Ni, respectively. As there are only two data points (one at 25 °C and one at 40 °C), the slopes in Figure 5.3 (b) and 5.4 (b) are exact.

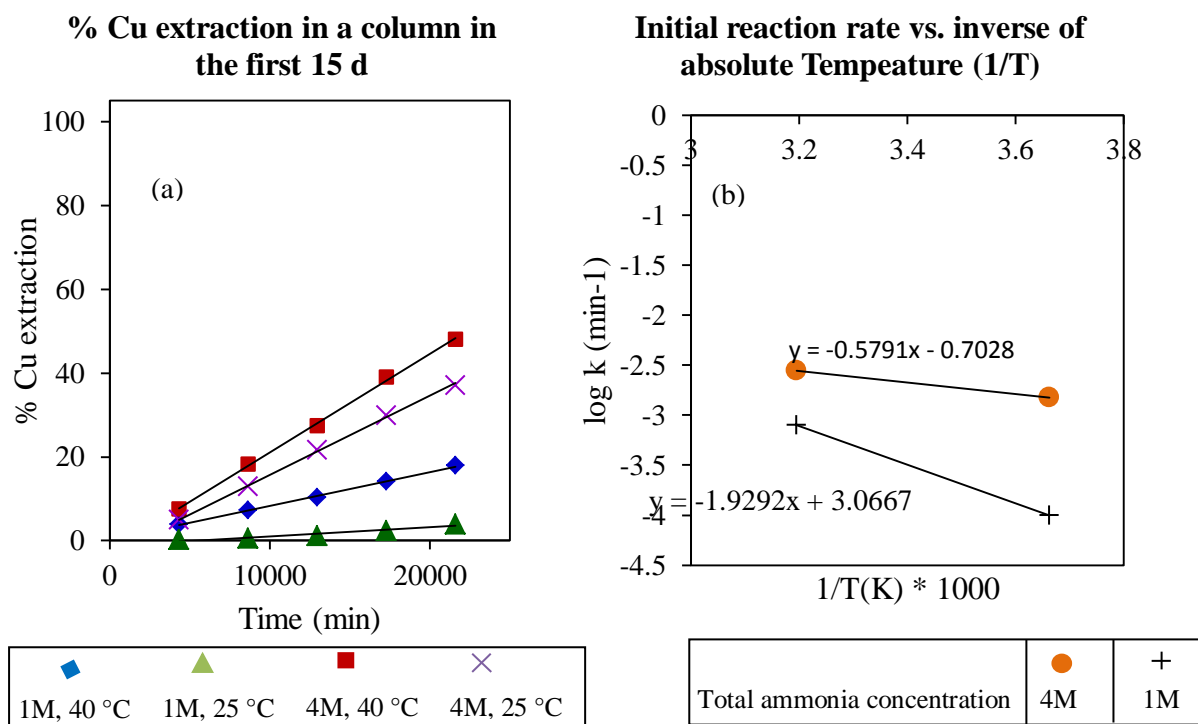


Figure 5.3: Graph (a) is a plot of the %Cu extraction in the first 15 days at two different temperatures and Graph (b) is a plot of the initial rates of reaction against the inverse of the absolute temperature. Total ammonia concentration was 1M and 4M at ambient temperature (25 °C) and 40°C.

Table 5.3: k and R^2 values for the slope of the regression lines in Figure 5.3 (a).

Concentration (M)	Temperature (°C)	Reaction rate k	R^2
4	40	0.0028	0.999
4	25	0.0017	0.999
1	40	0.0008	0.998
1	25	0.0001	0.936

Table 5.3 and 5.4 are the k and R^2 values obtained for all the slope regressions of Figure 5.3 (a) and 5.4 (a), respectively. The slopes are fairly linear with high correlation values. The rate of reaction increases as the temperature increases.

The 1 M curve suggests an E_a of 36.9 kJ/mol for Cu extraction, whilst the 4 M suggests an E_a of 11.1 kJ/mol. Due to time constraints only two temperatures were explored, one data point could be an outlier, hence, the results must be viewed with caution. Despite this limitation, the higher E_a value is close to that observed in the stirred tank experiment (33.6 kJ/mol). However, it cannot be ruled out also, that the 4 M tests operate in a different regime where mass transfer control becomes dominant. This is highly unlikely in tank experiments as these were done at high ammonia concentration (8 M). Bell et al. (1995) obtained E_a values of 31.4 kJ/mol and 37.7 kJ/mol and they suggest surface reaction rate control.

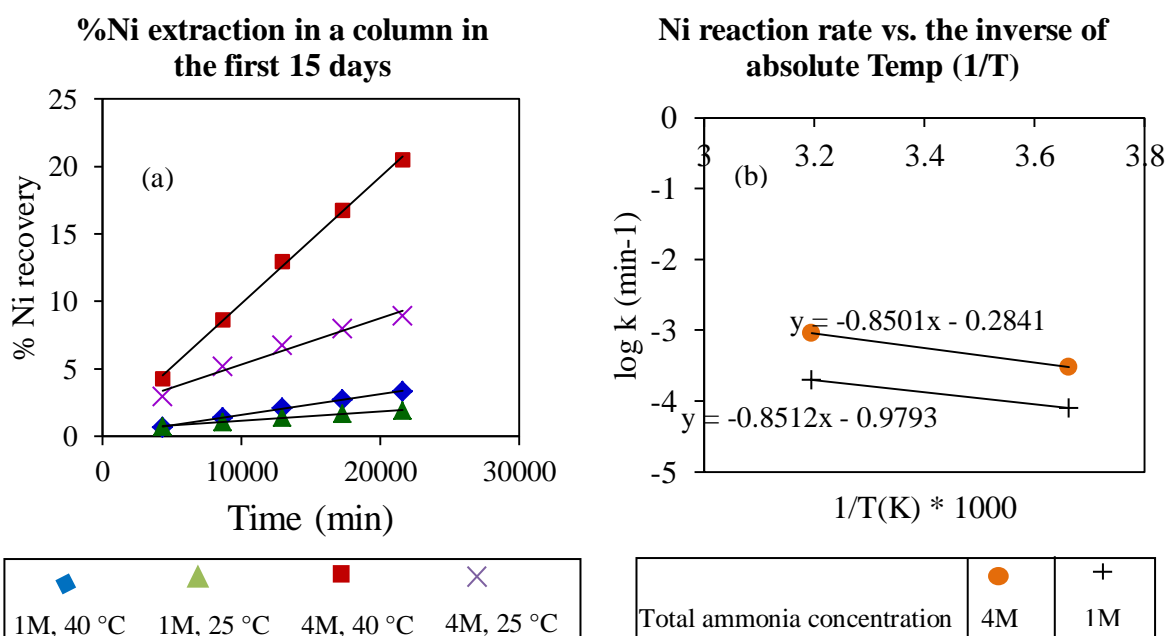


Figure 5.4: Graph (a) is a plot of the %Ni extraction in the first 15 days at two different temperatures and Graph (b) is a plot of the initial rates of reaction against the inverse of the absolute temperature. Total ammonia concentration was 1M and 4M at ambient temperature (25 °C) and 40°C

Table 5.4: k and R² values for the slope of the regression lines in Figure 5.4 (a)

Concentration (M)	Temperature (°C)	Reaction rate k	R ²
4	40	0.0009	0.999
4	25	0.0003	0.975
1	40	0.0002	0.999
1	25	0.0001	0.996

Ni extraction had a fairly linear regression passing through the origin. This was different in tanks. In columns the process is mass transfer controlled compared with tanks in which the process incorporates agitation. The way the material is packed in columns is such that the overall process diffusion at particle agglomerate level could be slow enough that even though there is an initial release of Ni, it would not enter the bulk solution stream through the bed any more rapidly than any Ni released by oxidation. The E_a obtained for both 1 M and 4 M ammoniacal lixiviants was 16.3 kJ/mol. The E_a in the column and the batch stirred tank reactor (15.8 kJ/mol) are similar, which is seen as a good indication of the E_a of Ni extraction in the present context and that its leaching is in both reactors controlled by mass transfer limitations. However, this does not have to mean the same mass transfer mechanism in both reactor settings.

5.3 Kinetic data analysis

In leach reactors, as the solid mineral is depleted, the interfacial area tends to be reduced, thereby reducing the overall rate of leaching over time, even if the concentrations of all the reagents remain unchanged. This effect was modelled using the shrinking core model, because the reacting surface is assumed to retract, leaving behind a layer of gangue material which includes silicates, carbonates and iron oxides and hydroxides. The ore particle is assumed to be approximately spherical in shape. The rate of reaction is governed either by the rate of diffusion of reactants through the outer layer to reach the reacting surface or by the kinetics of the dissolution reaction at the mineral surface or a combination of the two.

To determine the leaching reaction mechanism of the Platreef concentrates with ammoniacal lixiviant the results obtained were analysed using the shrinking core model. The following equations (25, 26 and 27) were used, whose derivation has been extensively explored in literature by Levenspiel (1999) and Sohn and Wadsworth (1979). Other authors such as

Szekely and Evans (1970), Pritzker (1996), Gbor et al. (2000), (Herreros et al. (2002) and Liddell (2005) have also applied these equations.

Spherical particles under surface chemical reaction control:

$$k_r t = 1 - (1 - X)^{1/3} \dots\dots\dots (25)$$

The rate of reaction is governed by the rate of diffusion of reactants through the outer layer to reach the reacting interface. The product layer diffusion model defining the rate equation is:

$$k_d = 1 + 2(1 - X) - 3(1 - X)^{2/3} \dots\dots\dots (26)$$

Spherical particles under mixed control model:

$$k_m t = 1 - 2(1 - X)^{1/3} + (1 - X)^{2/3} \dots\dots\dots (27)$$

where X is the fraction of reacted particle; k_r , k_d and k_m is the apparent rate constant for the surface reaction, product layer diffusion and mixed kinetic model, respectively.

5.3.1 Shrinking core model in batch stirred tank reactors

The results were analysed using the shrinking core model discussed above.

5.3.1.1 Shrinking core model for Cu conversion in tanks

Figure 5.5, 5.6 and 5.7 indicate surface reaction control, product layer diffusion control and mixed kinetic model control of Cu dissolution, respectively.

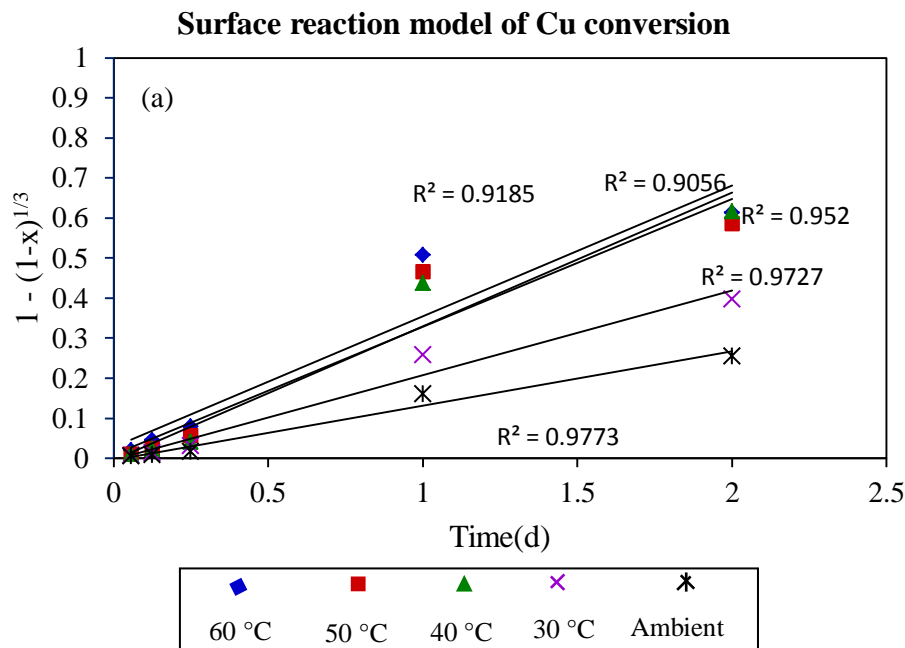


Figure 5.5: Surface reaction model at different temperatures for Cu dissolution in the stirred tank reactors.

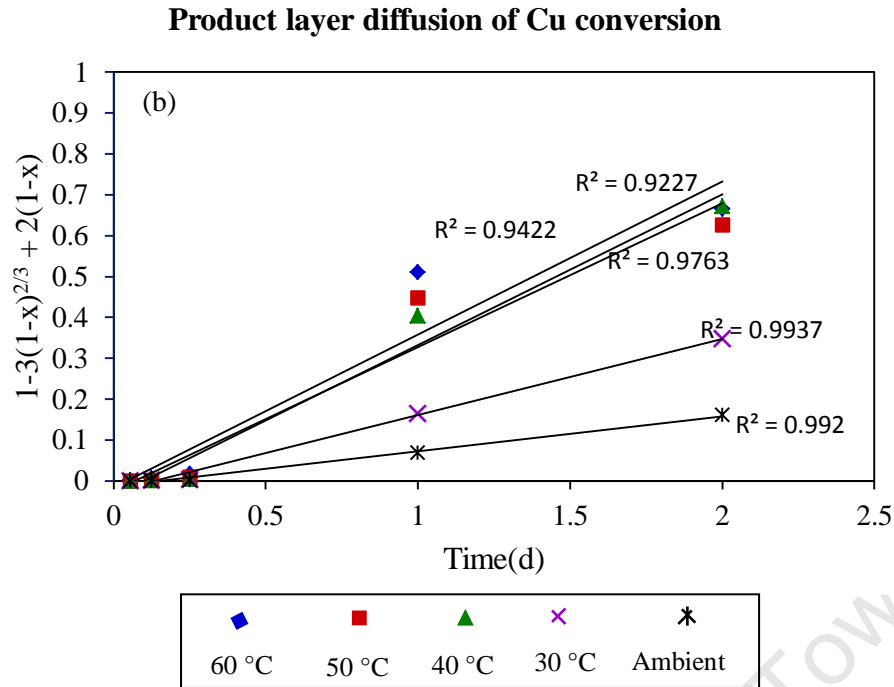


Figure 5.6: Product layer diffusion model at different temperatures for Cu dissolution in the stirred tank reactors.

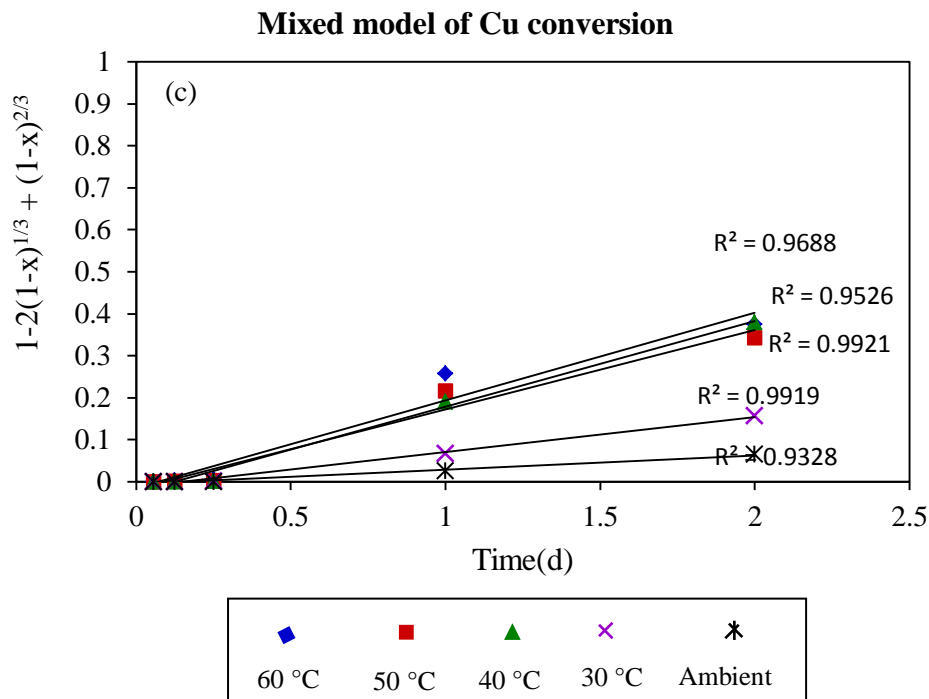


Figure 5.7: Graph of mixed control model at different temperatures for Cu dissolution in stirred tank reactors.

From the data analysed above for Cu the mixed control model gives the best fit overall. Both surface reaction model and the diffusion model a better fit at lower temperatures.

5.3.1.2 Shrinking core model for Ni conversion in tanks

Figure 5.8, 5.9 and 5.10 illustrate surface reaction control, product layer diffusion control and mixed kinetic model control of Cu dissolution, respectively.

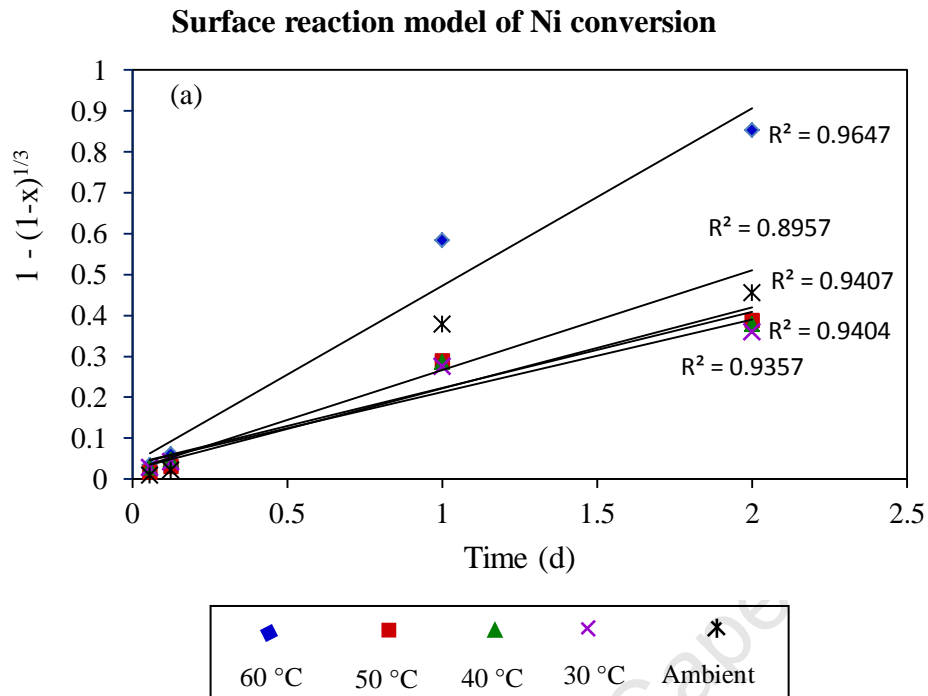


Figure 5.8: Graph of the surface reaction model at different temperatures for Ni dissolution in the stirred tank reactors.

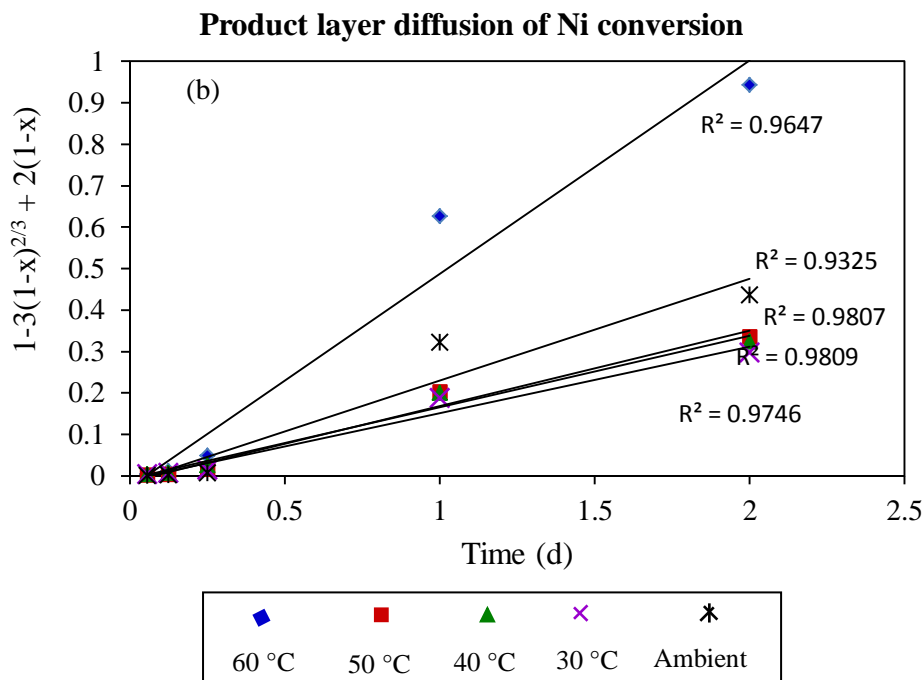


Figure 5.9: Graph of product layer diffusion model at different temperatures for Ni dissolution in the stirred tank reactors

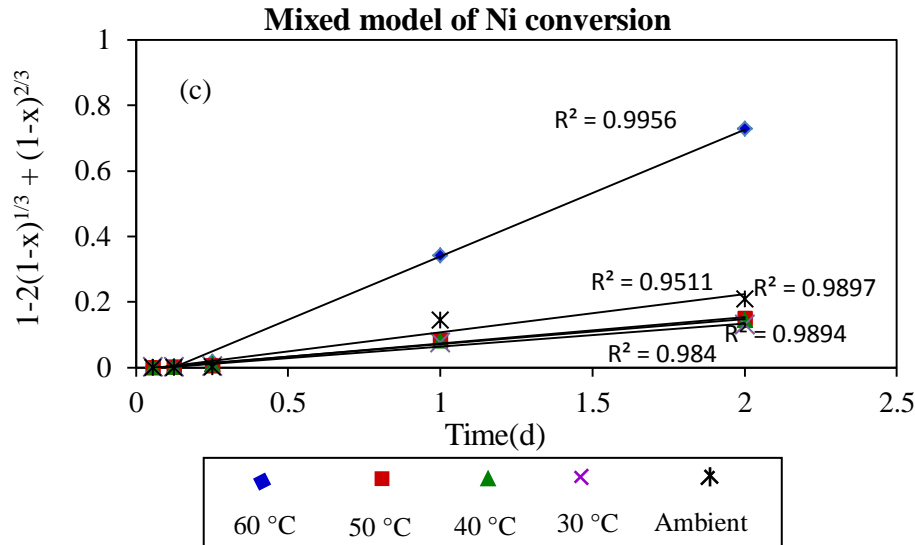


Figure 5.10: Graph of mixed control model at different temperatures for Ni dissolution in the tank reactors.

For Ni dissolution, the product layer diffusion model seem to fit the data better with high correlation values (>0.95), though the mixed control model indicates a good data fit. This implies that at different temperatures surface reaction or diffusion control may be observed.

5.3.2 Shrinking core model in columns

The results were analysed using the shrinking core model discussed in section 5.3.

5.3.2.1 Shrinking core model in columns for Cu dissolution

Figure 5.11, 5.12 and 5.13 illustrates surface reaction, product diffusion layer and mixed control in columns.

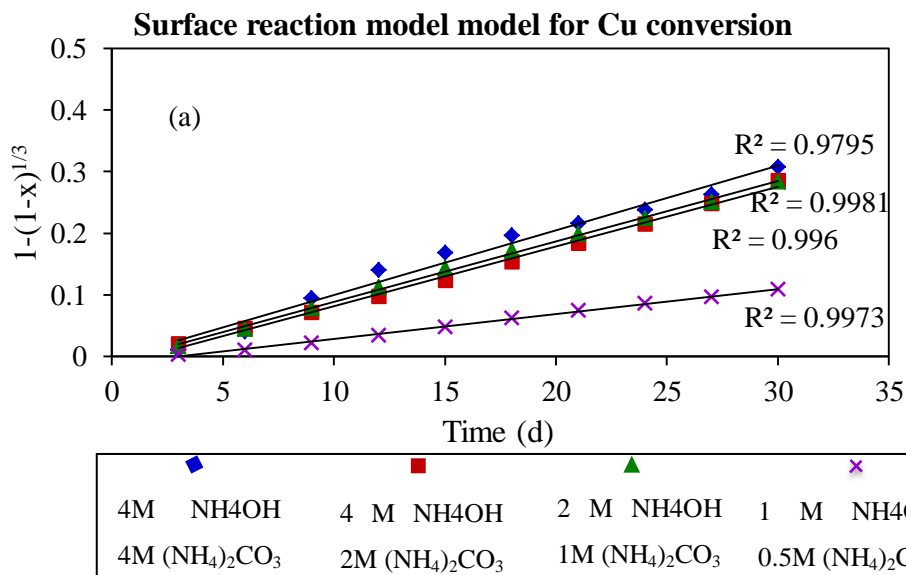


Figure 5.11: Graph of surface reaction model at different NH₃ concentrations for Cu dissolution in columns.

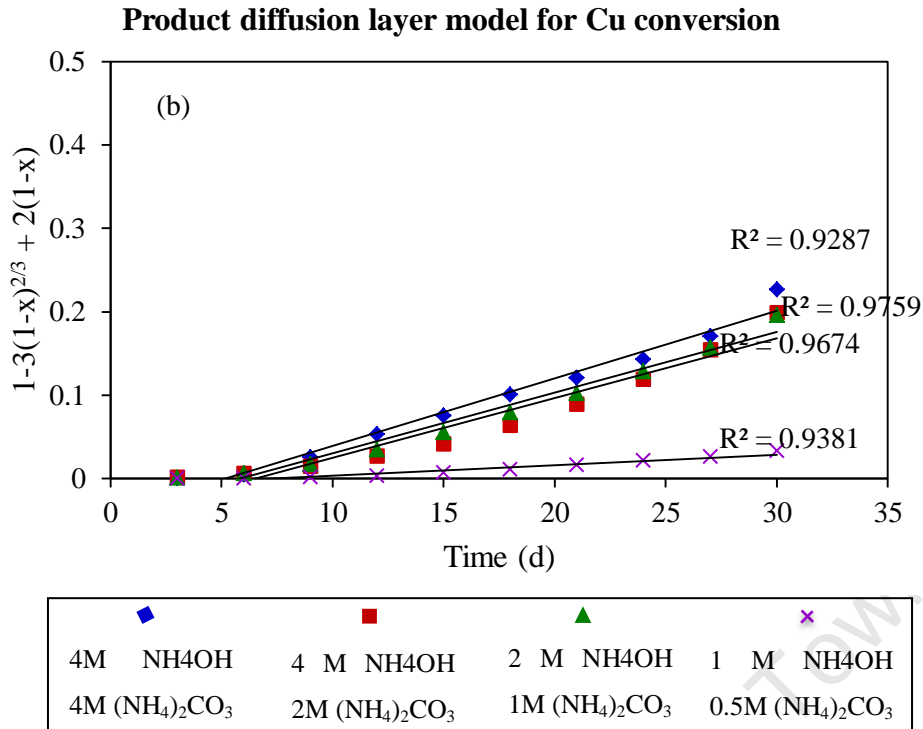


Figure 5.12: Graph of product layer diffusion model at different NH₃ concentration for Cu dissolution in columns.

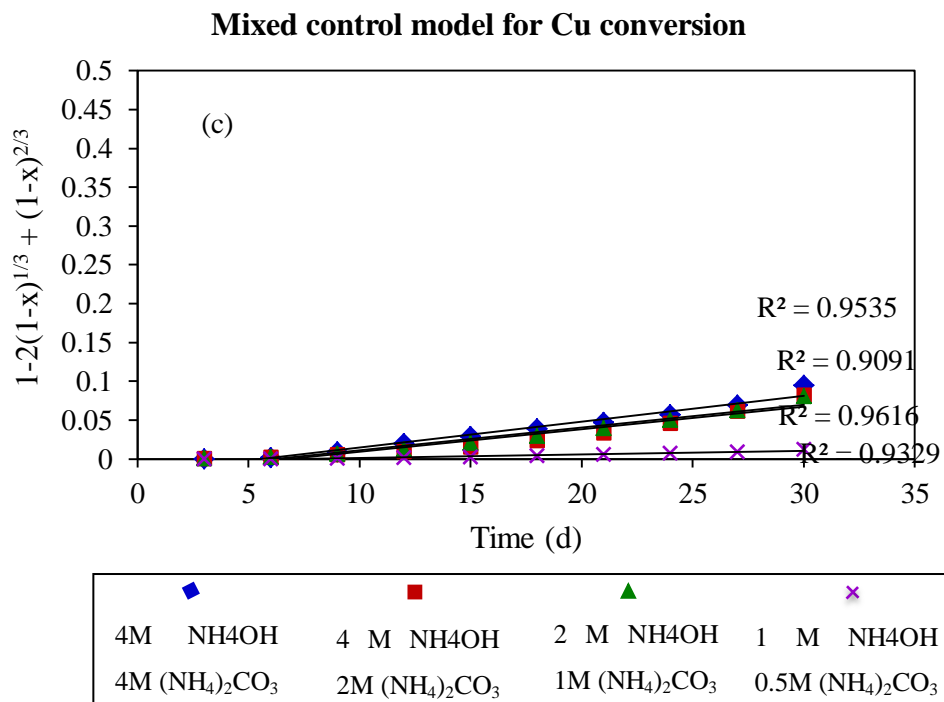


Figure 5.13: Graph of mixed control model at different NH₃ concentrations for Cu dissolution in columns.

Surface reaction model has the best fit on for Cu dissolution in columns, though the product layer model has equally high correlations in terms of copper dissolution, showing that the dissolution is under mixed control at different temperatures.

5.3.2.2 Shrinking core model for Ni conversion in columns

Figure 5.14, 5.15 and 5.16 illustrate surface reaction control, product layer diffusion control and mixed kinetic model control of Ni dissolution in columns.

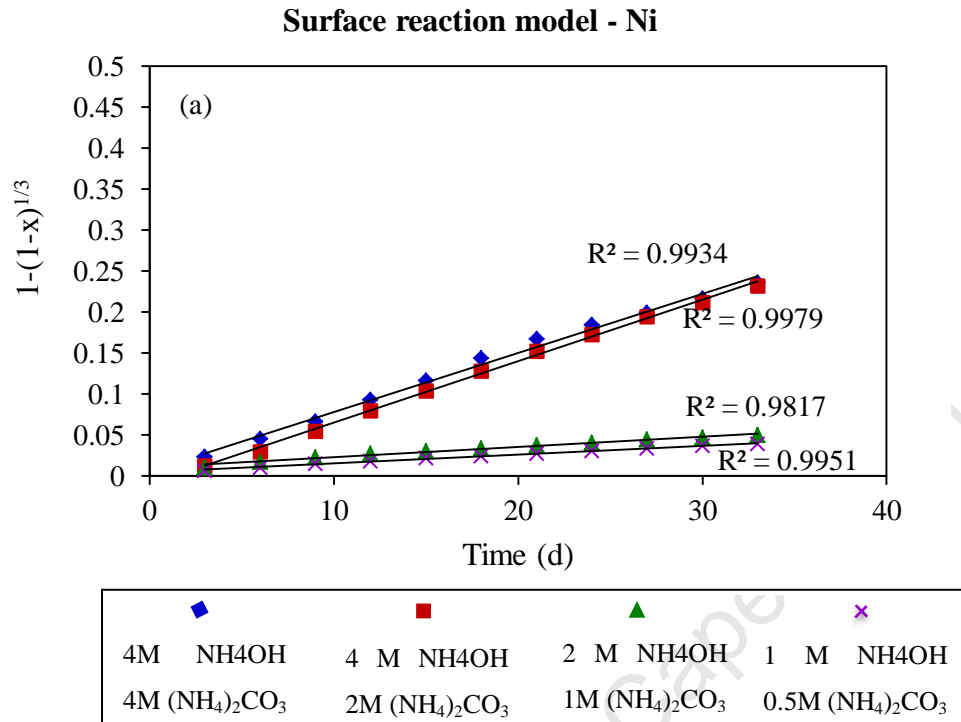


Figure 5.14: Graph of surface reaction model at different NH₃ concentrations for Ni dissolution in columns.

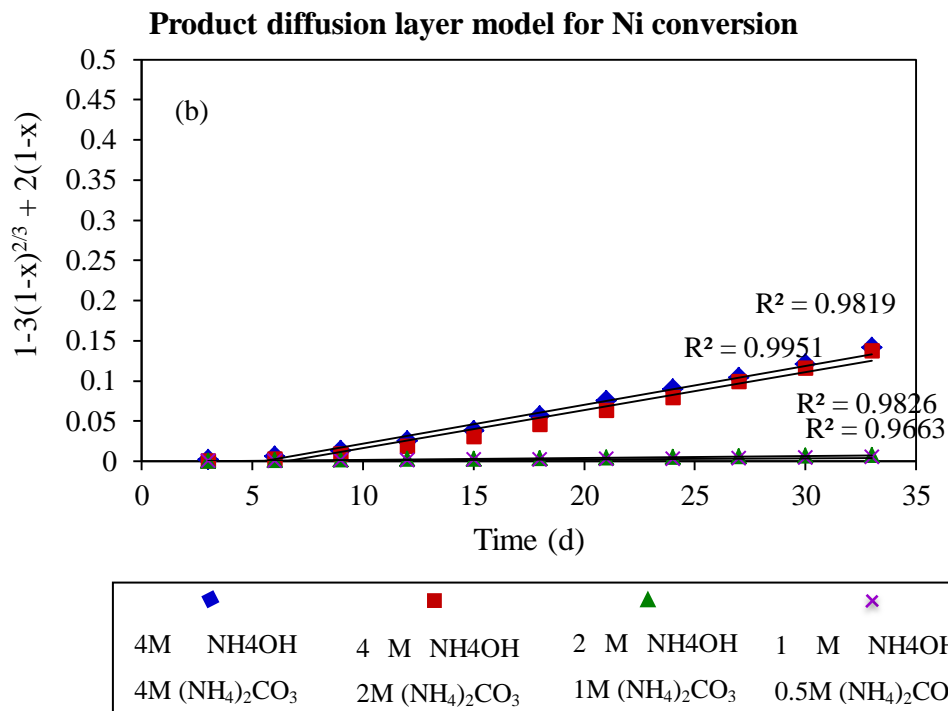


Figure 5.15: Graph of product layer diffusion model at different NH₃ concentration for Ni dissolution in columns.

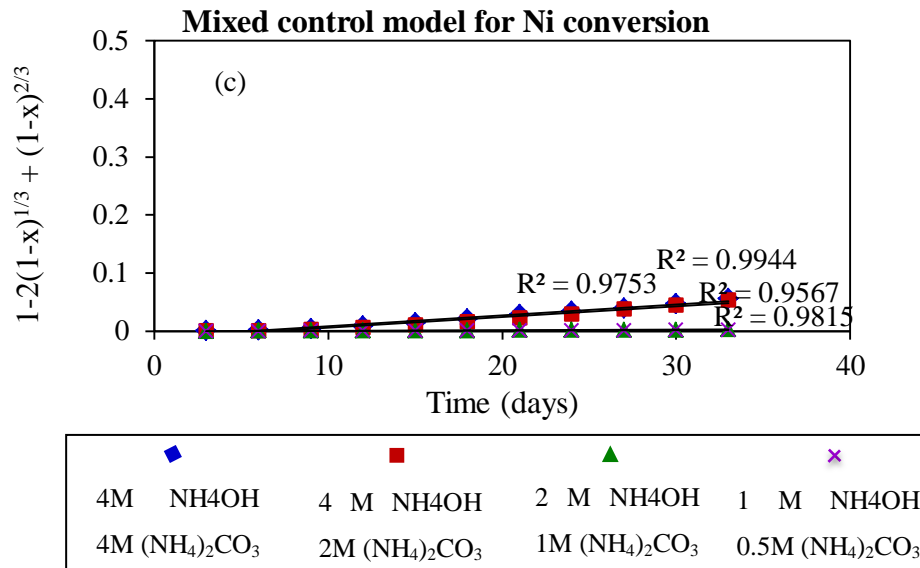


Figure 5.16: Graph of mixed control model at different temperatures for Ni dissolution in columns.

Figure 5.14, 5.15 and 5.16 illustrate the shrinking core model in the columns with respect to Ni dissolution. The product layer diffusion model and the surface reaction model have high correlations showing that the dissolution is under mixed control. Thus, the reaction is controlled by diffusion through the surface layer and surface chemical reactions. However, the activation energy suggests that the reaction is diffusion controlled.

All the models for Cu and Ni dissolution in tanks and columns have high correlation coefficients of approximately 0.9 or more. Unfortunately the close similarity of the curves makes this an unreliable way of distinguishing between these mechanisms.

5.4 Reaction order in terms of NH₃ in a batch stirred tank reactor

To quantify the effect of ammonia concentration, the order of the reaction (n) and the rate constant (k) were calculated by determining the slope from a linear regression of data points with a steep gradient. Figure 5.17 (a) and (b) illustrate the relationship of the initial rate of reaction with ammonia concentration in the tanks. To obtain the order of the reaction with respect to ammonia the following reactions were used:

$$\frac{dX}{dt} = k[NH_3]^n \dots\dots\dots (28)$$

$$\text{Log} \left(\frac{dX}{dt} \right) = \text{log } k + n \text{ Log}[NH_3] \dots\dots\dots (29)$$

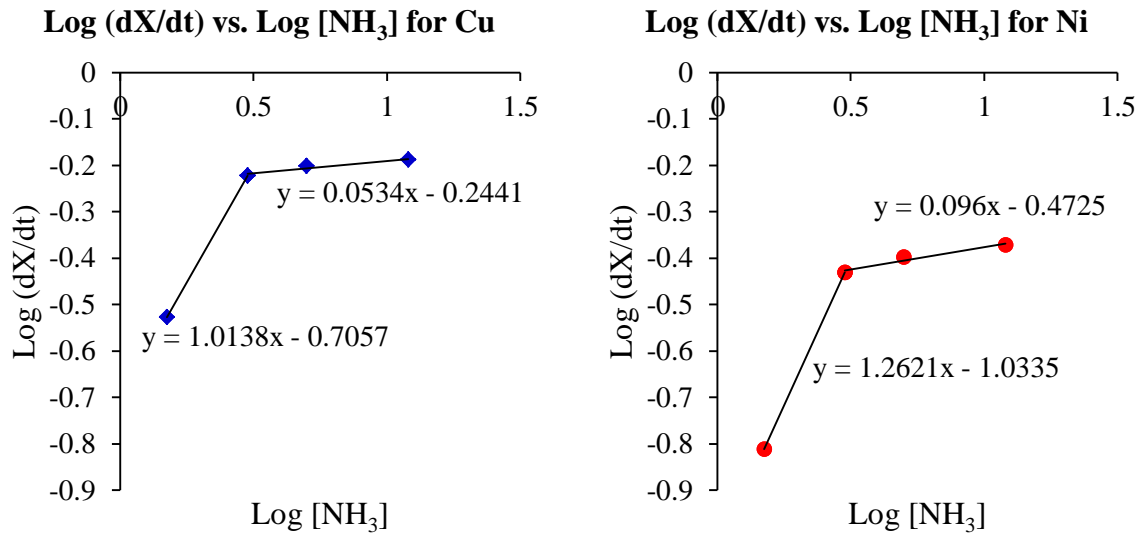


Figure 5.17 (a) and (b): Graph of $\text{Log}\left(\frac{dX}{dt}\right)$ vs. $\log [\text{NH}_3]$ in stirred tank reactors Cu and Ni conversion respectively.

The graph shows that the rate of reaction increased as the ammonia concentration increased up to approximately 3 M. Above 3 M, the rate of reaction became independent of the total ammonia concentration. The reaction order with respect to ammonia concentration less than 3 M is one for both Cu and Ni conversion. The order of the reaction is equal to zero with respect to the ammonia concentrations greater than 3 M, which have a gradient of 0.05 for the points ≥ 3 M for the graph of Cu and 0.09 for the points of Ni. The k value for Cu and Ni are 0.196 and 0.0925, respectively, obtained using the first two data points with ammonia concentration < 3 M. The graph shows that at 1 M the rate is slower compared to the other concentrations, which all have very similar rates of extraction. The trends obtained are similar to those obtained by Reilly and Scott (1977) using ammonia concentrations between 2.5 M and 7.0 M. Dutrizac (1981) also observed that at low levels of ammonia concentration, the rate increased sharply and was less substantially affected at higher ammonia levels. The reaction kinetics change from first order to zero order at ammonia concentrations greater than 3 M and this indicates that a different mechanism takes over and becomes rate limiting which could possibly be partial oxygen transport control.

5.5 Reaction order in terms of NH_3 in a column

Figure 5.18 (a) and (b) is a plot of the relationship between the rate of reaction with ammonia concentration in columns for Cu and Ni, respectively.

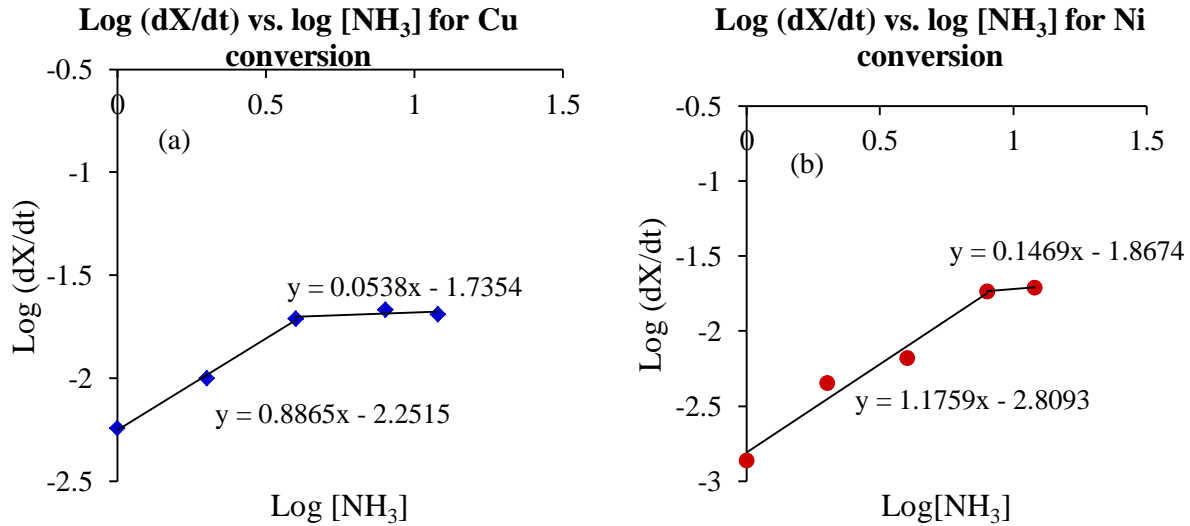


Figure 5.18 (a) and (b): Graph of $\text{Log} \left(\frac{dX}{dt} \right)$ vs. $\text{log} [\text{NH}_3]$ in columns for Cu and Ni respectively.

It can be observed that as the total ammonia concentration increases up to 4 M for Cu and between 4 and 6 M for Ni, the rate of reaction increases. However, at higher concentrations (> 4 M), the rate of reaction becomes independent of the ammonia concentration, because partial oxygen diffusion might possibly become the rate limiting step. The order of reaction is approximately one for both Cu and Ni at lower ammonia concentrations (< 4 M) and zero order at higher ammonia concentrations (> 4 M). The initial rates (k) are 0.0056 and 0.0016 with respect to Cu and Ni, respectively. Warren and Wadsworth (1978) and Lane and McDonald (1946) reported a first order NH_3 dependence.

5.6 Gas-Liquid mass transfer in columns and stirred tank reactors

Previous work done by Petersen (2010) has established that the rate of oxidation of a mineral concentrate in a GEOCOATTM heap is limited by the rate of oxygen mass transfer for which the following mass transfer coefficient ($k_L a$) was developed:

$$k_L a = 42.6 \exp \left(\frac{14\,000}{R} \left(\frac{1}{T_0} - \frac{1}{T} \right) \right) \left(\frac{1}{hr} \right) \dots \dots \dots (30)$$

R = Universal gas constant (8.314 kJ/mol/K), $T_0 = 20^\circ\text{C} = 293\text{K}$, T = Temperature (K)

Estimated column k_La values, calculated using equation 30 at different temperatures, are tabulated in Table 5.5.

Table 5.5: Estimated k_La values in columns at different temperatures

Temperature	k_La
Ambient	0.013 s^{-1}
40 °C	0.017 s^{-1}

Riet (1979) obtained the mass transfer coefficient using a stirred tank reactor as:

$$k_La = (1.022^{(T-20)})(0.016) \left(\frac{P_g}{V}\right)^{0.7} (u_s^{0.2}) \left(\frac{1}{s}\right) \dots\dots\dots (31)$$

P_g = power input by the impeller (W), V = volume (m^3), u_s = superficial gas velocity and T is the Temperature (°C). Estimated k_La values for batch stirred tank reactors at different temperatures were calculated using equation 31 and these are tabulated in Table 5.6. P_g/V has been estimated from the Applikon[®] manual and the volume of the liquid in the reactor. The u_s was obtained through calculations using the reactor diameter and the air flow-rate.

Table 5.6: Estimated k_La values in tank reactors at different temperatures, $P_g/V = 250 \text{ W/m}^3$, $u_s = 0.37 \times 10^{-2} \text{ ms}^{-1}$

Temperature	k_La
Ambient	0.28 s^{-1}
30 °C	0.31 s^{-1}
40 °C	0.38 s^{-1}
50 °C	0.48 s^{-1}
60 °C	0.59 s^{-1}

The estimated k_La values in the stirred tank reactors are 22 times higher than those in the columns (at the same temperature, i.e. ambient and 40 °C), which thus corresponds to higher oxygen mass transfer rates in the tanks. The impeller provides better mixing and this creates higher volumetric mass transfer coefficients. This points to an explanation why the reaction rate was significantly faster in the tanks as oxygen mass transfer was substantially higher.

According to Newton's law of cooling, the rate of oxygen mass transfer is described by:

$$r_{O_2} = k_La(c^* - c_b) \dots\dots\dots (32)$$

Where k_{La} is the volumetric mass transfer coefficient, c^* is the equilibrium concentration at the gas-liquid interface and c_b is the bulk concentration of oxygen in solution. If all of the oxygen in solution is used up, then the maximum rate of oxygen transfer is given by:

$$r_{O_2, supplied} = k_{La}(c^*) \dots \dots \dots (33)$$

In 2000, Tromans proposed a formula for the calculation of oxygen solubility in aqueous solutions as follows:

$$c^* = p_{O_2} \cdot k \cdot [1 + \kappa(C_i)^\gamma]^{-h} \dots \dots \dots (34)$$

The parameters κ , γ and h for aqueous ammonia as listed by Tromans (2000) are 0.0105, 1.0 and -1.0, respectively. The partial pressure for oxygen p_{O_2} is calculated as:

$$p_{O_2} = 0.21 P \dots \dots \dots (35)$$

Where P is the atmospheric pressure in these experiments = 1 atm.

The partition coefficient k is calculated from:

$$k = \exp\left\{\frac{0.046 \cdot T^2 + 203.35 \cdot T \cdot \ln\left(\frac{T}{298}\right) - (299.378 + 0.092 \cdot T) \cdot (T - 298) - 2.0591 \cdot 10^4}{8.3144 \cdot T}\right\} \dots \dots \dots (36)$$

where T is in K.

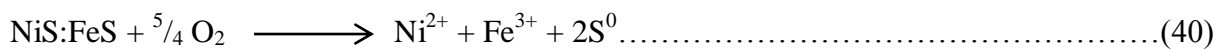
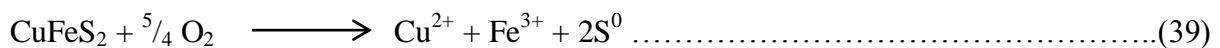
The rate of oxygen supplied was calculated using equation 33, 34, 35 and 36, whilst the rate of oxygen consumed was calculated using equation 37 for tanks and 38 for columns:

$$r_{O_2, consumed} = \left(\frac{\text{total oxygen consumed}}{\text{solution volume} \cdot \text{time}}\right) \left[\frac{\text{mol}}{\text{L} \cdot \text{s}}\right] \dots \dots \dots (37)$$

$$r_{O_2, consumed} = \left(\frac{\text{total oxygen consumed over 30 days}}{\text{liquid hold-up time}}\right) \left[\frac{\text{mol}}{\text{L} \cdot \text{s}}\right] \dots \dots \dots (38)$$

The liquid hold-up in tanks was assumed to be 0.2 L at any point in time.

Assumption: The stoichiometric equations describing the ammonia leaching of chalcopyrite and pentlandite are:



The rate of oxygen mass transfer was calculated over a basis of 1 day in tanks and 30 days in columns from experiments run at ambient temperature, a pH of 9.35 and 8 M total ammonia

concentration. The detailed calculations are in the Appendix A. The values are shown in Table 5.7.

Table 5.7: Rates of oxygen mass transfer at ambient temperature and pressure, at 8 M total NH_3 concentration.

Reactor	Rate of oxygen consumed ($r_{\text{O}_2, \text{consumed}}$)	Rate of oxygen supply ($r_{\text{O}_2, \text{supplied}}$)
Tanks	1.5×10^{-7} mol/L.s	6.94×10^{-5} mol/L.s
Columns	4.7×10^{-7} mol/L.s	3.22×10^{-6} mol/L.s

The oxygen consumption rate is higher in the columns than in the tanks although leaching is so much slower. This could be, because of the higher solid to liquid ratio in columns, which is about 100 times larger than in the tanks, and the leach rate only about 30 times slower, so therefore the net leaching rate is 3 times faster. The oxygen supply rate in columns is 22 times slower than in tanks because of the difference in k_{La} . The analysis indicates that in columns the rate of leaching is likely to be limited by oxygen mass transfer, whereas in tanks it is not as closely limited.

5.7 Evaporation rates of ammonia in batch stirred tank reactor system

Evaporation rates are highly dependent on the NH_3 concentration. For example, at a concentration of 0.5 M NH_4OH and 0.5 M $(\text{NH}_4)_2\text{CO}_3$ the ammonia loss/day is 0.01 mol/L/d from a 1 L solution, whilst 0.25 mol/L/d ammonia is lost when using a 4 M NH_4OH , 4 M $(\text{NH}_4)_2\text{CO}_3$, solution in the batch stirred tank reactor. Ammonia evaporation rates are less significant with temperature. Looking at a constant ammonia concentration of 4 M NH_4OH and 4 M $(\text{NH}_4)_2\text{CO}_3$ the rate of ammonia lost at ambient temperature, 40 °C and 50 °C is 0.18, 0.22 and 0.25 mol/L/d, respectively.

Table 5.8: Evaporation rates of ammonia in stirred tank reactor system

Ammonia concentration	Temperature	Ammonia losses/day
4 M NH_4OH , 4 M $(\text{NH}_4)_2\text{CO}_3$	50 °C	0.25 mol/L/d
4 M NH_4OH , 4 M $(\text{NH}_4)_2\text{CO}_3$	40 °C	0.22 mol/L/d
4 M NH_4OH , 4 M $(\text{NH}_4)_2\text{CO}_3$	Ambient	0.18 mol/L/d
2 M NH_4OH , 2 M $(\text{NH}_4)_2\text{CO}_3$	50 °C	0.10 mol/L/d
0.5 M NH_4OH , 0.5 M $(\text{NH}_4)_2\text{CO}_3$	50 °C	0.01 mol/L/d

5.8 Evaporation rates of ammonia in columns

In columns a similar trend of evaporation rates observed in tanks is noticed and is illustrated in Table 5.9. For example, looking at ambient temperature using 0.5 M NH_4OH and 0.25 M $(\text{NH}_4)_2\text{CO}_3$, 0.02 mol/L/d is lost in comparison to 0.55 mol/L/d lost in the columns with 4 M NH_4OH and 4 M $(\text{NH}_4)_2\text{CO}_3$ concentration. When temperature increases at a constant ammonia concentration the ammonia losses increase. For example, using a 2 M NH_4OH and 1 M $(\text{NH}_4)_2\text{CO}_3$ ammoniacal lixiviant, ammonia losses increase from 0.16 mol/L/d to 0.18 mol/L/d when temperature is increased from ambient to 40 °C.

Table 5.9: Evaporation rates of ammonia in the column system

Ammonia concentration	Temperature	Ammonia losses/day
4 M NH_4OH , 4 M $(\text{NH}_4)_2\text{CO}_3$	Ambient	0.55 mol/L/d
4 M NH_4OH , 2 M $(\text{NH}_4)_2\text{CO}_3$	Ambient	0.34 mol/L/d
2 M NH_4OH , 1 M $(\text{NH}_4)_2\text{CO}_3$	Ambient	0.16 mol/L/d
1 M NH_4OH , 0.5 M $(\text{NH}_4)_2\text{CO}_3$	Ambient	0.05 mol/L/d
0.5 M NH_4OH , 0.25 M $(\text{NH}_4)_2\text{CO}_3$	Ambient	0.02 mol/L/d
2 M NH_4OH , 1 M $(\text{NH}_4)_2\text{CO}_3$	40 °C	0.18 mol/L/d
0.5 M NH_4OH , 0.25 M $(\text{NH}_4)_2\text{CO}_3$	40 °C	0.03 mol/L/d

6.0 CONCLUSIONS AND RECOMMENDATIONS

The objective of this study was to investigate the technical feasibility of the ammoniacal leaching of a Platreef low-grade concentrate as an alternative route for base metal recovery, either in heaps or tanks. The initial experiments carried out were to evaluate whether the ammoniacal leaching process of a Platreef flotation concentrate would be possible in principle. This was confirmed following some preliminary laboratory testing in shake flasks. The best pH window established was between 9 and 10, with an optimum ammoniacal lixiviant of 4 M NH_4OH and 4 M $(\text{NH}_4)_2\text{CO}_3$ at ambient temperature. These results informed the design of experiments in tank reactors and columns which simulated tank leaching and heap leaching environments, varying temperature and ammonia concentration as key parameters.

The conclusions of this work within the range of data studied are listed below:

- In both systems an increase in temperature and ammonia concentration resulted in an increase in Cu and Ni extraction, with ammonia concentration having a significant effect. The use of room temperature is economically preferable.
- At low ammonia concentrations (<3 M in tanks and <4 M in columns) the order of the reaction is one and zero at higher NH_3 concentrations.
- For Ni dissolution, the activation energies were calculated as 15.8 kJ/mol and 16.3 kJ/mol in the batch stirred tank reactor and column respectively, indicating diffusion control.
- For copper dissolution, the activation energies were calculated as 33.6 kJ/mol and 36.9 kJ/mol in the tank and column respectively, indicating mixed control, with both surface kinetic and diffusion control.
- There is a significant amount of Ni extracted instantaneously in tanks but not in heaps. This phenomenon is not observed for Cu.
- The Ni and Cu leaching kinetics can be described using the shrinking core model. Model fits confirm that Ni dissolution is under diffusion control and Cu dissolution is under mixed kinetic control in both columns and batch stirred tank reactors, although the analysis does not provide decisive clarity on this.

- An increase in ammonia concentration resulted in significant ammonia losses, with higher losses in columns than tanks. An increase in temperature had only a slight effect in ammonia losses at the same ammonia concentration.
- The estimated $k_L a$ values were approximately 22 times higher in tank reactors than in the columns. It appears the columns are strongly oxygen supply limited, whereas in tanks this is not the case in the range of values tested.

The ammoniacal leaching process has been proved to be technically feasible in the laboratory, for Platreef flotation concentrate base metal recovery with almost complete extraction of Cu and Ni at high ammonia concentration. However, the high NH_3 concentration may not be economically suitable for industrial application, especially on a heap, due to evaporative losses, but there is an opportunity to recycle the ammonia and reduce losses in appropriately designed tank leach circuits.

Recommendations

At high NH_3 concentration the effect of passivation described in the literature did not seem to hinder the extraction of the base metals Cu and Ni, with near complete extraction in shake flasks and batch stirred tank reactors. However, it would be worthwhile to investigate the form in which the iron compounds are in, and if passivation significantly affects the process at lower NH_3 concentrations, as after a few days the graph flattens out under these conditions. It would be worthwhile to investigate if FeS_2 and FeS remain in their state or completely react to form iron oxide. Further study of the mineralogical transformations that may occur after leaching is recommended. The exact nature of the leach reactions in both tanks and columns need to be investigated to obtain a realistic estimate of the overall limiting factor. Especially the degree of leaching of FeS compounds needs to be followed (even if the Fe does not leach, all the S might be oxidised, in which case the analysis even for tanks is seriously flawed).

In future work the speciation between Cu(II) and Cu(I) should be established in the course of leaching in order to understand better the kinetics of the reaction, especially in the initial stages before the first copper is released. It is postulated that an increase in $\text{Cu(NH}_3)_4^{2+}$ as the reaction proceeded resulted in an increase in Cu and Ni extracted. Oxygen and the $\text{Cu(NH}_3)_4^{2+}$ complex have been observed to both work in the oxidation process of the

ammoniacal leaching reaction. It would be recommended that further study be done to investigate whether the real oxidant in the reaction is the oxygen or the $\text{Cu}(\text{NH}_3)_4^{2+}$ and how $\text{Cu}(\text{NH}_3)_4^{2+}$ influences the degree and rate of base metal leaching.

Ammonia losses at high concentrations are significant and detrimental if applied on a heap but may be possible in tanks. At low ammonia concentrations the process may be applied on both heap and tank environments, but further investigations would be required to establish a cost-effective concentration that is not detrimental to technical and environmental impact. One of the biggest drawbacks of ammonia leaching is the question of what to do with the product ammonium sulphate. Ammonium sulphate is a saleable by-product, but requires further purification before it can be used, making profitable production unlikely. Economic ways of processing the by-product ammonium sulphate need to be sought.

Because of the conflicting evidence in columns between diffusion at particle agglomerate level and oxygen mass transfer it is recommended that further study investigates the actual rate limiting factor.

Initial shake flask tests showed hardly any dissolution of Mg, Al, Ca, etc. It would be recommended that in future column studies these elements be monitored to observe if there is any significant dissolution due to the reduced kinetics.

The ammoniacal leaching process has been proved to work for base metal recovery from Platreef flotation concentrates in the laboratory. It is recommended that the residues be leached in the cyanide leaching process and the amenability of the precious metals compared to those with a pre-treatment stage of acid-bioleaching.

7.0 REFERENCES

- AB ACHEMA. 2006. *Safety Data Sheet, 197/2006/EB Regulation (REACH), Annex II. Ammonia solution*. Regulation. Safety.
- Altmaier, M., Gaona, X. and Fellhauer, D. 2010. *Intercomparison of redox determination methods on designed and near - natural aqueous systems*. KIT Scientific Reports 7572.
- Altman, K., Schaffner, M. and McTavish, S. 2002. Mineral Processing Plant Design, Practice and Control. In D.J. Barrat, H.N. Doug and A.L.E. Mular, Eds. Littleton, Colorado, USA: *Society for Mining, Metallurgy, and Exploration, Inc.* 1631-1643.
- Ash, M. and Ash, I. 2004. *Handbook of green chemicals*. 2nd ed. United States of America: Synapse Information Resources, Inc.
- Asselin, E. 2011. Thermochemistry of the Fe, Ni and Co-NH₃-H₂O systems as they relate to the Caron process: a review. *Minerals and metallurgical processing*. 28(4):169-175.
- Babcan, J. 1971. Synthesis of jarosite KFe₃(SO₄)₂OH₆. *Geol. 2b*. 22(2):299-304.
- Balashov, S. 2012. *Alexander Mining secures processing technology patent in DRC*. United Kingdom: Proactive Investors.
- Bartlett, R. 1998. *Solution Mining - Leaching and fluid recovery of materials*. 2nd ed. Netherlands: Gordon and Breach science publishers.
- Beckstead, L.W. and Miller, J. 1977a. Ammonia, oxidation leaching of chalcopryrite-reaction kinetics. *Metallurgical and materials transactions B*. 8(1):19-29.
- Beckstead, L.W. and Miller, J. 1977b. Ammonia, oxidation leaching of chalcopryrite-surface deposit effects. *Metallurgical and materials transactions B*. 8(1):31-38.
- Bell, S.L., Welch, G.D. and Bennett, P.G. 1995. Development of ammoniacal lixiviants for the in-situ leaching of chalcopryrite. *Hydrometallurgy*. 39(1-3):11-23.
- Benedict, C.H. and Kenny, L.L. 1924. Ammonia Leaching of Calumet and Hecla Tailings. *Mining and Metallurgy, American Institute of Mining and Metallurgical engineers Inc.*, 1297.
- Bhuntunkomol, K., Han, K.N. and Lawson, F. 1980. Leaching behaviour of metallic nickel in ammonia solutions. *Transaction Institution of Mining Metallurgy*. 89(Section C):C7-C13.
- Bjerrum, J., Haase, P. and Son. 1841. Metal ammine formation in aqueous solution.
- Bothara, K.G. 2008. Inorganic Pharmaceutical Chemistry. In Pragati Books Pvt. Ltd. 13.
- Bye, A.R. 2001. Mining the Platreef. *Appl. earth science. trans. inst. min. metallurgy B*. 110:B209-B210.

- Canterford, J.H. 1975. Treatment of nickeliferous laterites. *Minerals science and engineering*. 7:3-17.
- Caron, M.H. 1924. *Recovering values from nickel and cobalt ores*. 1487145. U.S.: .
- Caron, M.H. 1950. Fundamental and Practical Factors in Ammonia Leaching of Nickel and Cobalt Ores. *Journal of Metals*. 188:67-104.
- Cawthorn, R.G. 1999. The platinum and palladium resources of the Bushveld Complex, South Africa. *Journal of Science*. 95:481-489.
- Chase, C.K. 1980. Leaching and Recovery of Copper from As Mined Materials. In W.J. Schlitt, Ed. Warrendale, PA: SME-AIME. 95-103.
- Chen, T.T. and Cabri, L.J. 1986. Mineralogical overview of iron control in hydrometallurgy processing. *Iron control in Hydrometallurgy*. Dutrizac, J.E., Monhemius, A.J., Ed. Chichester, England: Ellis Horwood Ltd Publishers.
- Chuanhui, X., Newell, R., Quast, K. and Ellis, K. 2000. Ammonia Leaching: An Alternate Route for Copper Recovery. *MINPREX 2000, Australian Institute of Mining and Metallurgy*. 5:241-248.
- Collins, M.J. and Kofluk, D.K. 24 March 1998. U.S.5730776.
- Das, R.P. and Anand, S. 1995. Precipitation of iron oxides from ammonia-ammonium sulphate solutions. *Hydrometallurgy*. 38:161-173.
- Davies, D.S. Leuders, R.E., Spitz, R.A. and Frankiewicz, T.C. 1978. Nitric-Sulphuric acid leach process improvements. *107th Annual meeting of AIME*. February. Denver.
- Defreyne, J., Barr, G. and McCunn, G. 2004. CESL Process - Moving from Pilot to Production Scale. *Presentation at the International HYDRO-SULPHIDES*. 16-19 August 2004. Santiago, Chile.
- Dixon, P. and Madigan, D.C. 1975. *Hydrometallurgical recovery of Copper, Nickel or Zinc from sulphide ores by Oxidation in Ammoniacal Chloride or nitrate solutions*. U.S.3927170.
- Donnay, G., Corliss, L.M., Donnay, J.D.H., Elliot, N. and Hastings, J.M. 1958. Symmetry of magnetic structures: magnetic structure of chalcopyrite. In *Physics Review*. 1917 - 1923 ed.B112.
- Dreisinger, D. 2000. Introduction to Eh-pH diagrams, University of British Columbia. :26.
- Dresher, W.H. 2004. Producing Copper Nature's Way: Bioleaching. *CND: INNOVATIONS*. May 2004. 10.
- Duggan, J.E. 1928. Ammonia Leaching at Kennecott, Alaska.

- Dutrizac, J.E. 1981. Ammoniacal Percolation Leaching of Copper Ores. *Canadian Metallurgy Quarterly*. 20(3):307-315.
- Dutrizac, J.E. 1983. Jarosite-type compounds and their application in the metallurgical industry. *Hydrometallurgy, Research, Development and Plant Practice, Proceedings. 112th AIME Annual General Meeting*. 6 - 10 March. Osseo-Asare, K., Miller, J.D., Ed. Atlanta, Georgia: TMS-AIME. 531.
- Dutrizac, J.E. and Chen, T.T. 2009. The behaviour of scandium, yttrium and uranium during jarosite precipitation. *Hydrometallurgy*. 98(1-2):128-135.
- Duyvesteyn, W.P.C. and Sabacky, B.J. 1993. The Escondida process for copper concentrates. *Extractive Metallurgy of Copper, Nickel and Cobalt (The Paul, E. Quenan International Symposium) I: Fundamental Aspects*. Reddy, R.G. and Kleizenbach, R.N. Eds. Warrendale, PA: TMS. 881 - 910.
- Evans, D.J.I., Romanchuk, S. and Mackiw, K. 1964. Treatment of copper-zinc concentrates by pressure hydrometallurgy. *Canadian mining metallurgy, bull.* 57(678):857-866.
- Fittock, J.E. 1992. Nickel and Cobalt refining at QNI Pty Ltd. In 2nd ed. Yabulu, Queensland: AUSIMM Monograph, 19. 1-47.
- Forward, F.A. 1953. Ammonia pressure leach process for recovering nickel, copper and cobalt from Sherritt Gordon nickel sulphide concentrate. *Canadian Institute of Mining and Metallurgy, Bull.* 499:677.
- Forward, F.A. and Mackiew, V.N. 1955. Chemistry of the Ammonia Pressure Process for Leaching Ni, Cu and Co from Sherritt Gordon Sulphide Concentrates. *Journal of Metals, transactions AIME*. :454-463.
- Gbor, P.K., Ahmed, I.B. and Jia, C.Q. 2000. Behaviour of Co and Ni during aqueous sulphur dioxide leaching of nickel smelter slag. *Hydrometallurgy*. 57(1):13-22.
- Ghosh, M.K., Das, R.P. and Biswas, A.K. 2003. Oxidative ammonia leaching of sphalerite Part II: Cu(II) - catalysed kinetics. *International Journal Mineral Processing*. 70:221-234.
- Gowariker, V., Krishnamurthy, V.N., Gowariker, S., Dhanorhar, M. and Paranjape, K. 2009. *The Fertiliser Encyclopedia*. United States of America: John Wiley and Sons.
- Gruenewaldt, G.W., Sharpe, M.R. and Hatton, C.J. 1985. The Bushveld Complex: Introduction and Review *Economic Geology*. 80:803-812.
- Gupta, C.K. 2003. *Chemical metallurgy - Principles and Practice*. Germany: Wiley - VCH Verlag GmbH and Co. KGaA, WeinHem.
- Gupta, C.K. and Mukherjee, T.K. 1990. *Hydrometallurgy in extraction processes II*. Boston: CRC Press.

- Habashi, F. 1963. Kinetics and Mechanism of Copper Dissolution in Aqueous Ammonia. *Berichte der bunsengesellschaft für physikalische chemie*. 67(4):402-406.
- Halpern, J. 1953. Kinetics of the Dissolution of Copper in Aqueous Ammonia. *Journal of the Electrochemical Society*. 100(10):421-428.
- Harvey, T.J., Holder, N. and Stanek, T. 2002. Thermophilic bioleaching of chalcopyrite with GEOCOATTM Process. *Presented at Alta 2002 at Africa 2002 Ni/Co 8-Copper 7 Conference*. Golden, CO: Randol International, Ltd, Ed. Perth, Australia: 119-125.
- Haver, F.P. and Wong, M.M. 1971. Recovery of copper, iron, and Sulphur from chalcopyrite concentrates using a ferric chloride leach. *Journal of Metals*. 23:25-29.
- Haynes, W.M., Lide, D.R. and Raton, B. Eds. 2010. *Handbook of Chemistry and Physics*. 91st ed. London: Taylor and Francis.
- Herreros, O., Quiroz, R., Hernández, M.C. and Viñals, J. 2002. Dissolution kinetics of enargite in dilute Cl₂/Cl⁻ media. *Hydrometallurgy*. 64(3):153-160.
- Hyvarinen, O. and Hamalainen, M. 1999. *Method for producing copper in hydrometallurgical process*. U.S. 6007600.
- Implats, 2012. *Geological Settings: The Bushveld Complex*. [Online]. Available: http://www.financialresults.co.za/2012/implats_mr2012/index1c.php [2012, February 2012].
- Jandova, J. and Pedlick, M. 1994. Leaching behaviour of iron-nickel alloys in ammoniacal solution. *Hydrometallurgy*. 35(1):123-128.
- Johansson, C., Shrader, V., Suissa, J., Adutwum, K. and Kohr, W. 1999. Use of the GEOCOATTM process for the recovery of copper from chalcopyrite. *Bio-hydrometallurgy and the environment toward the mining of the 21st century*. R. Amils and A. Ballester, Eds. Amsterdam: Elsevier. 569 - 576.
- Jones, K. 1973. Ammonia. In *Comprehensive Inorganic Chemistry*. Eds. Bailar, J.C. Nyholm, H.J. and Trotman-Dickenson, A.F. Vol 2 ed. New York: Pergamon Press. 199-227.
- King, J.A., Dreisinger, D.B. and Knight, D.A. 1994. The Total Pressure Oxidation of Copper Concentrates. *Presentation at the CIMM District 6 Meeting*. March. Vancouver, B.C.: .
- Kingston, G.A. and El-Dousky, B.T. 1982. A contribution on the platinum-group mineralogy of the Merensky Reef at Rustenburg Platinum Mine. *Economic Geology*. 77:1367-1384.
- Kinloch, E.D. 1982. Regional trends in the platinum-group mineralogy of the critical Zone of the Bushveld Complex, South Africa. *Economic Geology*. 77:1328-1347.
- Kinnaird, J.A., Hutchinson, D. and Schurmann, L. 2005. Petrology and mineralisation of the southern Platreef: Northern limb of the Bushveld Complex, South Africa. *Mineralium Deposita*. 40(5):576-597.

- Kinnaird, J.A. and Nex, P. 2003. Mechanisms of marginal mineralisation in the Bushveld Complex. Applied Earth Science. *Transaction of the Institution of Mining Metallurgy B*. 112:B206-B208.
- Kotz, J.C. and Treichel, P.M.(.). 2003. *Chemistry and Chemical Reactivity*. Fifth ed. United States of America: Thomson Learning Inc.
- Kruesi, P.R., Allen, E.S. and Lake, J.L. 1973. Cymet process- hydrometallurgical conversion of base-metal sulphide to pure metals. *Canadian Institute of Mining and Metallurgy, Bull.* 66:81-87.
- Kuhn, M.C., Arbiter, N. and Kling, H. 1974. Anaconda's Arbiter process for copper. In Edmonton, Alberta: CIM Bull. 62.
- Lamya, R.M. 2007. A Fundamental Evaluation of the Atmospheric Pre-Leaching Section of the Nickel-Copper matte Treatment. University of Stellenbosch, South Africa.
- Lane, R.W. and McDonald, H.J. 1946. Kinetics of the Reaction between Copper and Aqueous Ammonia. *Journal of the American Chemical Society*. (9):1699-1704.
- Levenspiel, O. 1999. *Chemical Reaction Engineering*. Third ed. New York: Wiley.
- Liddell, K.C. 2005. Shrinking core models in hydrometallurgy: What students are not being told about the pseudo-steady approximation. *Hydrometallurgy*. 79:62-68.
- Lindsay, N.M. 1988. The processing and recovery of the Platinum - group elements. University of Witswatersrand, Johannesburg, South Africa.
- Lu, B.C.Y. and Graydon, W.F. 1955. Rates of Copper Dissolution in Aqueous Ammonium Hydroxide Solutions. *Journal of the American Chemical Society*. (23):6136-6139.
- Lundstron, M., Aroma, J. and Forsen, O. 2011. Microscopy and XRD investigation of the product layer formed during chalcopyrite leaching with copper (II) chloride. *Physicochemical problems of mineral processing* 46. 46:263-277.
- Mellor, W.J. 1928. A Comprehensive Treatise on Inorganic and Theoretical Chemistry. In VIII ed. London: Longmans, Green and Co. Ltd. 222.
- Meng, X. and Han, K.N. 1996. The Principles and Applications of Ammonia Leaching of Metals—A Review. *Mineral Processing and Extractive Metallurgy of Copper*. 16(1):23-61.
- Mizoguchi, T., Nakmura, J. and Ishii, H. 1978. Oxygen Pressurised Leaching of Metallic Nickel in Ammoniacal Ammonium Carbonate Solution. *J. Chem. Society, Japan*. 7:961-966.
- Morioka, S. and Shimakage, K. 1971. Fundamental Studies on the Ammonia Pressure Leaching of Metallic Nickel Powder. *Transaction institution of mining metallurgy*. 80 (Section C):C228-C234.

- Moyes, A.J. 2002. *The Intec Copper Process - Superior and Sustainable Copper Production'* (private communication).
- Moyes, J., Houllis, F. and Bhappu, R.R. 1999. The Intec Copper Process - Demonstration Plant Operating Experience and Results from the 1999 Campaign. *The Copper Concentrate Treatment Short Course, held in conjunction with Copper '99-Cobre '99*. October 1999. Phoenix, Arizona: 9-13.
- Mwase, J.M., Petersen, J. and Eksteen, J.J. 2012. A conceptual flowsheet for heap leaching of platinum group metals (PGMs) from a low-grade ore concentrate. *Hydrometallurgy*. 111-112(0):129-135.
- Myers, R.L. 2007. *The 100 most important compounds: a reference guide*. 26th ed. Westport, Conn: Greewood Press.
- Nelen, I.M. and Sobol, S.I. 1959. Mechanism of catalytic effect of copper during ammoniacal leaching in an autoclave. *Sb. tr. - gos. vses. Nauchno-issled. inst. tsvetnykh metal*. 15:577-584.
- Nevada-outback-gems.com/chalcopyrite 2012. *Chalcopyrite mineral facts*. [Online]. Available: http://nevada-outback-gems.com/mineral_information/Chalcopyrite_mineral_info.htm [2012, August].
- Newell, A.J.H. 2008a. *The Processing of Platinum Group Metals (PGM) - Part 1*. Runge, Inc. Australia: Pincock; Allen; Holt.
- Newell, A.J.H. 2008b. *The Processing of Platinum Group Metals (PGM) - Part 2*. Runge, Inc. Australia: Pincock, Allen and Holt.
- Nicol, M.J. 1975. An electrochemical investigation of the dissolution of copper, nickel, and copper-nickel alloys in ammonium carbonate solutions. *Journal of the South African Institute of Mining and Metallurgy*. :291-302.
- Nicol, M.J. 2008. *Hydrometallurgy. Study Guide*.
- NIOSH 1992. Recommendations for occupational safety and health: compendium of policy documents and statements. Cincinnati, OH: U.S. Department of Health and Human Services, Public Health Service, Centres for Disease Control, National Institute for occupational safety and health, DHHS (NIOSH) .
- Osseo-Asare, K., Lee, J., Kim, H. and Pickering, H. 1983. Cobalt extraction in ammoniacal solution: Electrochemical effect of metallic iron. *Metallurgical and Materials Transactions B*. 14(4):571-576.
- Outokumpu, 2005. *HydrocopperTM - A Unique and Effective Means of producing High - Quality Copper Products Directly from Copper Concentrate*.
- Park, K.H., Mohapatra, D., Reddy, B.R. and Nam, C.W. 2007. A study on the oxidative ammonia/ammonium sulphate leaching of a complex (Cu-Ni-Co-Fe) matte. *Hydrometallurgy*. 86(3-4):164-171.

- Penberthy, C.J., Oosthuizen, E.J. and Merkle, R.K.W. 2000. The recovery of platinum-group elements from the UG-2 chromitite, Bushveld Complex – a mineralogical perspective. *Mineralogy and Petrology*. 68:213-222.
- Penner, D., Michael, J. and Brown, W. 2005. A novel water conditioning adjuvant for use with formulated and nonformulated glyphosphate. *Journal of ASTM international*. 2(4):128-142.
- Peters, E. 1976. Direct Leaching of sulfides: Chemistry and applications. *Metallurgical and Materials Transactions B*. 7(4):505-517.
- Petersen, J. 2010. Determination of oxygen gas-liquid mass transfer rates in heap bioleach reactors. *Minerals Engineering*. 23:504-510.
- Petersen, J. and Dixon, D.G. 2002. Thermophilic heap leaching of a chalcopyrite concentrate. *Mineral Engineering*. 15(11):777-785.
- Porter, M. 2000. Nickel 2000 - The Major Nickel Deposits of the World, Deposit descriptions. *New Caledonian Geology and Nickel Deposits*. 28 May - 2 June. Sydney, NSW, Australia: Porter GeoConsultancy. PART B - South West Pacific Later.
- Prater, J.D., Queneau, P.B. and Hudson, T.J. 1970. The sulphation of copper iron sulphides with concentrated sulphuric acid. *Journal of Metals*. 22:23-27.
- Pritzker, M.D. 1996. Shrinking-core model for systems with facile heterogeneous and homogeneous reactions. *Chemical Engineering Science*. 51:3631-3645.
- Rao, K.S. 2000. The Role of Solids Characterisation Techniques in the Evaluation of Ammonia Leaching Behaviour of Complex Sulphides. *Mineral Processing and Extractive Metallurgy Review: An international journal*. (1):409-445.
- Rao, S.K., Das, R.P., Mukunda, P.G. and Ray, H.S. 1993. Use of X-ray diffraction in a study of ammonia leaching of multimetal sulfides. *Metallurgical and Materials Transactions B*. 24B(6):937-945.
- Reilly, I.G. and Scott, D.S. 1977. The leaching of a chalcopyrite concentrate in ammonia. *The Canadian Journal of Chemical Engineering*. 55(5):527-533.
- Riet, V.K. 1979. Review of Measuring Methods and Results in Nonviscous Gas-Liquid Mass Transfer in Stirred Vessels. *Ind. Eng. chem. process des. dev.* 18(3):357-363.
- Robinson, R.A. and Stokes, R.H. 1970. *Electrolyte Solutions*. Second ed. London: Butterworth.
- Roman, R.J. and Benner, B.R. 1973. The dissolution of copper concentrates. *Minerals Science and Engineering*. 5(1):3-24.
- Schwellnus, J.S.I., Hiemstra, S.A. and Gasparini, E. 1976. The Merensky Reef at the Atok Platinum Mine and its environs. *Economic Geology*. 71:249-260.

- Senaputra, A., Senanayake, G., Nicol, M.J. and Nikoloski, A.. 2008. Leaching Nickel and Nickel Sulfides in Ammonia/Ammonium Carbonate Solutions. *Hydrometallurgy 2008: Proceedings of the 6th International Symposium*. 17 - 28 August 2008. 560, Ed. 551-560.
- Shackleton, N.J., Malysiak, V. and O'Connor, C.T. 2007. Surface characteristics and flotation behaviour of platinum and palladium arsenides. *Int. J. miner. process.* 85:25-40.
- Shamaila, S. and O'Connor, C.T. 2008. The role of synthetic minerals in determining the relative flotation behaviour of Platreef PGE tellurides and arsenides. *Minerals Engineering*. 21:899-904.
- Sheng-Li, C. Xue-yi, G., Wen-tang, S. and Dong, L. 2010. Extraction of valuable metals from low grade nickeliferous laterite ore by reduction roasting - ammonia leaching method. *Journal of Central South University of Technology*. 17:765-769.
- Smith, F.L. and Harvey, A.H. 2007. Avoid common pitfalls when using Henry's Law. *Environmental Management*. :33-39.
- Sohn, H.Y. and Wadsworth, M.E. 1979. *Rate processes of extractive metallurgy*. New York: Plenum Press.
- Stanczyk, M.H. and Rampacek, C. 1966. *Oxidation leaching of copper sulfides in ammoniacal pulps at elevated temperatures and pressures*. 6808th ed. [Washington, D.C.]: U.S. Dept. of the Interior, Bureau of Mines.
- Stumm, W. and Morgan, J.J. 1996. *Aquatic Chemistry: Chemical Equilibria and Rates in Natural Waters*. Third ed. United States of America: John Wiley and Sons.
- Swinkels, G.M. and Berezowsky, R.M. Feb. 1978. The Sherritt-Cominco copper process - part 1: The process. *Canadian Mineral Metallurgical Bulletin*, 105-121.
- Szekely, J. and Evans, J.W. 1970. A structural model for gas—solid reactions with a moving boundary. *Chemical Engineering Science*. 25(6):1091-1107.
- Tozowa, K., Umetutsu, Y. and Sato, K. 1976. On chemistry of ammonia leaching of copper concentrates. In *The Extractive Metallurgy of Copper*. J.C. Yannopoulos and J.C. Argawal eds, Eds. New York:13.
- Tromans, D. 1998. Temperature and pressure dependent solubility of oxygen in water: a thermodynamics analysis. *Hydrometallurgy*. 48:327-342.
- Tromans, D. 2000. Oxygen solubility modelling in ammoniacal leaching solutions: Leaching of sulphide concentrates. *Minerals Engineering*. 13(5):497-515.
- Vermaak, C.F. and Hendricks, L.P. 1976. A review of the mineralogy of the Merensky Reef, with specific reference to new data on the precious metal mineralogy. *Economic Geology*. 71:1244-1269.

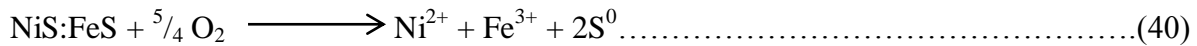
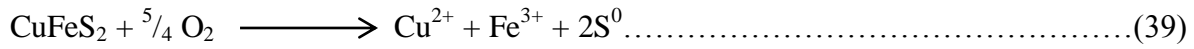
- Vermaak, M.K.G., Pistorius, P.C. and Venter, J.A. 2007. Fundamental electrochemical and Raman spectroscopic investigations of the flotation behaviour of PtAs₂. *Minerals Engineering*. 20:1153-1158.
- Viljoen, M.J. and Schurmann, L.W. 1998. Platinum - group metals. *The mineral resources of South Africa. Coun Geosci Handbook 16*. M.G.C. Wilson and C.R. Anhaeusser, Eds. 532-568.
- Warren, G. 1979. Electrochemical oxidation of chalcopyrite in ammoniacal solutions.
- Warren, G. and Wadsworth, M. 1984. The electrochemical oxidation of chalcopyrite in ammoniacal solutions. *Metallurgical and Materials Transactions B*. 15(2):289-297.
- Warren, G. and Wadsworth, M.E. 1978. The electrochemical oxidation of chalcopyrite in ammoniacal solutions. *AIME Annual Meeting*. 28 February - 2 March. Denver, Colorado: AIME preprint 78-B-68.
- Weiss, R.F. 1970. The solubility of nitrogen, oxygen and argon in water and seawater. *Deep sea research*. 17:721-735.
- Welham, N.J., Johnston, G.M. and Sutcliffe, M.L. 2010. *Method of ammoniacal leaching*. 2010/0180728 A1. U.S.: .
- Wiberg, E. and Holleman, A.F. 2001. Inorganic Chemistry. In Elsevier. 614.
- wiki.biomine.skelleftea.se. 2008. *Tank leaching*.
- Windholz, M., Budavari, S., Stroumstos, L.Y. and Fertig, M.N. 1976. *Merck Index*. 9th ed. Rahway, New Jersey: Merck and Co. Inc.
- www.galleries.com/pentlandite 2013. *The mineral pentlandite*. [Online]. Available: <http://www.galleries.com/pentlandite> [2013, January].
- Yamasaki, E. 1920. On the rate of metallic dissolution of metallic copper in aqueous ammonia. *Science reports Tohoku University, Japan*. 14(Series I : 9):160-220.
- Zapp, K.H. 2009. *Ammonium Compounds in Ullmann's Encyclopaedia of Industrial Chemistry 2012*. 90th ed. Wiley-VCH, Weinheim.

8.0 APPENDICES

APPENDIX A

Calculations of the rate of oxygen supplied and consumed

Assumption: The following stoichiometric equations describe the ammoniacal leaching of chalcopyrite and pentlandite:



Molecular mass of $\text{CuFeS}_2 = 63.55 + 55.85 + 2(32) = 183.55 \text{ g/mol}$

Molecular mass of $\text{NiS:FeS} = 58.69 + 55.85 + 2(32) = 178.54 \text{ g/mol}$

According to Newton's law of cooling, the rate of oxygen mass transfer is described by:

$$r_{\text{O}_2} = k_L a (c^* - c_b) \dots\dots\dots(32)$$

Where $k_L a$ is the volumetric mass transfer coefficient, c^* is the equilibrium concentration at the gas-liquid interface and c_b is the bulk concentration of oxygen in solution. If all of the oxygen in solution is used up, then the maximum rate of oxygen transfer is given by:

$$r_{\text{O}_2, \text{supplied}} = k_L a (c^*) \dots\dots\dots(33)$$

TANKS

Basis in Tanks: 1 day

Oxygen consumed for Cu leaching during Cu leaching of Platreef concentrates in tanks.

Volume of slurry	=	1 L
Amount of Cu leached in 1 day	=	261.8 mg/L
Moles of Cu leached in 1 day	=	$\frac{(261.8 \cdot 10^{-3}) \text{ g} \cdot 1 \text{ L}}{63.55 \text{ g/mol}}$
	=	0.00411 mol

From stoichiometric equation:

1 mole of CuFeS_2 : 1 mole of Cu

0.00411 moles: 0.00411 moles

\therefore 0.00411 mol CuFeS_2 leached theoretically

$$\begin{aligned}\text{Theoretical amount of O}_2 \text{ used} &= (0.00411 \times 1.25) \text{ mol} \\ &= 0.005134 \text{ mol}\end{aligned}$$

\therefore 0.005134 mol O₂ used in CuFeS₂ leach in 1L

Oxygen consumed during Ni leaching of Platreef concentrates in columns

$$\begin{aligned}\text{Volume of slurry} &= 1 \text{ L} \\ \text{Amount of Ni leached in 1 day} &= 385.6 \text{ mg/L} \\ \text{Moles of Cu leached in 1 day} &= \frac{(385.6 \cdot 10^{-3}) \text{ g} \cdot 1 \text{ L}}{58.69 \text{ g/mol}} \\ &= 0.00657 \text{ mol}\end{aligned}$$

From stoichiometric equation:

1 mole of NiS:FeS: 1 mole of Ni

0.00657 moles: 0.00657 moles

\therefore 0.00657 mol NiS:FeS leached theoretically

$$\begin{aligned}\text{Theoretical amount of O}_2 \text{ used} &= (0.00657 \times 1.25) \text{ mol} \\ &= 0.00821 \text{ mol}\end{aligned}$$

\therefore 0.00821 mol/L O₂ used in CuFeS₂ leach in 1L

Total amount of O₂ required: (0.005134 + 0.00821) mol/L = 0.0133 mol/L

$$r_{O_2, \text{consumed}} = \left(\frac{\text{total oxygen consumed}}{\text{solution volume} \cdot \text{time}} \right) \left[\frac{\text{mol}}{\text{L} \cdot \text{s}} \right] \dots \dots \dots (37)$$

$$\begin{aligned}\therefore \text{Rate of O}_2 \text{ consumed in tanks} &= 0.0133 \text{ mol/L.d} \\ &= \underline{\underline{1.54 \times 10^{-7} \text{ mol/L.s}}}\end{aligned}$$

Rate of oxygen supplied in tanks at ambient temperature:

For aqueous solutions Tromans (2000) proposes the following equation:

$$c^* = p_{O_2} \cdot k \cdot [1 + \kappa(C_i)^\gamma]^{-h} \dots \dots \dots (34)$$

where C_i refers to the molality of the salt i in solution. The parameters κ , γ and h for aqueous ammonia as listed by Tromans (2000) are 0.0105, 1.0 and -1.0, respectively.

The partial pressure of oxygen is calculated as:

$$p_{O_2} = 0.21 P \dots\dots\dots(35)$$

Where P is the atmospheric pressure in these experiments = 1 atm.

The partition coefficient k is calculated from:

$$k = \exp\left\{\frac{0.046 \cdot T^2 + 203.35 \cdot T \cdot \ln\left(\frac{T}{298}\right) - (299.378 + 0.092 \cdot T) \cdot (T - 298) - 2.0591 \cdot 10^4}{8.3144 \cdot T}\right\} \dots\dots\dots(36)$$

where T is in K

$$k = 1.2788 \times 10^{-3}$$

$$\begin{aligned} c^* &= 0.21 \cdot 1.2788 \cdot 10^{-3} \cdot [1 + 0.0105(8)^{1.0}]^{-1.0} \\ &= 2.5 \times 10^{-4} \text{ mol/kg H}_2\text{O} \\ &\sim 2.5 \times 10^{-4} \text{ mol/L} \end{aligned}$$

$$\begin{aligned} \text{Rate of O}_2 \text{ supplied in tanks} &= k_{La} \times c^* \\ &= 0.28/\text{s} \times 2.5 \times 10^{-4} \text{ mol/L} \\ &= \underline{\underline{6.94 \times 10^{-5} \text{ mol/L.s}}} \end{aligned}$$

COLUMNS

Basis in columns: 30 days

Oxygen consumed during Cu leaching of Platreef concentrates in columns

$$\begin{aligned} \text{Amount of Cu leached in 30 days} &= 6583.6 \text{ mg} \\ &= 0.104 \text{ mol} \end{aligned}$$

1 mole of CuFeS₂: 1 mole of Cu

0.104 moles: 0.104 moles

∴ 0.104 mol CuFeS₂ leached

Theoretical amount of O₂ used = 0.104 * 1.25 = 0.129 mol

∴ 0.129 mol O₂ used in CuFeS₂

Oxygen consumed during Ni leaching of Platreef concentrates in columns

$$\begin{aligned}\text{Amount of Ni leached in 1 day} &= 5404.9 \text{ mg} \\ &= 0.092 \text{ mol}\end{aligned}$$

1 mole of NiS:FeS: 1 mole of Ni

0.092 moles: 0.092 moles

∴ 0.092 mol CuFeS₂ leached

Theoretical amount of O₂ used = 0.092 x 1.25 = 0.115 mol

∴ 0.115 mol O₂ used in NiS:FeS leach

Total amount of O₂ required: (0.129 + 0.115) mol = 0.244 mol

$$r_{O_2, consumed} = \left(\frac{\text{total oxygen consumed over 30 days}}{\text{liquid hold-up-time}} \right) \left[\frac{\text{mol}}{\text{L.s}} \right] \dots \dots \dots (38)$$

$$\begin{aligned}\therefore \text{rate of O}_2 \text{ used in columns} &= \frac{0.244 \text{ mol}}{\frac{0.2 \text{ L}}{d}} \\ &= \frac{0.244 \text{ mol}}{0.2 \times 30 \times 3600 \text{ L.s}} \\ &= \underline{\underline{4.71 \times 10^{-7} \text{ mol/L.s}}}\end{aligned}$$

Rate of oxygen supply in columns at ambient temperature (298K)

The equilibrium concentration at the gas-liquid interface is calculated using the equations (34, 35 and 36) above is:

$$\begin{aligned}c^* &= 0.21 \cdot 1.2788 \cdot 10^{-3} \cdot [1 + 0.0105(8)^{1.0}]^{-1.0} \\ &= 2.5 \times 10^{-4} \text{ mol/kg H}_2\text{O} \\ &\sim 2.5 \times 10^{-4} \text{ mol/L}\end{aligned}$$

$$\begin{aligned}\text{Rate of O}_2 \text{ supply in columns} &= k_L a \times c^* \\ &= 0.013/\text{s} \times 2.5 \times 10^{-4} \text{ mol/L} \\ &= \underline{\underline{3.22 \times 10^{-6} \text{ mol/L.s}}}\end{aligned}$$

Appendix B: Material Safety Data Sheet (MSDS): Ammonia**1. Chemical Product**

Product Name: Ammonia

Chemical Name: Ammonia

Common Names/Synonyms: Ammonia Anhydrous; Anhydrous Ammonia

2. Composition, Information on Ingredients

INGREDIENT	% VOLUME	PEL-OSHA ¹	TLV-ACGIH ²	LD ₅₀ or LC ₅₀ Route/Species
Ammonia FORMULA: NH ₃ CAS: 7664-41-7 RTECS #: BO0875000	100.0	50 ppm TWA	25 ppm TWA 35 ppm STEL	LC ₅₀ 2000 ppm/4H

¹ As stated in 29 CFR 1910, Subpart Z (revised July 1, 1993)² As stated in the ACGIH 1994-95 Threshold Limit Values for Chemical Substances and Physical Agents**3. Hazards Identification****Emergency Overview**

Irritating or corrosive to exposed tissues. Inhalation of vapours may result in pulmonary edema and chemical pneumonitis. Slightly flammable.

Route of Entry:

Skin Contact Yes	Skin Absorption No	Eye Contact Yes	Inhalation Yes	Ingestion No
---------------------	-----------------------	--------------------	-------------------	-----------------

Health Effects:

Exposure Limits Yes	Irritant Yes	Sensitization No
Teratogen No	Reproductive Hazard No	Mutagen Yes
Synergistic Effects None Reported		

Carcinogenicity: -- NTP: No IARC: No OSHA: No

- Eye Effects: Mild concentrations of product will cause conjunctivitis. Contact with higher concentrations of product will cause swelling of the eyes and lesions with a possible loss of vision.
- Skin Effects: Mild concentrations of product will cause dermatitis or conjunctivitis. Contact with higher concentrations of product will cause caustic-like dermal burns and inflammation. Toxic level exposure may cause skin lesions resulting in early necrosis and scarring.
- Ingestion Effects: Since product is a gas at room temperature, ingestion is unlikely.
- Inhalation Effects: Corrosive and irritating to the upper respiratory system and all mucous type tissue. Depending on the concentration inhaled, it may cause burning sensations,

coughing, wheezing, shortness of breath, headache, nausea, with eventual collapse. Inhalation of excessive amounts affects the upper airway (larynx and bronchi) by causing caustic-like burning resulting in edema and chemical pneumonitis. If it enters the deep lung, pulmonary edema will result. Pulmonary edema and chemical pneumonitis are potentially fatal conditions.

NFPA HAZARD CODES		HMIS HAZARD CODES		RATINGS SYSTEM
Health:	3	Health:	3	0 = No Hazard
Flammability:	1	Flammability:	1	1 = Slight Hazard
Reactivity:	0	Reactivity:	0	2 = Moderate Hazard
				3 = Serious Hazard
				4 = Severe Hazard

4. First Aid Measures

- Eyes: Flush contaminated eye(s) with copious quantities of water. Part eyelids to assure complete flushing. Continue for a minimum of 15 minutes. Persons with potential exposure to ammonia should not wear contact lenses.
- Skin: Remove contaminated clothing as rapidly as possible. Flush affected area with copious quantities of water. In cases of frostbite or cryogenic "burns" flush area with lukewarm water. Do not use hot water. A physician should see the patient promptly if the cryogenic "burn" has resulted in blistering of the dermal surface or deep tissue freezing.
- Ingestion: Not specified. Seek immediate medical attention.
- Inhalation: Prompt medical attention is mandatory in all cases of overexposure. Rescue personnel should be equipped with self-contained breathing apparatus. Conscious persons should be assisted to an uncontaminated area and inhale fresh air. Quick removal from the contaminated area is most important. Unconscious persons should be moved to an uncontaminated area, given mouth-to-mouth resuscitation and supplemental oxygen. Keep victim warm and quiet. Assure that mucus or vomited material does not obstruct the airway by positional drainage.

5. Fire Fighting Measures

Conditions of Flammability: Non-flammable		
Flash point: None	Method: Not Applicable	Auto-ignition: Temperature: 1274 °F (690 °C)
LEL(%): 16		UEL(%): 25
Hazardous combustion products: None		
Sensitivity to mechanical shock: None		
Sensitivity to static discharge: None		

- **Fire and Explosion Hazards:** The minimum ignition energy for ammonia is very high. It is approximately 500 times greater than the energy required for igniting hydrocarbons and 1000 to 10,000 times greater than that required for hydrogen.
- **Extinguishing Media:** Water fog. Use media suitable for surrounding fire.
- **Fire Fighting Instructions:** If possible, stop the flow of gas. Since ammonia is soluble in water, it is the best extinguishing media-not only in extinguishing the fire, but also absorbing the escaped ammonia gas. Use water spray to cool surrounding containers.

6. Accidental Release Measures

Evacuate all personnel from affected area. Use appropriate protective equipment. If leak is in user's equipment, be certain to purge piping with inert gas prior to attempting repairs.

7. Handling and Storage

Electrical Classification:

Class 1, Group D.

Earth-ground and bond all lines and equipment associated with the ammonia system. Electrical equipment should be non-sparking or explosion proof. Gaseous or liquid anhydrous ammonia corrodes certain metals at ambient temperatures. The presence of oxygen enhances the corrosion of ordinary or semi-alloy steels. The addition of water inhibits this enhancement. Keep anhydrous ammonia systems scrupulously dry.

Use only in well-ventilated areas. Valve protection caps must remain in place unless container is secured with valve outlet piped to use point. Do not drag, slide or roll cylinders. Use a suitable hand truck for cylinder movement. Use a pressure regulator when connecting cylinder to lower pressure (<500 psig) piping or systems. Do not heat cylinder by any means to increase the discharge rate of product from the cylinder. Use a check valve to trap in the discharge line to prevent hazardous back flow into the cylinder.

Protect cylinders from physical damage. Store in cool, dry, well-ventilated area away from heavily trafficked areas and emergency exits. Do not allow the temperature where cylinders are stored to exceed 125°F (52 °C). Cylinders should be stored upright and firmly secured to prevent falling or being knocked over. Full and empty cylinders should be segregated. Use a "first in-first out" inventory system to prevent full cylinders from being stored for excessive periods of time. For additional handling recommendations, consult Compressed Gas Association Pamphlets P-1 and G2. Never carry a compressed gas cylinder or a container of a gas in cryogenic liquid form in an enclosed space such

as a car trunk, van or station wagon. A leak can result in a fire, explosion, asphyxiation or a toxic exposure.

8. Exposure Controls, Personal Protection

INGREDIENT	% VOLUME	PEL-OSHA ²	TLV-ACGIH ³	LD ₅₀ or LC ₅₀ Route/Species
Ammonia FORMULA: NH ₃ CAS: 7664-41-7 RTECS #: BO0875000	100.0	50 ppm TWA	25 ppm TWA 35 ppm STEL	LC ₅₀ 2000 ppm/4H

¹ Refer to individual state of provincial regulations, as applicable, for limits which may be more stringent than those listed here.

² As stated in 29 CFR 1910, Subpart Z (revised July 1, 1993)

³ As stated in the ACGIH 1994-1995 Threshold Limit Values for Chemical Substances and Physical Agents.

- Engineering Controls: Use local exhaust ventilation to reduce concentrations to within current exposure limits. A laboratory type hood is suitable for handling small or limited quantities.
- Eye/Face Protection: Gas tight chemical goggles or full-face piece respirator.
- Skin Protection: Protective gloves made of any suitable material.
- Respiratory Protection: Level C respiratory protection with full face piece or self-contained breathing apparatus should be available for emergency use. Air purifying respirators must be equipped with suitable cartridges. Do not exceed maximum use concentrations. Do not use air purifying respirators in an oxygen deficient/immediately dangerous to life and health (IDLH) atmosphere. Consult manufacturer's instructions before use.
- OTHER/GENERAL PROTECTION: Safety shoes, safety shower, eyewash "fountain".

9. Physical and Chemical Properties

PARAMETER	VALUE	UNITS
Physical state (gas, liquid, solid)	: Gas	
Vapour pressure at 70°F	: 94	psia
Vapour density at 60°F (Air = 1)	: 0.62	
Evaporation point	: Not Available	
Boiling point	: -28	°F
	: -33.3	
°C Freezing point	: 107.9	
°F		
	: -77.7	°C
pH	: Not	
Available Specific gravity	:	
Not Available Oil/water partition coefficient		
: Not Available Solubility (H ₂ O)		
: Very soluble Odour threshold		
: Not Available		
Odour and appearance	: A colourless gas with a pungent odour.	

10. Stability and Reactivity

- Stability: Unstable
- Conditions to Avoid (Stability): None
- Incompatible Materials: Reacts vigorously with fluorine, chlorine, HCl, HBr, nitrosyl chloride, chromyl chloride, nitrogen dioxide, trioxxygen difluoride, and nitrogen trichloride
- Hazardous decomposition products: Hydrogen at very high temperatures: 1544 °F (840 °C)
- Conditions to avoid (polymerization): None
- Hazardous polymerization: Will not occur.

11. Toxicological Information

- Mutagenic: Genetic mutations observed in bacterial and mammalian test systems.
- OTHER: Toxic effects to the respiratory system, senses, liver, kidneys and bladder observed in mammalian species from prolonged inhalation exposures at above 100 ppm.

12. Ecological Information

Other Environmental Information: The reportable quantity is the minimum quantity of a material that when released, requires reporting to the appropriate Federal, State and local officials. Notification requirements are found under CERCLA Section 103(a). Initial notification may be by telephone, radio, or in person. A written follow-up notice is also required.

13. Disposal Considerations

Do not attempt to dispose of residual waste or unused quantities. Return in the shipping container properly labelled, with any valve outlet plugs or caps secured and valve protection cap in place to BOC Gases or authorized distributor for proper disposal.

14. Transport Information

PARAMETER	United States DOT	Canada TDG
PROPER SHIPPING NAME:	Ammonia, Anhydrous, liquefied	Ammonia, Anhydrous, liquefied
HAZARD CLASS:	2.2	2.4 (9.2)
IDENTIFICATION NUMBER:	UN 1005	UN 1005
SHIPPING LABEL:	NONFLAMMABLE GAS	CORROSIVE GAS

15. Regulatory Information

Ammonia is listed under the accident prevention provisions of section 112(r) of the Clean Air Act (CAA) with a threshold quantity (TQ) of 10,000 pounds.